TURUN
YLIOPISTO
UNIVERSITY
OF TURKU

DIAGNOSTIC AND PROGNOSTIC VALUE OF FREE PAPP-A IN CORONARY ARTERY DISEASE

Clinical Studies with Novel Immunoassay

Emilia Tuunainen (née Engström)

TURUN YLIOPISTON JULKAISUJA – ANNALES UNIVERSITATIS TURKUENSIS
SARJA – SER. F OSA – TOM. 17 | TECHNICA – INFORMATICA | TURKU 2022

TURUN
YLIOPISTO
UNIVERSITY
OF TURKU

DIAGNOSTIC AND PROGNOSTIC VALUE OF FREE PAPP-A IN CORONARY ARTERY DISEASE

Clinical Studies with Novel Immunoassay

Emilia Tuunainen (née Engström)

TURUN YLIOPISTON JULKAISUJA – ANNALES UNIVERSITATIS TURKUENSIS
SARJA – SER. F OSA – TOM. 17 | TECHNICA – INFORMATICA | TURKU 2022

University of Turku

Faculty of Technology
Department of Life Technologies
Biotechnology Unit
Doctoral programme in Clinical
Research, DPCR

Research Director

Professor Emeritus, Kim Pettersson
Biotechnology Unit
Department of Life Technologies
University of Turku, Turku, Finland

Supervised by

Assistant professor, Saara Wittfooth
Biotechnology Unit
Department of Life Technologies
University of Turku, Turku, Finland

Professor, Antti Saraste
Heart Center
Turku University Hospital, Turku, Finland

Reviewed by

Adjunct Professor, Päivi Laitinen
HUS Diagnostiikkakeskus
HUSLAB

Professor, Jari Laukkanen
Cardiology, Department of Medicine
University of Eastern Finland

Opponent

Professor, Ola Hammarsten
Department of Clinical Chemistry and
Transfusion Medicine
University of Gothenburg

The originality of this publication has been checked in accordance with the University of Turku quality assurance system using the Turnitin OriginalityCheck service.

ISBN 978-951-29-9048-1 (PRINT)
ISBN 978-951-29-9049-8 (PDF)
ISSN 2736-9390 (Print)
ISSN 2736-9684 (Online)
Painosalama, Turku, Finland 2022

Matildalle ja Ainolle

Minä suojelen sinua kaikelta,
mitä ikinä keksitkin pelätä.
Ei ole sellaista pimeää,
jota minun hento käteni ei torjuisi.

Anni Sinnemäki

UNIVERSITY OF TURKU
Faculty of Technology
Department of Life Technologies
Biotechnology Unit
EMILIA TUUNAINEN: Diagnostic and Prognostic Value of Free PAPP-A in Coronary Artery Disease – Clinical Studies with Novel Immunoassay
Doctoral Dissertation, 169 pp.
Doctoral Programme in Clinical Research, DPCR
November 2022

ABSTRACT

Complications of coronary artery disease are the number one cause of death worldwide, so identification of high-risk individuals is crucial. Pregnancy-associated plasma protein A (PAPP-A) is a candidate cardiac-risk related biomarker, which has been linked to poorer outcome in various cardiovascular patients. Especially, the free form of PAPP-A (fPAPP-A) is linked to cardiovascular events, but thus far no direct assay detecting fPAPP-A has been published. Most available assays measure total PAPP-A and are widely used in prenatal screening where high concentration changes occur. Thus, cardiac-related slight fPAPP-A changes might be undetectable with total PAPP-A assays. Also, PAPP-A is released to circulation after heparin treatment, which is a common anticoagulant used in dissolving thrombus. This might question the ability of PAPP-A to be used as a marker for haparinized patients.

In this thesis, first direct immunoassay targeting fPAPP-A was created and its analytical and clinical performance as cardiac-risk related biomarker was evaluated. The analytical performance of the fPAPP-A assay was evaluated against current guidelines. The risk of death or myocardial infarction in patients admitted to hospital due to chest pain was studied and compared to tPAPP-A and indirect fPAPP-A assays. The developed assay was also used in predicting obstructive CAD in suspected chronic CAD patients. The disease extent and severity was determined with hybrid computed tomography and positron emission tomography myocardial perfusion imaging. Correlation of heparin-induced release of fPAPP-A and atherosclerotic burden was studied in suspected chronic CAD patients.

The developed assay sensitively measured fPAPP-A. The risk of death or myocardial infarction correlated with increasing circulating fPAPP-A concentration. Also, fPAPP-A in combination with contemporary cTnI further improved the risk-predictive capability. Accordingly, the fPAPP-A level was elevated in chronic CAD patients who were diagnosed with obstructive CAD. As a biomarker, fPAPP-A outperformed traditional risk factors and other evaluated biomarkers in predicting obstructive CAD. Heparin-induced release of fPAPP-A to circulation was not associated with clinical coronary atherosclerotic characteristristics observed with coronary computed tomography angiography.

KEYWORDS: Pregnancy-associated plasma protein A, atherosclerosis, coronary artery disease, biomarker, immunoassay, risk prediction

TURUN YLIOPISTO
Teknillinen tiedekunta
Bioteknologian laitos
Biotekniikka
EMILIA TUUNAINEN: Suoralla menetelmällä mitattu vapaa PAPP-A diagnostisena ja ennustavana merkkiaineena sepelvaltimotaudissa
Väitöskirja, 169 s.
Turun kliininen tohtoriohjelma, TKT
Marraskuu 2022

TIIVISTELMÄ

Sepelvaltimotautiin liittyvät komplikaatiot ovat yleisin kuolinsyy maailmassa, jonka vuoksi korkean riskin potilaiden tunnistaminen ajoissa on tärkeää. Raskauteen liittyvä plasmaproteiini A (PAPP-A) on lupaava merkkiaine, joka on yhdistetty erilaisilla sydänpotilailla heikompaan selviytymiseen ilman sydäntapahtumia. Erityisesti PAPP-A:n vapaa muoto (fPAPP-A) on liitetty sydäntapahtumiin, mutta suoraa määritysmenetelmää fPAPP-A:lle ei ole vielä kehitetty. Useimmat määritykset mittaavat kaikkia PAPP-A:n muotoja ja niitä käytetään raskauden-aikaiseen seulontaan, jolloin pitoisuusmuutokset ovat suuria. Tällaisella määrityksellä mitattuna sydäntapahtumien yhteydessä tapahtuvat pienet fPAPP-A -muutokset saattavat jäädä huomioimatta. PAPP-A:ta vapautuu verenkiertoon myös verihyytymien liuottamiseen käytetyn hepariinilääkityksen vuoksi. Tämä saattaa kyseenalaistaa PAPP-A:n käytön merkkiaineena hepariinilääkityillä potilailla.

Väitöskirjatyössä kehitettiin ensimmäinen suora fPAPP-A:ta mittaava immunomääritys. Määrityksen analyyttista toimivuutta evaluoitiin kliinisen kemian ohjeistusten mukaisesti. FPAPP-A:n käyttöä sydänkohtaukseen tai kuolemaan liitettynä merkkiaineena tutkittiin rintakivun vuoksi sairaalaan saapuneilta potilailta ja tuloksia verrattiin epäsuoralla menetelmällä mitattuun fPAPP-A:han sekä kaikkia PAPP-A:n muotoja mittaavaan määritykseen. Lisäksi, fPAPP-A:n yhteyttä ahtauttavaan sepelvaltimotautiin tarkasteltiin epäillyillä vakaaoireisilla sepelvaltimotautipotilailla. Sepelvaltimotaudin vakavuuden ja laajuuden määrittäimiseen käytettiin hybridikuvantamista, jossa hyödynnetään tietokonetomografiaa ja isotooppitutkimusta. Samoilla potilailla tutkittiin myös hepariinin vapauttaman fPAPP-A:n yhteyttä sepelvaltimotaudin vaikeusasteeseen.

Kehitetty määritys oli herkkä mittaamaan fPAPP-A:ta. Kohonnut fPAPP-A oli yhteydessä suurentuneeseen sydänkohtauksen tai kuoleman riskiin. Yhdistettynä sydänperäisen troponiini I:n kanssa, kyky ennustaa riskä parani entisestään. Lisäksi, ahtauttavaa sepelvaltimotautia sairastavilla potilailla oli kohonnut fPAPP-A -pitoisuus ja fPAPP-A toimi paremmin kuin perinteiset riskitekijät tai muut mitatut merkkiaineet. Hepariinin vuoksi verenkiertoon vapautunut fPAPP-A ei ollut yhteydessä selvaltimotaudin vakavuuteen tai laajuuteen.

ASIASANAT: Raskauteen liittyvä plasmaproteiini A, sepelvaltimotauti, merkkiaine, immunomääritys, riskin ennustaminen

Table of Contents

Abbreviations

ACS	Acute coronary syndrome
AHA	American Heart Association
AP	Angina pectoris
Apo	Apolipoprotein
AUC	Area under the curve
BP	Blood pressure
BSA	Bovine serum albumin
CABG	Coronary artery bypass graft surgery
CAC	Coronary artery calcium
CAD	Coronary artery disease
CHD	Coronary heart disease
CI	Confidence interval
CLSI	Clinical And Laboratory Standards Institute
CMR	Cardiac magnetic resonance
cPAPP-A	Complexed PAPP-A
CRP	C-reactive protein
CSA	Cross-sectional area (of the lumen)
CT	Computed tomography
CTA	Computed tomography angiography
cTn	Cardiac troponin
(c)TnI	(Cardiac) troponin I
(c)TnT	(Cardiac) troponin T
CVD	Cardiovascular disease
ECG	Electrocardiogram
EF	Ejection fraction
ELISA	Enzyme-linked immunosorbent assay
ESC	European Society of Cardiology
fβ-hCG	Free beta human chorionic gonadotropin
fPAPP-A	Free PAPP-A i.e., non-complexed PAPP-A
FRS	Framingham Risk Score
GAG	Glycosaminoglycan

HDL-C	High-density lipoprotein cholestrol
HF	Heart failure
HR	Hazard ratio
hs	High-sensitivity
HU	Hounsfield unit
ICA	Invasive coronary angiography
IDL	Intermediate-density lipoproteins
IGF	Insulin-like growth factor
IGF-R1	Type 1 insulin-like growth factor receptor
IGFBP	Insulin-like growth factor binding protein
IL	Interleukin
i.v.	Intravenous
IVUS	Intravascular ultrasound
LAD	Left anterior descending artery
LDL	Low-density lipoprotein
LDL-C	Low-density lipoprotein cholesterol
LiH	Lithium heparin
LM	Left main coronary artery
LMWH	Low molecular weight heparin
lncRNA	Long non-coding RNA
LNR	Lin-Notch repeat
LoB	Limit of Blank
LoD	Limit of Detection
LoQ	Limit of Quantitation
Lp(a)	Lipoprotein A
Lp-PLA2	Lipoprotein-associated phospholipase A2
mAb	Monoclonal antibody
MACE	Major adverse coronary event
MBF	Myocardial blood flow
MCP-1	Monocyte chemoattractant protein 1
MI	Myocardial infarction
miRNA	Micro RNA
MLA	Minimal lumen area
MMP	Matrix metalloproteinase
MPI	Myocardial perfusion imaging
MPO	Myeloperoxidase
MRI	Magnetic resonance imaging
NST-ACS	Non-ST segment elevation acute coronary syndrome
NSTEMI	Non-ST segment elevation myocardial infarction
NT-proBNP	N-terminal prohoromone of brain-type natriuretic peptide

OCT	Optical coherence tomography
OR	Odds ratio
PAPP-A	Pregnancy-associated plasma protein A
PCI	Percutaneous coronary intervention
PET	Positron emission tomography
proMBP	Proform of eosinophil major basic protein
ROC	Receiver-operator characteristic
rPAPP-A	Recombinantly produced non-complexed PAPP-A
RR	Risk ratio
SARS-CoV-2	Severe acute respiratory syndrome coronavirus 2
s.c.	Subcutaneous
SCR	Short consensus repeat
SD	Standard deviation
SPECT	Single photon emission computed tomography
ST2	Stanniocalcin 2
STEMI	ST segment elevation myocardial infarction
T2D	Type 2 diabetes mellitus
TC	Total cholesterol
TCFA	Thin-cap fibroatheroma
TG	Triglyceride
TNF-α	Tumour necrosis factor α
tPAPP-A	Total PAPP-A, complexed and non-complexed forms together
TSA	Tris-buffered saline with azide
UAP	Unstable angina pectoris
UFH	Unfractionated heparin
VLDL	Very-low-density lipoprotein
VSMC	Vascular smooth muscle cell

List of Original Publications

This dissertation is based on the following original publications, which are referred to in the text by their Roman numerals:

I Tuunainen E, Lund J, Danielsson J, Pietilä P, Wahlroos V, Pudge K, Leinonen I, Porela P, Ilva T, Lepäntalo M, Pulkki K, Voipio-Pulkki L-M, Pettersson K, Wittfooth S. Direct immunoassay for free pregnancy-associated plasma protein A (PAPP-A). *J Appl Lab Med* **3**(3):438–449. (2018)

II Tuunainen E, Maaniitty T, Knuuti J, Pettersson K, Wittfooth S, Saraste A. Free PAPP-A as a biomarker: heparin-induced release is not related to coronary atherosclerotic burden. *Clin Chem Lab Med* 57(7):e155–e158. (2019)

III Tuunainen E, Nammas W, Maaniitty T, Knuuti J, Wittfooth S, Saraste A. Circulating free pregnancy-associated plasma protein A is elevated in chronic coronary artery disease. [manuscript]

1 Introduction

The prevalence of cardiovascular diseases (CVDs) is relatively high and currently CVD is the leading cause of death throughout the world.[1] The disease has become so common that the American Heart Association (AHA) has estimated that one in three people will suffer some form of CVD during their lifetime. Clinically, coronary artery disease (CAD) and ischemic stroke are the two most prevalent forms of CVD.[2] These are causing major financial burden in the form of increasing healthcare costs, especially in developing or low-income countries.[3]

The condition behind CVD and coronary heart disease (CHD) is atherosclerosis. The disease is very complex by nature and factors contributing to the development and progression of atherosclerosis are genetic or related to lifestyle. Prevention of the disease progression is the key therapy that needs to be applied in order to avoid future severe cardiac-related complications. Therefore, critical processes in the progression of atherosclerosis need to be identified and usually more than one risk factor must be targeted when aiming to reduce the risk.[4] The reduction of CVD morbidity and mortality rely on the primary and secondary prevention where the control of modifiable risk factors play a crucial role.[5]

Measurement of various circulating biomolecules, i.e., biomarkers, are used in aid to diagnose CVD and in monitoring the disease progression or response to therapy. Biomarkers are indicators of biochemical changes behind atherosclerosis and thus used in the assessment of disease status. Results of biomarker levels can be used independently or in conjunction with other methods to determine individual's risk of future cardiovascular events.[6] Generally, various risk scores use biomarker measurements together with known risk factors (e.g., sex, age, smoking and diabetes status) and blood pressure (BP) measurement when generating the individual's risk score. The calculated risk score can be taken into account when designing suitable therapy and later to determine the achieved response.[7] Biomarker levels and risk scores are easy to obtain but the most accurate approximation of the atherosclerosis status in coronary arteries is achieved with different imaging modalities. Primarily, the diagnosis of CAD is recommended to be obtained with non-invasive methods over invasive imaging, but the selection of the method depends on patient needs and available resources. Guidelines generated by European Society of Cardiology (ESC)

give instructions for selecting suitable imaging method when diagnosing chronic CAD. For evaluating the extent and severity of CAD, both anatomical and ischemic characteristics are required.[6]Even though massive leaps in CVD diagnosis and therapy have been accomplished, still a substantial residual risk of a cardiac event remains. With current diagnostic tools and available therapies, the life expectancy of diseased individuals has increased. Still, many individuals suffer from these diseases and despite therapy, the quality of life of these individuals is affected. Thus, improving existing or creating new methods to diagnose CVD and determine the risk of cardiac events remains as a critical task for scientists worldwide and across disciplines.[8]

2 Literature Review

2.1 Coronary artery disease (CAD)

2.1.1 Atherosclerosis

Atherosclerosis develops over long period of time and the first pathological change observed in animal models is the hyperlipidaemia-induced macrophage infiltration of the intima.[9] However, atherosclerotic lesions in animals have limited resemblance to humans and therefore progression of atherosclerosis and plaque morphology have been studied in more detail during autopsy.[10] Initiation of atherosclerosis is summarized by Libby *et al.*[11]: Accumulation of low-density lipoprotein (LDL) particles into the innermost layer of the vessel wall, intima, begins the development of atherosclerosis. After oxidative and other modifications, the LDL particles become proinflammatory and start to gather circulating monocytes which later differentiate to macrophages.

Based on autopsy findings, different plaque morphologies have been categorized by AHA consensus group already in the 1990s and have been later complemented. Adaptive intimal thickening (AHA type I) and fatty streaks (AHA type II) are signs of non-progressive atherosclerosis. At least 30% of neonates have acentric intimal thickening. In fatty streaks, intimal macrophages have intra- and extracellular lipid deposits which are also called foam cells.[10] AHA types III–VI are classified as being signs of progressive atherosclerosis. Pathological intimal thickening (AHA type III), also referred to as intermediate lesions or atheromas, is the first type of progressive atherosclerotic plaques. Here, lipid pools rich in proteoglycans are located close to medial wall and are likely accumulated due to the loss of smooth muscle cells by apoptosis in the area. Also, microcalcification can be observed. Fibroatheromas (AHA type IV) are the first advanced lesions where an acellular necrotic core, accumulated cellular debris and cholesterol monohydrate, and lack of extracellular matrix are present. Fibroatheromas have distinctly formed fibrous cap between the lumen and the necrotic core and at this point the fibrous cap is quite thick and generally non-flow limiting.[12] When the fibrous cap becomes clearly identifiable and further thickens, there is a large number of apoptotic macrophages present. These macrophages harbour the contents of necrotic core and eventually the enlarged

necrotic core and thickened fibrous cap start to restrict the flow (AHA type V).[10,13] Thin-cap fibroatheroma (TCFA, AHA type VI) has a large necrotic core and a thin fibrous cap that is prone to rupture, hence it is called a vulnerable plaque. Fibrous caps of vulnerable plaques are infiltrated by numerous macrophages and T-cells.[10,12,14]

The main causes for fatal thrombosis by coronary plaques are plaque rupture, plaque erosion and eruptive nodular calcification. In plaque rupture the thrombus is in connection with the necrotic core and the fibrous cap is completely ruptured or partially fractured. If the thrombus is not connected with the necrotic core or deep intima, then the thrombus is a result of erosion and usually non-occlusive. Eruptive nodular calcification occurs when dense calcified bodies are spread out to the luminal space thus hardening the vessel wall. Due to mechanical stress towards nodular calcification, the fibrous cap of the atheroma disrupts. This results in thrombosis, which, however, is generally minor and non-occlusive.[12]

Intraplaque haemorrhage increases the size of the necrotic core. Red blood cells function as a source of free cholesterol which is then absorbed to the expanding necrotic core. Leaky *vasa vasorum* is the likely cause for intraplaque haemorrhage because it infiltrates the plaque when the lesion thickens.[15] Healed plaque rupture is identified by a break in the fibrous cap with overlaying visible repair process. The repair reaction involves smooth muscle cells that, depending on the healing phase, are surrounded by proteoglycans and/or collagen. Amount of healed plaque ruptures seems to correlate with the extent of narrowing of the lumen.[16,17]

Coronary calcification is a typical feature of advanced fibroatheroma. Calcification is mostly seen in healed plaque ruptures and as nodular calcification in fibrous plaques.[16,17] Calcification starts when smooth muscle cells of the plaque secrete blisters which contain calcium-binding proteins. This active and regulated process initiates the passive sedimentation of calcium salts.[18] Calcification increases with age and diabetics have greater calcification than non-diabetics.[19] Calcification in single plaques is usually considered to stabilize the plaque but extensive calcification is a sign of vast atherosclerosis, thus indicating increased risk for atherosclerotic complications in the future.[20] Four different types of calcifications are seen: speckled, focal nodular, multifocal, and diffuse. TCFAs usually contain speckled calcification which makes diagnosing with calcium-based imaging more difficult. In ruptures, multifocal or diffuse calcification is a common finding and rupture without any calcification is rare. Healed plaque ruptures mainly contain diffused calcification. Nodular calcification is the least common form of calcifications, and it is associated with tortuous arteries of the elderly.[21]

2.1.2 Factors contributing to atherosclerosis

Epidemiological studies since 1940s have tried to identify risk factors that are associated with cardiovascular mortality. Some well-established risk factors are modifiable, such as smoking, hypertension, diabetes, dyslipidaemia, obesity, and physical inactivity, while some are non-modifiable, like age, sex, and family history of premature CHD. Prevention of cardiac events highly relies on controlling the modifiable risk factors by lifestyle changes, pharmacological management or in most severe cases, cardiovascular surgery.[22–24]

Both active and passive (second-hand) cigarette smoking accelerates the progression of atherosclerosis. Smoking harms the endothelial cells of the arteries by weakening the ability of cells to produce nitrogen oxide and thus results in an active inflammatory state. Also, compounds in the smoke gasses oxidise LDL particles, which enhances the accumulation of monocytes which later differentiate to macrophages and together with LDL particles transforms into foam cells.[25] Smoking, however, is a reversible risk factor and there is a clear decline in the risk even after 6 months after smoking has been stopped.[26]

High BP, i.e., hypertension, affects the arterial intima by accelerating division of smooth muscle cells and by activating endothelial cells in the artery to become proinflammatory. The division of smooth muscle cells causes thickening of the intima and the proinflammatory endothelial cells initiates the cascade of monocyte gathering leading to the formation of foam cells. BP levels above 120 mmHg systolic and above 80 mmHg diastolic is considered as elevated. To increase early intervention of high BP, also classification of "prehypertension" has been suggested where 120–139 mmHg systolic and 80–89 mmHg diastolic BP mandates intervention. Treatment of hypertension with multidrug therapy reduces the risk of cardiovascular events.[27]

Dyslipidaemia, i.e., abnormalities in lipid levels, increases the risk of cardiovascular events. Increased circulating concentrations of total cholesterol (TC) and LDL cholesterol (LDL-C), low high-density lipoprotein cholesterol (HDL-C) and elevated triglyceride (TG) levels independently increase CHD mortality risk. Increase of TG concentration affects to other lipids and enhances proatherogenic properties of them. Statins (HMG-CoA reductase inhibitors) have been proven effective medication for dyslipidaemia by inhibiting cholesterol synthesis in the liver. Statins reduce LDL-C and TG and to some extent increase HDL-C concentration.[28,29]

There are growing numbers of individuals diagnosed with type 2 diabetes mellitus (T2D) and also substantial numbers of cases are undiagnosed. In T2D patients, the fasting blood glucose level is ≥126 mg/dL. Almost 40% of US adult population has prediabetes with fasting blood glucose level at 100–125 mg/dL while normal level is considered to be <100 mg/dL.[30] T2D increases atherosclerotic burden

by increasing TG concentration, decreasing HDL-C concentration, and creating smaller LDLs (small dense LDLs) which are more atherogenic. Also, hyperglycaemia accelerates atherogenesis by affecting macrovascular and microvascular circulation. Treatment and control of T2D decreases CHD mortality.[31]

The term metabolic syndrome is used when one individual has multiple metabolic factors that are not related to each other. Such factors can be increased waist circumference (abdominal obesity), increased plasma TG concentration, decreased plasma HDL-C concentration, elevated BP, and raised fasting glucose concentration in plasma. These metabolic factors independently can advance the progression of atherosclerosis and in combination as metabolic syndrome the proatherosclerotic effect is even more evident. Metabolic syndrome is progressive pathological state which significantly increases the risk of T2D and atherosclerotic changes in arteries. Lifestyle changes along with proper medication are most suited treatments for metabolic syndrome.[32]

Genetic factors confound the non-modifiable and independent risk factor of premature CHD. Genetic associations in CHD are widely studied but still largely unexplained. Gene mutations have been found that lead to familial hypercholesterolemia and hypertension but usually these are a result of interaction between environmental factors and multiple genes. Familial CHD is defined as premature if the onset age for father is <55 years and for mother <65 years.[33]

Other unmodifiable risk factors are sex and advancing age. Both men and women are at risk of developing CHD but in men the development occurs roughly 10 years earlier than in women. The differences are based on metabolic characteristics and lifestyle habits. The risk of CHD increases in women after menopause. Due to the progressive nature of atherosclerosis, it is only natural that decades-long changes in arteries start to have clinical impact when getting older. However, based on other risk factors, the risk between individuals of same age may vary considerably.[23]

Modifiable risk factor of CHD that might reduce progression of the disease is the increase of physical activity. Physical inactivity has an undesired effect on cholesterol, insulin resistance and BP. Moderate-intensity physical activity daily, vigorous-intensity physical activity 3 days a week and strength training activities 2 days a week are recommended.[34]

Currently several global risk calculators are available to assess the risk of developing CHD, such as Framingham Risk Score (FRS)[29], SCORE risk assessment model[35] and FINRISK-calculator[36]. The aim of the calculators and scores is to identify the individuals at greater risk of CHD and to monitor overall risk of individuals who already have CHD in treatment. Reducing risk factors at population level is achieved by modifying lifestyle habits towards healthier and/or with the effect of medication.[7]

2.1.3 Clinical presentation of CAD

Early-stage coronary atherosclerosis is usually clinically asymptomatic even though progression of the disease has already begun. First, arterial lumen is preserved by enlargement of the vessel wall area (positive remodelling) but when plaque starts to affect vessel lumen (negative remodelling) atherosclerosis becomes clinically visible.

The primary clinical symptom of chronic obstructive CAD is chest pain called angina pectoris (AP). AP evolves when plaque formation manifests as symptoms of ischemia. Myocardial ischemia is defined as lack of oxygen supply to certain regions of the myocardium. In myocardial ischemia the coronary flow reserve is reduced and generally at least 50% diameter stenosis is observed. Thereby the myocardium has increased metabolic demand of oxygen but is not receiving sufficient supply of it. Symptoms of typical AP are pressure on the chest (i), the pain/discomfort begins or becomes worse during exercise (ii) and relieves with rest or nitroglycerine medication (iii). Additionally, the pain may radiate to left arm, neck, or jaw, be present after eating, is repeatable and includes shortness of breath. If all of the criteria i–iii are not fulfilled, the AP is classified as atypical and if only one or none of the criteria are met, the symptoms are considered as non-anginal origin.[37]

Atherothrombosis is present on the surface of an unstable, eroded or ruptured atherosclerotic plaque where platelet rich thrombus has been formed. This is an acute condition which needs to be identified and treated quickly after the onset of symptoms. Acute coronary atherothrombosis presents as acute coronary syndrome (ACS).[38] The acute form of atherothrombosis begins with a rupture of a TCFA. This is usually the cause of sudden death due to acute myocardial infarction (MI) and is most frequently found in proximal arteries and with non-obstructive diameter stenosis (<50%), i.e., ruptured plaque does not narrow the lumen (as in positive remodelling).[39]

Formation of platelet-rich thrombus due to plaque rupture and erosion leads to ACS, either ST segment elevation MI (STEMI), non-ST segment elevation MI (NSTEMI) or unstable angina pectoris (UAP). Acute coronary atherothrombosis is associated with ischemia and anginal pain at rest. STEMI is typically associated with a total occlusion of a coronary artery and biomarkers of cardiac injury or necrosis are elevated, most commonly cardiac troponins (cTns) are used. In NSTEMI there is not diagnostically detectable elevation of ST segment in electrocardiogram (ECG), but cTns are abnormal or above reference range which indicates ischemia. In UAP, symptoms, such as chest pain, might be similar, but biomarker levels are undetectable or remain within reference range.[40] Percutaneous coronary intervention (PCI) or anti-thrombotic and anti-platelet medications targeting the acute atherothrombotic process are used to treat ACS.[41,42]

2.2 Imaging methods for CAD

2.2.1 Stress echocardiography

Echocardiography utilizes ultrasound which resonates at over 20 000 Hz frequency. The echocardiographic picture forms when applied ultrasound reflects as it encounters interfaces of two acoustically different tissues. The greater the difference in tissues, the greater echo is reflected. As ultrasound proceeds in tissue, it weakens, and the frequency of the ultrasound determines how well it penetrates tissue and how well resolution is achieved in the picture. Ultrasound of smaller frequency penetrates further into tissue, but the resolution is coarse and with higher resolution the picture resolution is more precise but only at close distance. In echocardiography, ultrasound is sent and received in turns which defines the pulse repletion frequency, i.e., how many pictures are formed per second. When imaging the heart, the number of pictures per second need to be high in order to have real time structural motion captured. When applying an array of ultrasound waves, it is possible to create 2-dimensional grey-scale pictures and even 3-dimensional pictures.[43]

The 2-dimensional grey-scale picture is the foundation for echocardiographic pictures. Depending on the amplitude of the echo, brighter and darker areas are formed. Higher amplitude of the echo is portrayed brighter in the picture. The resolution of the picture can be enhanced by strengthening weaker echoes and post-processing of the image.[43]

In stress echocardiography, the 2-dimensional echocardiography is combined with stress induced by physical or pharmacological manner.[44] The main reason for performing stress echocardiography is to detect myocardial ischemia in patients with suspected or known CAD. Changes in the wall motion are accurate measures for detecting and localizing underlying CAD.[45] Stress is most commonly induced by exercise, dobutamine or dipyridamole. In case patient is not eligible for exercise, drugs are used to obtain stress. Drugs are also preferred because physical activity can make the sonographic examination more difficult e.g., due to hyperventilation or excessive chest wall movement.[46] Dobutamine increases the oxygen demand of myocardium[47] while dipyridamole is a vasodilator which reduces the subendocardial flow supply[48].

Principally, there are four types of responses to stress which can be seen with stress echocardiography. The myocardium can be classified as normal, ischemic, ischemic viable or necrotic. The accuracy of stress echocardiography is affected by e.g., obesity and lung disease and quality can be improved by utilizing harmonic imaging and ultrasound contrast agents such as dissolvent gas bubbles.[44]

Stress induced with either exercise, dobutamine or dipyridamole results in comparable diagnostic accuracies in detecting CAD[49] In a meta-analysis by Knuuti et al., the sensitivity and the specificity of stress echocardiography detecting anatomically significant CAD was 85% and 82%, respectively.[50] When applying pre-test probability of significant CAD (as guided by ESC[6]) to the calculations of positive and negative likelihood ratios[51] the stress echocardiography has post-test probability of ruling-in and ruling-out anatomically significant CAD if pre-test probability is ≤48% and ≥56%, respectively.[50]

The wall abnormalities (presence or absence) diagnosed with stress echocardiography also provide prognostic information. The induced stress by either exercise, dobutamine or dipyridamole is widely studied and results in similar prognoses independent of the method used.[49] In a study of 9 000 patients, the annual risk of detecting myocardial ischemia for patients with normal stress echocardiography was 0.4–0.9%, indicating good prognosis.[52] For a positive stress echocardiography test, combination with clinical parameters (diabetes, renal dysfunction or received therapy) and more detailed analysis of the echo can divide patients in intermediate (1–3% annual risk for hard coronary events, i.e., MI or death) and high-risk classes (>10%). A negative stress echocardiography can divide patients as having low (1–3%) or very low (<0.5%) annual risk of hard coronary events. Nevertheless, stress echocardiography is not recommended as the first-line imaging method for patients with suspected or known CAD, but for patients with inconclusive stress ECG test.[49]

2.2.2 Invasive coronary angiography

Invasive coronary angiography (ICA) has been the most widely and longest used method in detecting coronary stenosis in patients with suspected chronic CAD, UAP, NSTEMI or STEMI. ICA is performed by catheterization and is an invasive procedure.[42,53,54] Femoral artery is commonly used to enable arterial access, but radial artery is increasingly used as a safer option. Coronary catheter is placed in the ascending aorta and after removing the access sheath, imaging is performed fluoroscopically.[54,55] Iodinated contrast agent is injected selectively to left or right coronary artery systems. Patient is imaged from multiple angles to achieve best possible view of the arteries.[54] ICA can be converted from diagnostic procedure into therapeutic one. ICA is the only imaging method where is an option to simultaneously perform revascularization procedure. Despite the risks of complications during ICA, it remains as the reference standard for the diagnosis of CAD.[54]

With ICA the main diagnostic goal is to estimate the presence and degree of stenosis (**Figure 1**). Commonly, this is done with visual examination by the

operative professional. Visual estimation has proven to be very reliable method (79–93% agreement with autopsy studies) even though under-estimation of the stenosis degree is possible. Also, overestimation can happen e.g. because of overlapping vessels. Errors in the estimates of the stenosis degree may be caused due to subjective view of the operator that increase the intra- and inter-operator variation. ICA provide any information on the functional aspects caused by coronary stenosis.[56] Accuracy in determining luminal narrowing is highly improved with quantitative coronary angiography where computer software-assisted analysis decreases inter-operator variation.[57]

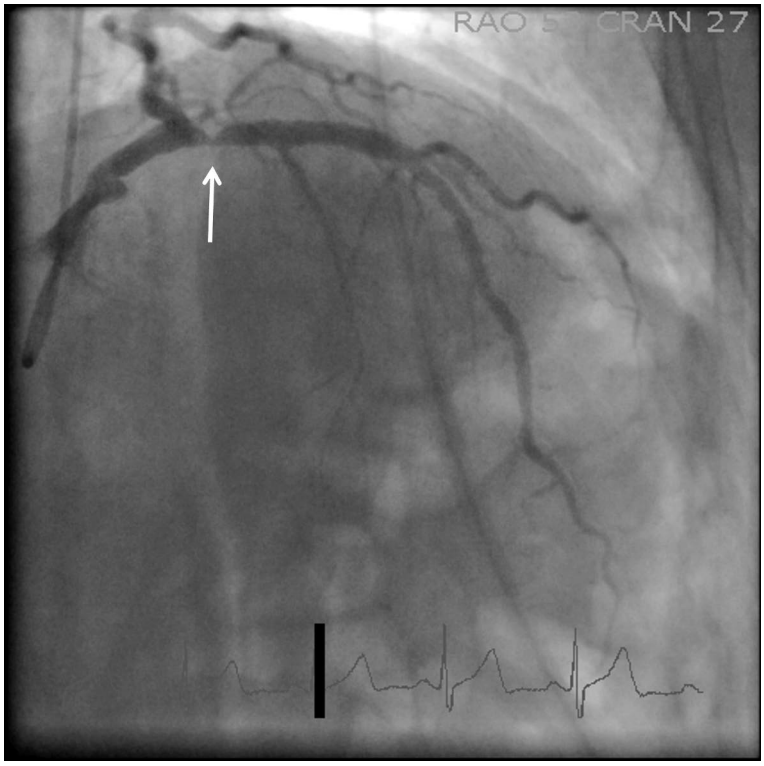

Figure 1 Severe stenosis observed with invasive coronary angiography in the proximal left anterior descending artery.

Thrombus and acute plaque rupture are visible with ICA. These can be observed as reduction in distal flow or as defect in intraluminal filling. ICA is routinely used during PCI and before coronary artery bypass graft surgery (CABG). Even before injecting contrast agent, coronary calcification and existing stent appear as dark area within opaque material in ICA. Stent can be differentiated from calcification due to structured form.[58]

ICA can guide clinicians to suitable therapy for a patient. Decision of revascularization by PCI or CABG can be made with information obtained during ICA. Risk for adverse cardiac events is higher if stenosis is observed in proximal segments of the arterial tree or there are multiple atherosclerotic segments. Obstructive CAD is usually defined as >50% stenosis in left main (LM) coronary artery or >70% stenosis in another major epicardial artery.[58] Based on ICA, several scores are available to calculate the risk of poorer cardiovascular outcome and guide in the selection of therapy. Commonly, these utilize the proximity, severity, and extent of coronary artery stenoses. The Duke Prognostic Score[59] and the Syntax Score[58] assess this risk with information obtained by ICA.

2.2.3 Intravascular imaging

Intravascular ultrasound (IVUS) is an imaging technique, which enables visualization of the vessel wall and characteristics of a plaque. Imaging is possible with high frequency ultrasound, and it provides cross-sectional images of the coronary arteries with 150–200 μm resolution. IVUS uses catheter where at the tip is a small transducer and the catheter is able to reach even distal segments in the coronary artery tree. To acquire the image, motorized catheter pullback of 0.5 mm/s is used.[60]

With IVUS all the layers of arterial wall can be differentiated: intima as a bright layer, media as a dark stripe, and adventitia as multiple bright echoes. Narrowing of the lumen due to atherosclerosis is also detectable with IVUS and calcified plaques are shown as echo-bright with acoustic shadowing behind the calcified area .[60]

With IVUS, the percent plaque burden and the lumen area stenosis can be calculated by measuring cross-sectional area (CSA) of the lumen and external elastic membrane CSA. Plaque burden is determined as a ratio of atheroma CSA and external elastic membrane CSA. Stenotic area can be calculated by subtracting minimum lumen CSA from reference CSA and dividing this with reference lumen CSA.[61] Minimal lumen area (MLA) in the normal reference population has been determined to be 7.5 mm^2. MLA >7.5 mm^2, however, does not seem to significantly predict poorer outcome in patients.[62] Determination of intermediate coronary lesions can be difficult to assess with IVUS, especially in the LM. When IVUS is compared to parameters evaluating hemodynamic influences of stenosis, such as myocardial perfusion and fractional flow reserve, it correlates only moderately.[63] The sensitivity and specificity of IVUS have been improved by stringent classification of MLA and stenosis percentage.[64]

IVUS can be used for guidance when performing PCI. Additionally, IVUS can aid in finding the optimal position for the stent, thus avoiding complications.[65] Future cardiac events could be determined by assessing plaque progression with IVUS, but

it needs further validation since the utility has been demonstrated only in small studies.[66,67] Plaque composition can be assessed with IVUS as well. Non-calcified, fibrotic, partially calcified, and calcified plaques are visible with grey-scale IVUS. Due to strong acoustic signals with shadowing, separation between types in overlapping plaques might be difficult. Radiofrequency IVUS can improve the differentiation of plaque types by producing a colour map of the plaque where dense calcium is presented as white, necrotic core as red, fibrofatty tissue as light green and fibrous tissue as dark green. This way TCFA, thick-cap fibroatheromas, pathologic intimal thickening, fibrotic plaque, and fibrocalcific plaque can be differentiated.[68,69] In PROSPECT-study, lesion characteristics detected with radiofrequency IVUS were associated with adverse cardiovascular events. Still, finding of TCFA showed low specificity.[70]

Optical coherence tomography (OCT) is a method with substantially higher resolution than in IVUS (4–20 μm). Instead of ultrasound, the OCT uses near-infrared light where adjacent biological tissues reflect the light and produce cross-sectional two-dimensional image. With OCT, the imaging of vulnerable plaque is possible. OCT accurately can detect thin fibrous cap, lipid pools and increased macrophage infiltration. OCT is mainly used to guide PCI and may improve the prognosis compared to ICA alone.[71,72]

Near-infrared spectroscopy utilizes emitting light from organic molecules and measures a proportion of light that is returned. With near-infrared spectroscopy, the chemical composition of plaque can be determined, and it is displayed as a probability of a lipid core. Visually, yellow colour indicates lipid rich or lipid core in plaque while red colour means zero probability of a lipid core. Method correlates well with histology and has been investigated for imaging vulnerable plaques.[73,74]

2.2.4 Cardiovascular magnetic resonance

Magnetic resonance imaging (MRI) is a non-invasive imaging method where ionizing radiation is not required. With MRI it is possible to obtain 3-dimensional images of high quality. Cardiac magnetic resonance (CMR) should be performed with ECG synchronization in order to increase resolution and to minimize motion artifact. However, MRI should not be performed on patients with internal metal objects like pacemaker or aneurysm clip. Also, nephrogenic systemic fibrosis may develop due to contrast enhanced MRI scans.[75]

CMR angiography can be performed as T1 or T2 weighted. T1 weighting is applicable when accurate evaluation of myocardial structure is required. In such images blood appears dark and cardiac tissues bright.[76] In T2 weighting, blood is visible as bright areas while cardiac structures are relatively darker.[77] This is especially useful when imaging stenosis and plaques with lipid deposition which

appear as dark. T2 weighting is typically utilized in CMR angiography.[77] In contrast enhanced CMR, gadolinium-based contrast materials are used. With contrast enhanced CMR, myocardial perfusion can be imaged along with MI and fibrosis depending on the timing of the contrast agent injection.[76]

CMR angiography is sensitive tool in determining ≥50% stenosis, but compared to conventional ICA, native vessel CMR angiography might produce false positive results due to difficulties in interpreting the coronary segments. Recently, specificity of CMR angiography detecting ≥50% stenosis has improved but is still behind accuracy of computed tomography angiography (CTA).[77,78] Nonetheless, CMR imaging has shown to detect large, calcified lesions and is sensitive enough in assessing CABG patency.[79] Yet, CMRA is not recommended routinely for the detection of CAD.[77]

CMR imaging of myocardial perfusion can be performed during pharmacological stress test with adenosine or dipyramidole. Perfusion is evaluated through wall motion abnormalities and distorting myocardial contraction. Defect in perfusion indicates reduction in blood flow. Using intravenous contrast agent during CMR stress test improves the diagnostic accuracy of the method and even enable quantification of subendocardial infarctions and ischemia.[80,81] Sensitivity and specificity of CMR detecting anatomically significant CAD based on meta-analysis is 90% and 80%, respectively, and detecting functionally significant CAD, 89% and 87%, respectively. Thus, CMR is better at ruling-in diagnoses of either anatomically or functionally significant CAD.[50]

Since non-obstructive lesions are the most common place of cardiovascular events, MRI has also been used to identify vulnerable plaques in large arteries. It can be used to characterize the thickness of the vessel wall, atheroma volume in atherosclerotic lesions and plaque composition (e.g., lipid-rich necrotic core). This is possible due to suitable contrast agents or molecular imaging agents such as ferromagnetic particles[82] and gadolinium-based peptides[83]. Imaging of coronary arteries is challenging due to small size and continuous motion during cardiac cycle.[84,85] Some studies have shown that imaging e.g., thoracic aorta or carotid artery can perform plaque assessment with close correlation to histologic specimens.[84,86] Non-coronary plaques can also be serially imaged with MRI, meaning that it is possible to follow remodelling and plaque progression in relation to treatment.[87–89]

2.2.5 Coronary calcium imaging

Noncontrast cardiac computed tomography (CT) is a useful method to detect and quantify calcified atherosclerosis. Imaging can be performed with electron beam CT or multidetector CT. In electron beam CT, rotating x-rays from electron gun are subjected around the patient and high temporal resolution is achieved. Currently,

multidetector scanners are preferred and noncontrast CT can be performed before contrast CTA to quantify calcium (**Figure 2**). Noncontrast multidetector CT should be performed in late diastole to acquire best possible quality of the image.[90]

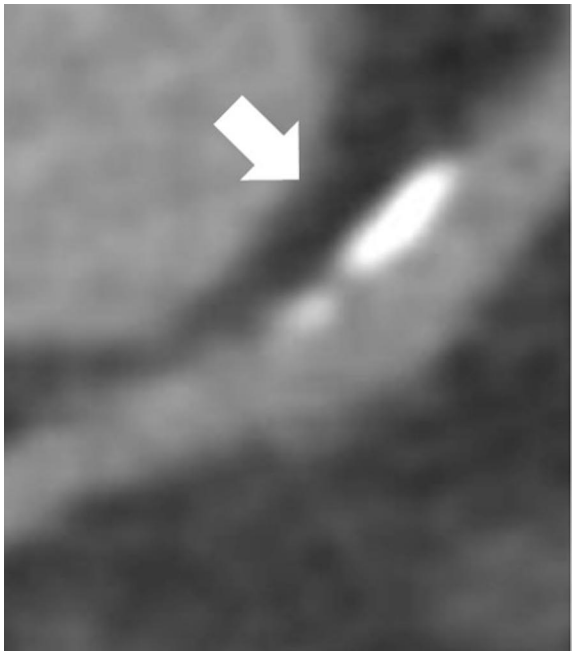

Figure 2 Noncontrast computed tomography detecting calcification. Calcification appears as white in the noncontrast CT image.

Agatston method is used to quantify coronary calcium, which assesses the area and density of the calcification. Attenuation value >130 Hounsfield unit (HU) is classified as calcified lesion. The calcium score is calculated based upon the attenuation values. In each segment of the coronary tree, the calcified area is calculated and multiplied with a density weighting factor. The total calcium score is the summation of all the segmental calcium scores. Usually, the total calcium score is used in the risk assessment. One unit of calcium score indicates of calcium score 1 is that at least 3 closely located voxels (3-dimensional pixels) in the image exceed the HU threshold of 130. Calcium score of 0 indicates that there is no detectable coronary calcium.[90]

There is strong evidence of the relationship between coronary artery calcium (CAC) and cardiovascular outcomes. Therefore, screening of CAC may be considered in patients with intermediate risk of coronary events by clinical risk factors, such as FRS.[91] Also, Multi-Ethnic Study of Atherosclerosis tool could be utilized in the evaluation of CAC by determining the relative risk [CAC score above

the 75th percentile for age, sex, and ethnicity] or absolute risk (CAC score above 300).[92] With noncontrast CT two types of calcifications can be observed, small spotty foci of calcium and large area of calcium, and these have different influence on the risk even though CAC score could be the same. Spotty calcification is associated with greater risk. Additionally, distribution of calcification plays a role in the risk assessment. Observed LM or 3-vessel [LM, left anterior descending (LAD) and right coronary artery] CAC is more severe than 1- or 2-vessel CAC and thus prognostically more important.[91,93,94] Calcium scanning with noncontrast CT is a non-invasive method and based on the acquired information, could inform about the need for lifestyle intervention or medical therapy.[95,96]

2.2.6 Coronary computed tomography angiography

In recent years coronary CTA has emerged as one of the leading modalities in assessing coronary arteries. With coronary CTA it is possible to acquire a high-resolution image of coronary arteries, cardiac structures, aorta, and other large vessels while using modest radiation exposure to patient. Also, plaque features such as size, remodelling of the vessels, lipid deposition and degree and pattern of plaque calcification, can be characterized with coronary CTA. Especially, coronary CTA can be used to rule-out obstructive CAD with high diagnostic accuracy.[97–99]

In CT the gantry rotating around the patient includes both the x-ray source and the detector. When x-ray enters the body, the travelling of the x-ray photons depends on the tissue density. The detector records the photons that pass through the target (tissue) rather than those absorbed by the tissue, meaning the interaction between photon and tissue's atoms, do not reach the detector at all. CT image is a graphical description of this attenuation of x-rays in the body. Attenuation of photons is described with attenuation coefficient (μ). The more photons are detected, the lower the μ is. Also, μ reflects the tissue density. The μ is higher with higher tissue density. However, μ is not constant in tissue, it also depends on the tissue thickness and energy of the x-ray photon. By adjusting the energy of the x-ray photon, the image noise, radiation dose and tissue contrast can be controlled.[100]

The scintillation detector measures and records the x-ray photons and transforms it into light. Then the light is converted to electrical signal by the photodiode and finally to digital signal by the computer. The needed data acquisition system is located between the detector and computer. The data acquisition system transforms the measured radiation beams into binary data, which is further sent to computer for processing. To generate the image, multiple complicated mathematical calculations are needed and thus, reconstruction algorithms are used for the raw electrical signal to get complete computerized CT image. The brightness of the image can be calculated with formula where tissue μ is compared to water μ. In the HU scale of

CT number, the value of water is set as 0 and therefore, the calculated value of particular tissue is a number relative to density of water. Air has a CT number of -1 1000, while bone has a value of +1 000. There are indicated CT numbers for atheroma, fat, fibrous tissue, calcium, thrombus, blood, etc. which are used when interpreting coronary CT images.[100]

Due to relatively small size and constant moving, multidetector-row CT is the desired choice when imaging coronary arteries. In multidetector-row CT instead of a single detector in one dimensional arrangement, there are multiple detectors, where individual detectors in each row are further divided into multiple detector elements and two-dimensional array is formed. When increasing the detector number, fewer gantry rotations are needed to acquire the complete CT image. Currently, multidetector-row CT devices use 64, 128, 256 or even 320 detector rows and CT image of coronary arteries can be achieved with just one gantry rotation where scan length is shorter and thus the radiation exposure to the patient lower.[101].

To decrease motion artifact, ECG-gating is used. Highest image quality is acquired when the heart rate is ≤60 beats/min and imaged during middle to late diastole phase. Heart rate can be slowed down with oral or intravenous beta blockers. Also, to enhance the dilation of arteries, a sublingual nitroglycerin can be administrated before imaging. The vasodilation improves the image quality. Additionally, coronary CTA requires intravenous administration of iodinated contrast agent. To image coronary arteries, they need to be filled with contrast agent as much as possible so amount of 50–110 mL is used with infusion rate 4–6 mL/s.[98,102] Much can be done to decrease the radiation exposure without major effect to image quality. Currently, combination of various methods reducing radiation exposure is preferred and radiation dose during coronary CTA imaging can be <4 mSv.[103]

For coronary CTA imaging there are multiple guidelines available on its performance[102], reporting and interpretation of results[104], and radiation exposure minimalization[103]. Likewise, the key to successful coronary CTA imaging is the proper patient selection and guiding criteria for this are available.[105] Additionally, training requirements throughout medical disciplines is crucial and thus advised.[106]

With coronary CTA, non-calcified, partially calcified and calcified atherosclerotic plaques are visible. Also, stages of atherosclerosis are identifiable due these three types of plaques visualized in coronary CTA.[107] An example of CTA image is shown in **Figure 3**. Multiple studies have compared coronary CTA with ICA for the detection of obstructive CAD.[108,109] In detecting significant stenosis (≥50% of lumen diameter), the sensitivity and specificity with coronary CTA was on average 98% and 88%, respectively, resulting in negative predictive value of over 95%.[110] Hence, coronary CTA is widely used as the preferable non-invasive method in excluding obstructive CAD.[105]

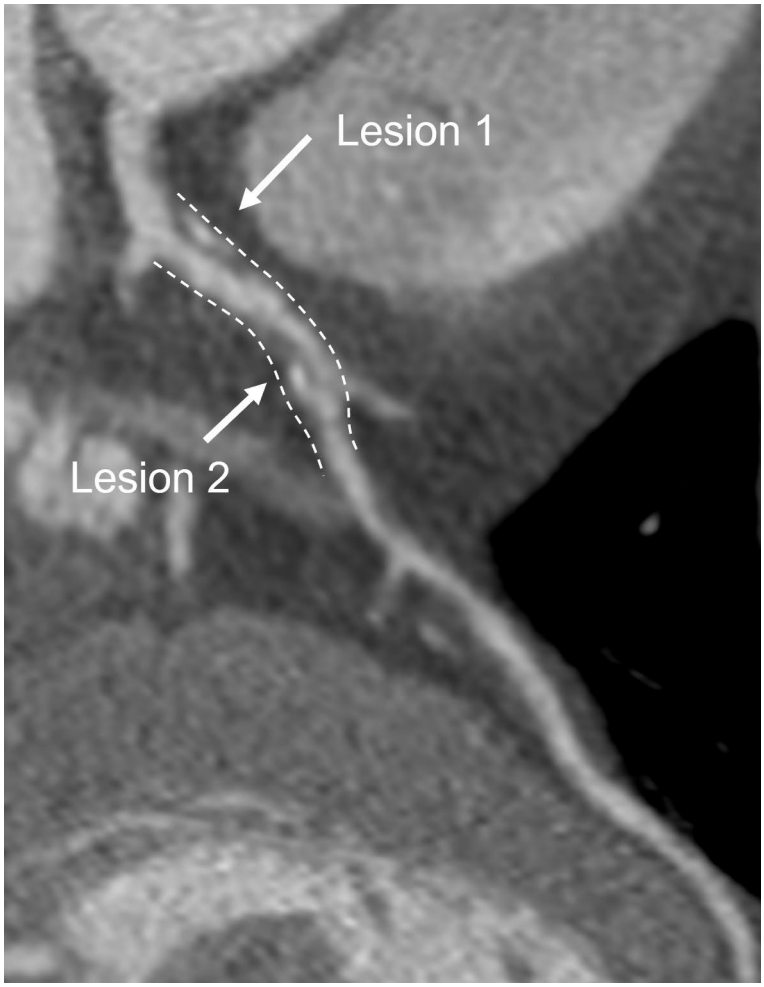

Figure 3 Coronary computed tomography angiography image of proximal left anterior descending artery. In lesion 1 mild stenosis (25–49%) is observed. In lesion 2 there is moderate stenosis (50–69%) with positive remodelling.

Coronary CTA uses semi-quantitative scale in defining lumen stenosis:[104]

1. Normal arteries do not have any plaques or stenosis visible.
2. Plaques causing <25% lumen diameter stenosis considered as minimal.
3. Plaques causing 25%–49% lumen diameter stenosis considered as mild.
4. Plaques causing 50%–69% lumen diameter stenosis considered as moderate.
5. Plaques causing 70%–99% lumen diameter stenosis considered as severe.
6. Total occlusion causes 100% lumen diameter stenosis.

According to guidelines, lumen diameter stenosis should be evaluated throughout the coronary tree. The coronary tree has been divided into standard segments, such as the 18-segment coronary tree shown in **Figure 4**.[104]

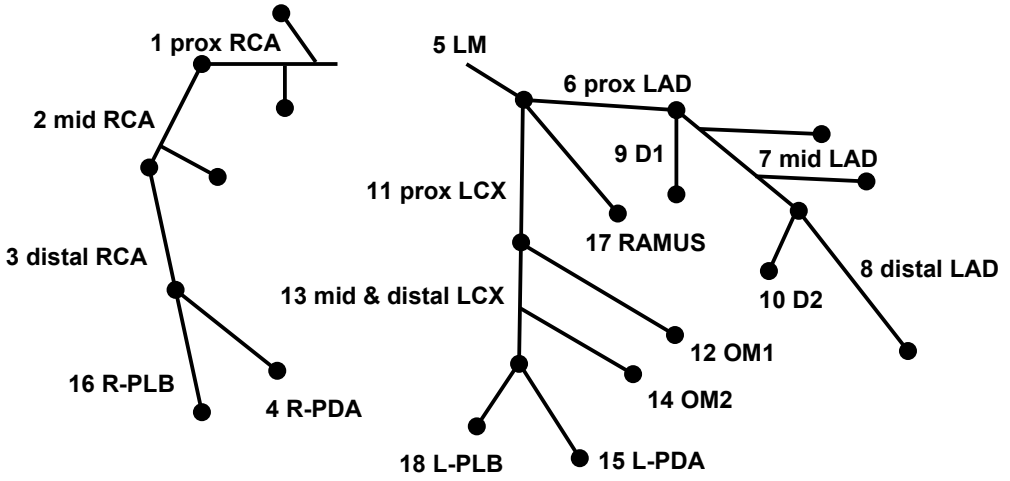

Figure 4 Segmentation of coronary tree. 1 = proximal right coronary artery (RCA), 2 = mid RCA, 3 = distal RCA, 4 = right posterior descending artery (R-PDA), 5 = left main (LM) atery, 6 = proximal left anterior descending (LAD) artery, 7 = mid LAD, 8 = distal LAD, 9 = first diagonal branch (D1), 10 = second diagonal branch (D2), 11 = proximal left circumflex (LCX) artery, 12 = first obtuse marginal (OM1) artery, 13 = mid and distal LCX, 14 = second obtuse marginal (OM2) artery, 15 = left PDA (L-PDA), 16 = right posterior-lateral branch (R-PLB), 17 = Ramus intermedus artery, 18 = left PLB (L-PLB). Adapted from Uusitalo *et al.*[116]

The reproducibility of atherosclerotic plaque characterization by coronary CTA is highly dependent on the observer. Detection of calcified and non-calcified components is quite similar across observers, but measurement of total and non-calcified plaque volumes can vary.[111] Better reproducibility is obtained in non-calcified lesions and in LAD artery. The reproducibility is further enhanced with the use of standardized and automated softwares.[112]

Coronary CTA is effective prognostic tool in determining stenosis and plaque characteristics. Based on these, increased rate of adverse cardiovascular events can be predicted. A meta-analysis concluded that patients with obstructive coronary CTA (lumen stenosis ≥50%) had significantly higher annual risks of major adverse coronary event (MACE) and death, 8.8% and 2.2%, respectively, than non-obstructive (1.4% and 0.7%, respectively) or normal coronary CTA patients (0.17% and 0.15%, respectively).[113] Therefore, coronary CTA can function as an independent predictor[114] but also as additive to CAC score and other clinical predictors[115]. Different types of scores can be also calculated which indicate the future risk. For example, CTA risk score by Uusitalo *et al.* takes into account the

plaque burden, severity, location and the composition of plaque and is superior in predicting cardiovascular events in suspected CAD patients.[116] Coronary CTA is not recommended for screening of asymptomatic patients due to the exposure to ionizing radiation.[105]

2.2.7 Radionuclide myocardial perfusion imaging

Single photon emission compute tomography (SPECT) and positron emission tomography (PET) are used in myocardial perfusion imaging (MPI). In MPI, target is to study differences in blood flow before and after exercise- or drug-induced stress. Flow-limiting epicardial CAD detected as perfusion defect in MPI has both diagnostic and prognostic utility. Quantitation of myocardial blood flow (MBF) in absolute terms is possible with PET-MPI, while evaluation of defects in relative distribution of perfusion is done with SPECT-MPI.

SPECT-MPI

In SPECT-MPI distribution of radiotracer in the myocardium is evaluated in multiple slices of the heart, which are reformatted from 3-dimensional data set of 180° planar projection images.[117] Most common radiotracers used in SPECT-MPI are thallium-201 (^{201}Tl) and technetium-based ^{99m}Tc sestamibi and ^{99m}Tc tetrofosmin.[118] The ^{99m}Tc radioisotopes are preferred over ^{201}Tl because of higher energy level, resulting in better specificity, and lower tissue attenuation and scatter, resulting in lesser radiation exposure and higher image resolution. ECG-gated image acquisition is also possible with ^{99m}Tc.[117,119] Yet, linear response of tracer uptake with increasing MBF is not achieved.[118] Stress-inducing is performed either by exercise or pharmacologically with vasodilator, such as dipyridamole, adenosin or regadenoson. In case of severe asthma or obstructive pulmonary disease, dobutamine can be used.[120]

In SPECT-MPI, ischemic areas are identified as having reduced tracer uptake during stress. Gated images can be used in quantifying regional function and evaluating left ventricular ejection fraction (LVEF) and volume. Reduced tracer uptake in SPECT corresponds closely to lumen diameter stenosis of at least 50%–70%. The radiation exposure is comparable to ICA, 7–9 mSv. As with coronary CTA, there are attempts to reduce the radiation exposure. In SPECT these include imaging only during the stress, using wide-beam reconstruction and resolution recovery. Cadmium zinc telluride and cesium iodide crystals have better detector efficiency which enables faster SPECT acquisition.[121]

In a meta-analysis of 79 SPECT-MPI studies, the sensitivity and specificity in diagnosing obstructive stenosis (>50%) was 86% and 74%, respectively.[122] In

multivessel-disease there is a possibility of false negative diagnosis, since SPECT is based on assessment of relative perfusion differences and balanced ischemia can remain unnoticed.[123,124] Assessment of myocardial viability can be performed with ^{201}Tl based on intact cell membrane and preserved Na-K ATPase activity. First baseline imaging is performed, and viability imaging is done 18–24 hours from baseline. Remaining uptake of radiotracer is visible in viable areas with initially reduced perfusion.[125]

SPECT-MPI also has prognostic capabilities. Normal perfusion is indication of good outcome since only less than 1% of individuals will suffer from MI or cardiovascular death within a year, which is in the level of general population. On the other hand, annual event rate was 5.9% in patients with moderately or severely abnormal perfusion.[126] Similarly, in another study annual incidence rate was 1.2% in low-risk SPECT scans and 8.3% in abnormal scans.[127] Diabetics with abnormal perfusion have shown high prevalence of LM disease, 3-vessel disease or 2-vessel CAD including LAD.[128] General event risk is 7% annually, which can vary depending on the severity of perfusion defects.[122,126] Also, patients with reduced ejection fraction (EF) of 30%–39% had a yearly event rate of 7.6% while with EF of ≥50% it was 1.8%. In the same study, patients with EF<40% and severe ischemia, the annual cardiac event rate was 20% while patients with EF ≥40% had event rate of 8% with-in 2-year follow-up period.[129] Clinically stable patients with normal SPECT-MPI have 5-year warranty period on developing CAD which is, however, influenced by patient age, sex, diabetes status, and renal function.[130]

PET-MPI and hybrid PET-CT imaging

Inflammatory activity is typical for vulnerable plaques, and the presence of inflammatory cells can be imaged with PET. When combining metabolic PET images with anatomically accurate CT images, it is possible to identify high-risk lesions. Imaging of inflammation by PET is mainly based on uptake of glucose analogue ^{18}FDG (fluorine-18 labelled deoxyglucose) in macrophages. The half-life of ^{18}FDG is 110 minutes.

In PET imaging, distribution of a radiotracer within a body is imaged as a static image or series of images over time. Emission of positron (radiotracer) occurs when the radiotracer is in close proximity to tissue's atoms (electrons). Annihilation takes place and both ions disappear and transform into energy as gamma rays (photons). PET scanner detects these gamma rays travelling to opposite directions and determines where the photons originated through detectors that surround the patient in the process called co-incidence detection. The produced image shows the location in body where annihilation occurred.[131]

The tracer has to be a compound which metabolism and/or distribution in the body is known. Myocardial perfusion can be imaged with ^{13}N-ammonia, ^{82}Rubidium (^{82}Rb), ^{15}O-water and most recently with ^{18}F-flurpiridaz. Metabolism can be imaged with physiological substrates such as ^{18}FDG, ^{11}C-acetate, or ^{11}C-palmitate. The positron emitting radionuclides are produced by cyclotron (^{18}FDG, ^{13}N-ammonia and ^{15}O-water) or a strontium-82 (^{82}Sr) generator (^{82}Rb). Either reduced myocardial tracer uptake or reduced myocardial blood flow during stress indicates ischemia in PET-MPI. Absolute MBF can be measured with ^{13}N-ammonia, and it has a half-life of 10 minutes.[131] The 110-minute half-life of ^{18}F-fluripidaz enables both exercise and pharmacological stress imaging.[132] The half-life of ^{82}Rb is 76 seconds but accurate quantification of MBF is possible.[133] The ^{15}O-water has ideal kinetics for measuring quantitative myocardial blood flow and it has a half-life of around two minutes.[131]

When combined with CT imaging, the CT scan is performed first, and it is followed by PET-MPI. Physically scanners are located in the same machine, but scans cannot be performed simultaneously. This combination of the two methods is called hybrid PET-CT imaging. Because of the prior CT imaging of the target area, the PET signal can be evaluated together with detailed anatomy. Typically, attenuation correction is also based on CT.[134]

The PET-MPI enables the detection of location, severity, and extent of myocardial perfusion abnormalities. Distal coronary microcirculation assessment is also possible due to the capability of PET-MPI to measure MBF in absolute units.[135] MBF determined with PET-MPI can be visualized with polar map, where the colour represents the amount of MBF (**Figure 5**). The measurement of MBF opens the possibility for clinician to guide therapy, evaluate risk factors and monitor progression before advanced CAD.[136]

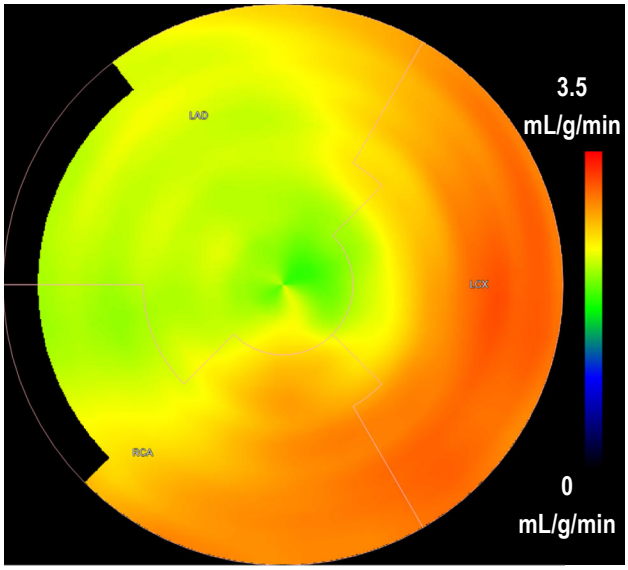

Figure 5 Polar map of positron emission tomography (PET) myocardial perfusion imaging. The scan was performed under adenosine stress and PET performed with ^{15}O-water. Reduced myocardial blood flow (MBF) was observed in the left anterior descending (LAD) artery, where the MBF was 1.9–2.1 mL/g/min. MBF in the left circumflex (LCX) artery was 2.7 mL/g/min and in the right coronary artery (RCA) 2.6 mL/g/min.

In diagnosing obstructive CAD (≥50% stenosis), PET-MPI had sensitivity of 92% and specificity of 85%, which are both better than with SPECT-MPI.[137,138] Similar to SPECT-MPI, the annual event rate is significantly increased in patients with abnormal PET-MPI results.[139] PET-MPI is also eligible tool for the detection of viability based on glucose metabolism in viable myocardium assessed by ^{18}FDG.[140] Even though PET-MPI is more expensive and not as easily available than SPECT, it has lower radiation exposure and better diagnostic performance.[138] Because of the high diagnostic accuracy and advances in the technology, such as enhanced temporal and spatial resolution, tracers with high myocardial extraction and automated attenuation correction, PET imaging as a technology, especially when combined to hybrid PET-CT imaging, is the future of CAD evaluation.[141]

2.3 Clinical risk scores for CAD

2.3.1 Framingham risk score

The FRSs are based on Framingham Heart Study which was started in the town of Framingham, Massachusetts, in 1948 and initiated by the National Heart Institute (currently the National Heart, Lung, and Blood Institute, NHLBI). The original purpose

of the study was to study individuals who had not yet developed any symptoms of cardiovascular disease or had MI or cerebrovascular attack in order to find common factors that advance the development of cardiovascular diseases. The Original Cohort (Gen1) consisted of 5 209 men and women, and they were followed until 2014. In 1971 started the second cohort, the Offspring Cohort, (Gen2) which consisted of the offspring and their spouses of the original cohort (5 124 individuals). Follow-up of Gen2 cohort is still on-going. The collection of the Generation 3 Cohort (Gen 3) started in 2002 and these participants are the offspring of Gen2 cohort (4 095 individuals). The follow-up of Gen3 cohorts remains active as well.[142] Additionally, in 1994 a new cohort was formed to reflect community diversity in Framingham and the surrounding towns. This Omni Cohort 1 included 506 men and women of African American, Hispanic, Asian, Indian, Pacific Islanders and Native American origins. In 2003 the offspring of Omni Cohort 1 were enrolled in the study as Omni Cohort 2 (410 individuals).[143]

The Framingham Heart Study populations have enabled the discovery of multiple risk factors of various cardiovascular diseases. First, risk factors for developing CHD were determined. These risk factors were identified in a study, which consisted of the Original Cohort (Gen1). In total 838 men and 227 women developed CHD during the follow-up period. Based on Gen1 12-year follow-up data, a sex-based algorithm was established where the 10-year risk of CHD can be evaluated.[29] In the study BP, TC, LDL-C, HDL-C, age, diagnosis of diabetes and smoking status were associated with the development of CHD. In the algorithm concentration of either TC or LDL-C can be used. Calculation of 10-year risk of CHD is shown in **Table 1**.

Table 1 Factors included in the calculation of 10-year risk of coronary heart disease.

Step 1: Age					
Years	LDL-C points		TC points		
	Men	Women	Men	Women	
30-34	-1	-9	[-1]	[-9]	
35-39	0	-4	[0]	[-4]	
40-44	1	0	[1]	[0]	
45-49	2	3	[2]	[3]	
50-54	3	6	[3]	[6]	
55-59	4	7	[4]	[7]	
60-64	5	8	[5]	[8]	
65-69	6	8	[6]	[8]	
70-74	7	8	[7]	[8]	
Step 2: Cholesterol					
LDL-C			TC		
mg/dL	mmol/L	LDL-C points, men / women	mg/dL	mmol/L	TC points, men / women
<100	<2.59	-3 / -2	<160	<4.14	[-3] / [-2]
100-129	2.60-3.36	0 / 0	160-199	4.15-5.17	[0] / [0]
130-159	3.37-4.14	0 / 0	200-239	5.18-6.21	[1] / [1]
160-190	4.15-4.92	1 / 2	240-279	6.22-7.24	[2] / [1]
≥190	≥4.92	2 / 2	≥280	≥7.25	[3] / [3]

Table 1 continues

Step 3: HDL-C

mg/dL	LDL-C points		TC points	
	Men	Women	Men	Women
<35	2	5	[2]	[5]
35-44	1	2	[1]	[2]
45-49	0	1	[0]	[1]
50-59	0	0	[0]	[0]
≥60	-1	-2	[-2]	[-3]

Step 4: Blood pressure

Systolic (mmHg)	Diastolic (mmHg), LDL-C [TC] points, men / women (if different)				
	<100	80-84	85-89	90-99	≥100
<120	0 [0] / -3 [-3]	0 [0]	1 [1] / 0 [0]	2 [2]	3 [3]
120-129	0 [0]	0 [0]	1 [1] / 0 [0]	2 [2]	3 [3]
130-139	1 [1] / 0 [0]	1 [1] / 0 [0]	1 [1] / 0 [0]	2 [2]	3 [3]
140-159	2 [2]	2 [2]	2 [2]	2 [2]	3 [3]
≥160	3 [3]	3 [3]	3 [3]	3 [3]	3 [3]

Step 5: Diabetes

	LDL-C / [TC] points	
	Men	Women
No	0 / [0]	0 / [0]
Yes	2 / [2]	4 / [4]

Step 6:Smoker

	LDL-C / [TC] points	
	Men	Women
No	0 / [0]	0 / [0]
Yes	2 / [2]	2 / [2]

Step 7: Sum points from steps 1-6

Step 8: Determine CHD risk				**Step 9: Compare to average person your age**	
LDL-C points	10-year CHD risk	TC	10-year CHD risk	Age (years)	Average 10-year CHD risk
≤-3	1%			Men	
-2	2% / 1%	[≤-2]	[2%] / [1%]	30-34	3%
-1	2%	[-1]	[2%]	35-39	5%
0	3% / 2%	[0]	[3%] / [2%]	40-44	7%
1	4% / 2%	[1]	[3%] / [2%]	45-49	11%
2	4% /3%	[2]	[4%] / [3%]	50-54	14%
3	6% / 3%	[3]	[5%] / [3%]	55-59	16%
4	7% / 4%	[4]	[7%] / [4%]	60-64	21%
5	9% / 5%	[5]	[8%] / [4%]	65-69	25%
6	11% / 6%	[6]	[10%] / [5%]	70-74	30%
7	14% / 7%	[7]	[13%] / [6%]	Women	
8	18% / 8%	[8]	[16%] / [7%]	30-34	<1%
9	22% / 9%	[9]	[20%] / [8%]	35-39	<1%
10	27% / 11%	[10]	[25%] / [10%]	40-44	1%
11	33% / 13%	[11]	[31%] / [11%]	45-49	2%
12	40% / 15%	[12]	[37%] / [13%]	50-54	3%
13	47% / 17%	[13]	[45%] / [15%]	55-59	7%
14	≥56% / 20%	[14]	[≥53%] / [18%]	60-64	8%
15	≥56% / 24%	[15]	[≥53%] / [20%]	65-69	8%
16	≥56% / 27%	[16]	[≥53%] / [24%]	70-74	11%
≥17	≥56% / ≥32%	[≥17]	[≥53%] / [≥27%]		

Abbreviations used in the table: LDL-C, low-density lipoprotein cholesterol; TC, total cholesterol; HDL-C, high-density lipoprotein cholesterol; CHD, coronary heart disease.

The calculated risk of CHD is compared to average risk of the same age group, e.g. 55-year old male having risk of 31% is almost 2-fold higher than the average risk of a male in same age group (31% / 16% = 1.94).[29] In general, 10-year CHD risk at 20% or over is considered to be elevated and in need of intervention.[35] The 10-year risk of CHD can also be calculated using sex-specific equations derived from multivariate-adjusted relative risk model.[29] Besides 10-year risk of CHD, currently risk algorithims for various cardiovascular disease outcomes are available (**Table 2**).

Table 2 Risk prediction algorithms for various cardiovascular disease outcomes.

Outcome	Risk calculator
First atrial fibrillation (AF)	FHS Atrial Fibrillation score (10-year risk)[144] Predictors: Age, male sex, BMI; systolic BP, treatment for hypertension, PR interval, significant murmur, prevalent heart failure
First heart failure (HF) in AF	Heart Failure in Atrial Fibrillation (10-year risk)[145] Predictors: Age, BMI, left ventricular hypertrophy, diabetes, significant murmur, prevalent MI
Cardiovascular disease (CVD)	FHS Cardiovascular Disease (10-year risk)[146] Predictors: Age, diabetes, smoking, treated and untreated systolic BP, TC, HDL-C, BMI replaicing lipids in a simpler model
Hard CVD	Cardiovascular Disease (30-year risk)[147] Predictors: Male sex, age, systolic BP, use of antihypertensive treatment, smoking, diabetes, TC, HDL-C, BMI replaicing lipids in a simpler model
Congestive HF	Congestive Heart Failure (4-year risk)[148] Predictors: Age, left ventricular hyperthrophy, heart rate, systolic BP, CHD, valve disease, diabetes, BMI, vital capacity (some models), cardiomegaly (some models)
Hard CHD (MI or coronary death)	Hard Coronary Heart Disease (10-year risk)[149] Predictors: Age, TC, HDL-C, systolic BP, treatment for hypertension, smoking
CHD	Coronary Heart Disease (10-year risk)[29] Predictors: Age, diabetes, smoking. JNC-V BP categories, NCEP TC categories, LDL-C
First CHD	Coronary Heart Disease (2-year risk)[150] Predictors: Age, systolic BP, smoking, fasting lipid level (TC and HDL-C), physician diagnosis of diabetes at the current or previous examination, use of antihypertensive medication
Subsequent CHD	Recurrent Coronary Heart Disease (2-year risk)[150] Predictors: Age, systolic BP, smoking, fasting lipid level (TC and HDL-C), physician diagnosis of diabetes at the current or previous examination
Diabetes	Type 2 Diabetes Mellitus (fasting blood glucose at or above 126 mg/dL) (8-year risk)[151] Predictors: Age, sex, fasting glucose above 100 mg/dL, BMI, HDL-C, TG above 150 mg/dL, BP, parental history of diabetes
Incident fatty liver (on CT scan)	Fatty Liver Disease[152] Predictors: Age, sex, BMI, alcohol use, TG concentration

Table 2 continues	
Incidence of hypertension	Hypertension (1-, 2- and 4-year risks)[153] Predictors: Age, male sex, BP, BMI, parental hypertension, smoking
Intermittent claudication	Intermittent Claudication (4-year risk)[154] Predictors: Age, sex, serum cholesterol, hypertension, smoking, diabetes, CHD
Stroke	Stroke (10-year risk)[155] Predictors: Age, systolic BP, diabetes, smoking, prior CVD, AF, left ventricular hypertrophy, use of hypertensive medication
	Stroke after Atrial Fibrillation (5-year risk)[156] Predictors: Age, sex, systolic BP, diabetes, prior stroke or ischemic attack

Abbreviations used in the table: AF, atrial fibrillation; FHS, Framingham Heart Study; BMI, body mass index; BP, blood pressure; HF, heart failure; MI, myocardial infarction; CVD, cardiovascular disease; TC, total cholesterol; HDL-C, high-density lipoprotein cholesterol; CHD, coronary heart disease; JNC-V, 5th Report of the Joint National Committee on prevention, detection, and treatment of high blood pressure; NCEP, The National Cholesterol Education Program; LDL-C, low-density lipoprotein cholesterol; TG, triglyceride; CT, computed tomography.

The Framingham Heart Study is still on-going and has produced massive amount of information on major risk factors for cardiovascular outcomes. Technologies have evovled greatly since the beginning of the study, so also studies of genetic patterns underlying CAD are evaluated. This enables the generation of more complex models, which might yield novel findings of ways to prevent and treat CAD. The Framingham Heart Study continues to be one of the world's leading epidemological studies and it is expanding to further areas of reasearch, such as dementia.[157]

2.3.2 SCORE risk charts

SCORE risk assessment models have been created by ESC. The SCORE2 and SCORE2-OP risk models published in June 2021 followed the original SCORE-algorithm. SCORE2 risk prediction model evaluates the 10-year risk of CVD in Europe while SCORE2-OP is intended to be used in older persons in four geographical risk regions in Europe and it estimates the incident cardiovascular event risk.

The SCORE-project (Systematic Coronary Risk Evaluation) was initiated by ESC and the 2nd Joint Task Force of the European Societies on Coronary Prevention in aim to create a tool for clinical practise to estimate the total CVD risk in European people. The risk algorithms based on Framingham Heart Study might overestimate the CVD risk in some European countries which are considered as low-risk countries. Multiple clinical datasets were obtained and pooled from 12 different European countries and cardiovascular mortality was studied as an endpoint. Based

on SCORE-project, risk charts for men and women were created, where age (40, 50, 55, 60 and 65 years), smoking status, systolic BP (20 mmHg intervals) and either TC or TC/HDL-C-ratio were used as predictors. Also, low- and high-risk countries had separate risk charts. In SCORE charts, the individual's risk is compared to the risk of optimal values of same age group (**Table 3**). As an example, a smoking person with the highest systolic BP and TC (or TC/HDL-C-ratio) has 12-times higher risk than non-smoking person with the lowest systolic BP and TC (or TC/HDL-C-ratio). For systolic BP and TC (or TC/HDL-C-ratio) the value in the chart is selected which is the closest measure from the patient. Additionally, the risk is reported as a percentage where color-coding of the risk number is categorized into seven classes (<1%, 1%, 2%, 3%–4%, 5%–9%, 10%–14% and ≥15%). The predictive value of the charts was evaluated with individuals between ages 45 and 64, and areas under the curve (AUCs) of receiver-operator characteristic (ROC) curves were 0.71–0.84.[35]

Table 3 An example of SCORE risk chart for total cardiovascular mortality (55-year old male in low-risk country).

Systolic blood pressure (mmHg)	Non-smoker					Smoker				
180	3	3	4	5	6	6	7	8	10	12
160	2	3	3	4	4	4	5	6	7	8
140	1	2	2	2	3	3	3	4	5	6
120	1	1	1	2	2	2	2	3	3	4
	4	5	6	7	8	4	5	6	7	8
	Total cholesterol (mmol/L)									

The SCORE2 is an updated algorithm of SCORE and additionally to cardiovascular mortality as an endpoint, non-fatal CVD risk was added as an endpoint. Since SCORE was first introduced in early 2000s, the CVD burden has shifted more towards non-fatal incidences, so the update roughly 20 years later was well-justified. The SCORE2 was validated in individuals with the age of 40–69 years and without prior CVD or diabetes. Prospectively 45 study cohorts from 13 European countries were included in the updated model algorithm and it was further externally validated using 25 prospective cohorts not included in the establishment of the model.[158]

The primary outcome in the SCORE2 study was CVD expressed as cardiovascular mortality, non-fatal MI and non-fatal stoke. In addition, countries were subdivided into low-, moderate-, high- and very high-risk regions to reflect the national risk status more precisely according to WHO age- and sex-standardized overall CVD mortality rates. The classification into these risk-regions was done by

evaluating the population-based risk profile inside the nation, thus leading to classification of average risk-region.[158]

The SCORE2 risk charts are formed similarly as SCORE risk charts, separately for different age groups, both sexes, smoking status, and risk-region. Systolic BP and non-HDL-C were likewise used in the model. Here, non-HDL-C means all other forms of cholesterol besides HDL-C and is calculated as subtracting HDL-C from TC. Predictors in the SCORE2 risk charts are shown in **Table 4**. Besides giving the individuals risk compared to individual with lowest non-HDL-C and systolic BP in the same age group, also color-coded risk percentages are given (**Table 4**). The SCORE2 outperformed the original SCORE, thus giving better indication of the individuals' risk in fatal or non-fatal cardiovascular events.[158]

Table 4 Predictors in the SCORE2 algorithm and risk classes.

Predictor	**Categories**	
Risk-region	Low	Moderate
	High	Very high
Sex	Male	Female
Smoking	Non-smoker	Smoker
Age	40–44	45–49
	50–54	55–59
	60–64	65–69
Systolic blood pressure (mmHg)	100–119	120–139
	140–159	160–179
Non-HDL-C (mmol/L)	3.0–3.9	4.0–4.9
	5.0–5.9	6.0–6.9
Risk class	**<50 years**	**50–69 years**
Green	<2.5%	<5%
Orange	2.5% to <7.5%	5% to <10%
Red	≥7.5%	≥10%

Abbreviation used in the table: HDL-C, high-density lipoprotein cholesterol.

Specifically for older persons, SCORE2-OP was established where either 5- or 10-year risk of CVD can be estimated. The SCORE2-OP algorithm is similarly derived as SCORE2 but with higher age classes: 70–74, 75–79, 80–84 and 85–89. Also, risk percentage classes are higher than in SCORE2: <7.5% (green), 7.5% to <15% (orange) and ≥15% (red). The SCORE2-OP risk charts give clinicians valuable information and more accurate estimate on CVD risk especially for the elderly people in whome risk of CVD is already initially higher. Lowering of CVD

risk predictor values shows the decrease in risk compared to patients current status which can be used to guide intervention and treatment.[159]

2.3.3 FINRISK calculator

The FINRISK calculator was created with data collected from Finnish individuals in the FINRISK study since 1972 and the study is on-going. The FINRISK calculator was first published in 2007 where data from 1982–2007 was utilized.[36] The calculator gives the 10-year risk assessment of getting MI, stroke or either of them, and is intended to be used for people aged 30–74.[160] Predictors used in the calculator are similar to FRS and SCORE since it is based on those, but FINRISK algorithm is generated specifically for Finnish population considering the prevalence of cardiovascular diseases and fatal or non-fatal events from registers.[36]

Besides age, sex and smoking status, the increased level of TC, decreased level of HDL-C, elevated systolic BP and diagnosis of T2D are considered risk factors in Finnish population as well as parental medical history (MI before the age of 60 or stroke before the age of 75). The personal risk value is compared to the risk of a person with same sex and age but optimal values for the other risk factors. Also, risk comparison to a person of same sex and age with average risk factor values of a Finnish person is reported. With results from FINRISK calculator Finnish people are encouraged to lifestyle changes targeting prevention and it also serves as a guiding tool of treatment for clinicians.[160]

Genetic susceptibility of CVDs is high in Finland and for that reason parental history questions were added to the FINRISK 2.0 calculator. Also, risk factors for MI and stroke are slightly different so separate algorithms were generated for these. The calculator based on FINRISK 2.0 study uses the same risk factors for determining the risk of CVD-related events within 10 years as the original FINRISK calculator. However, based on study findings a new algorithm for indicating stroke within 10 years a new algorithm was established. Elevated systolic BP, smoking and low HDL-C level were considered risk factors for suffering a stroke within 10 years. For FINRISK 2.0 calculator cohort size increased and algorithm calculation methods were altered from the original FINRISK calculator, which enabled more accurate estimation for both endpoints.[161]

2.4 Biochemical markers for CAD

2.4.1 Lipid profile

Lipids play a key role in the development of atherosclerosis and can be used as risk predictive markers of future cardiovascular events. Currently multiple types of lipids

can be measured from blood sample: cholesterol (TC, LDL-C, HDL-C and oxidized LDL), TGs, lipoprotein A [Lp(a)], apolipoprotein B (ApoB), lipoprotein-associated phospholipase A2 (Lp-PLA2) and ceramides.

Cholesterol

The traditional lipid panel consists of TC, LDL-C, HDL-C, and TGs. Currently, also non-HDL-C and oxidized LDL values are used.

Lipids play a crucial role in the development and progression of atherosclerosis. Libby *et al.*[162] have summarized the recent knowledge on atherogenesis and how lipids are involved in it. The liver secretes very-low-density lipoproteins (VLDLs), which contain cholesterol and TGs. On the surface of endothelial cells, lipoprotein lipase detaches fatty acids from TG particles and remaining particles end up in the liver where they are quickly metabolized or transformed to LDL, HDL or intermediate-density lipoprotein (IDL) particles.

Human body tries to get rid of excess LDL particles and cholesterol through LDL receptors on liver cells, but the more LDL receptors are occupied in the liver, the more LDL particles are released from the liver into the circulation thus increasing the LDL-C concentration in the circulation. Nutrition has a major role on the amount of LDL particles released from the liver receptors to circulation. Some of the LDL particles in the circulation proceed through endothelium to LDL receptors on the cells of most inner layer of the arteries, intima. The sphere-shaped LDL particle attaches to proteoglycan receptors on the intima through ApoB100 protein (later referred as ApoB) located on the outer layer of the LDL particle. Besides the single ApoB protein, the outer layer also includes phospholipids and cholesterol. The core of an LDL particle is full of cholesterol esters and TGs. Through receptors on the intima, LDL particles are oxidised or modified to form which macrophages recognise and take up uncontrollably. In macrophages the modified LDL particles are transferred into lysosomes for lysing and the esterification of cholesterol starts. The macrophages uptake as much cholesterol esters as they can and eventually transform into foam cells. In the excess of LDL particles, the lipid core in the atheroma starts to form when modified LDL particles transfer even further from the intima, into the musculoelastic layer. There these particles accumulate and form fatty droplets. Dying foam cells release the cholesterol from within which then merges with the fatty droplets. The process of very-low-density lipoprotein particle originating from the liver and eventually forming atheroma with lipid core is a continuous process and especially risk factors described in chapter 2.1.2 are in key role in the initiation and progression of atherosclerosis.

An HDL particle is a similar sphere as an LDL particle, but half the size and the surface contains multiple apolipoproteins of which apolipoprotein A1 (ApoA1) is

the most crucial. In the liver, HDL particles are able to some extent remove LDL particles on LDL receptors. HDL particles and immature pro-β-HDL particles can remove cholesterol from the foam cells in the developed fatty streaks, thus HDL particles have antiatherogenic properties. However, the ability of HDL particle to intake cholesterol and cholesterol esters is limited because of imbalance between LDL and HDL particle amounts. Also, HDL particles encounter such modifications in the intima that reduces the cholesterol uptake.

Laboratory measurements of TC are accurate, precise, and well-standardized. TC is the measurement of cholesterol esters and free cholesterol from all lipoproteins. Ascorbic acid, bilirubin, TG, and haemolysis can, however, interfere TC assays. In HDL-C assays, first non-HDL components need to be removed from the sample. This creates differences between assays and can show as bias in routine use. In TG assays, mono-, di-, and triglycerides are hydrolysed to glycerol and free fatty acids. The total serum glycerol concentration is measured.[163] TG is very heterogenic analyte which can create overestimation in certain rare genetic diseases. The LDL-C concentration in mg/dL unit is usually calculated by using the Friedewald formula (1)[164]. For the use of Friedewald formula in the estimation of LDL-C concentration, fasting sample is required. The Friedewald formula is applicable when TG concentration is less than 150 mg/dL and completely invalid if TG concentration is above 400 mg/dL.[165]

$$[LDL - C] = [TC] - [HDL - C] - [0.20 \times TG] \quad (1)$$

Another formula called Martin/Hopkins has been created where TG values are divided by adjustable factor which is derived from median TG/VLDL ratio in general population of all ages (N=1 350 908). This formula is not as affected by TG as the Friedewald formula but still the Friedewald formula is mostly used.[165] The direct measurement of LDL-C is also possible, but it is laborious and not in routine use, except in research laboratories. Non-HDL-C is characterized as all other lipoproteins except HDL-C: the concentration of HDL-C is subtracted from the TC concentration. Non-HDL-C, therefore, represents the combination of cholesterol in LDL, IDL, VLDL, and chylomicron particles as well as VLDL and chylomicron remnants and Lp(a).[163] Measurement of oxidized LDL is currently possible with enzyme-linked immunosorbent assays (ELISAs) but it is not measured routinely as part of lipid profile.[166] The clinical evidence of oxidized LDL association with progression of human atherosclerosis is insufficient, and limited data is not supportive on using oxidized LDL as therapeutic target.[11] The desired lipid values for adults are shown in **Table 5**. These limits may vary by e.g., sex, ethnicity, and CVD status.

Table 5 Desired values of lipid parameters in adults.

Analyte		Desired value	
		mmol/L	mg/dL
TC[a, 167]		<5.0	<190
HDL-C[a]	Men	>1.0[168]	>40[163]
	Women	>1.2[168]	>50[163]
TG[b, 167]	Fasting	<1.7	<150
	Non-fasting	<2.0	<175
LDL-C[a] (calculated[c])[167]	Low- to moderate-risk patients	<3.0	<115
	High-risk patients	<2.5	<100
	Very high-risk patients	<1.8	<70
	TG multiplication factor in formula	0.45	0.2
Non-HDL-C[167]	Moderate-risk patients	<3.8	<145
	High-risk patients	<3.3	<130
	Very high-risk patients	<2.5	<100
oxidized LDL[166]		<45 U/L	

Abbreviations used in the table: TC, total cholesterol; HDL-C, high-density lipoprotein cholesterol; TG, triglyceride; LDL-C, low-density lipoprotein cholesterol.
[a]For TC, HDL-C and LDL-C, mmol/L is converted to mg/dL by multiplying with factor of 38.6.
[b]For TGs, mmol/L is converted to mg/dL by multiplying with factor of 88.5.
[c]Calculation method for LDL-C uses Friedewald formula.

Due to the strong causative role of LDL particles in atherosclerosis, the measurement of LDL-C is used to describe the state and progression of atherosclerosis. The possibility to calculate LDL-C when TC, HDL-C and TGs are measured has already existed since the 1970s.[164] The predictive value of high LDL-C or TC and low HDL-C has been utilized already in the first FRS algorithm and lowering of LDL-C in the circulation has been proven an efficient way to reduce the risk of advancing atherosclerosis.[167] However, LDL particles are not solely responsible of the development and progression of atherosclerosis. Also, very low LDL-C concentrations reached with efficient LDL-lowering therapy increase the variation in the calculation with Friedewald formula.[165] Thus, updated methods are needed in order to find the high-risk individuals even at lower age. The determination of non-HDL-C has shown promise as such method. With non-HDL-C, the concentration comprises of all atherogenic particles, not just LDL and in clinical assessment it has in some cases proven more accurate tool than LDL-C alone.[169] In a meta-analysis of medicated patients, the 1% decrease in non-HDL-C also decreased 1% the relative risk for CHD.[170] Moreover, the determination of non-HDL-C enables the usage of non-fasting samples in lipid concentration measurement, since highly variable TGs are not account for.[167] Especially, non-

HDL-C has been shown to be superior to LDL-C in CVD risk-prediction when LDL-C is in optimal level. When non-HDL-C approach was utilized, the individuals in need of preventive therapy doubled.[171]

Lipoprotein A

In Lp(a), the plasminogen-like ApoA1 is bound to LDL and ApoB via a disulfide bond.[172,173] Lp(a) may vary in size due to the number of repeats of two tri-loop structures (KIV, "kringles") in ApoA1. There are 10 types of KIV and the number of type 2 (KIV_2) repeats define the size of ApoA1 isoforms and thus the size of Lp(a).[174] With smaller ApoA1 size the concentration of Lp(a) in the circulation is higher. Consequently, Lp(a) levels are inversely correlated with ApoA1 size.[172,175] Also, the number of KIV_2 repeats have an effect on Lp(a) levels, causing variation of Lp(a) levels between individuals.[176] The level of Lp(a) varies between individuals, but it remains quite constant throughout life.[172,173] Additionally, single-nucleotide polymorphisms rs10455872 and rs3798220 influence the Lp(a) levels between individuals.[177]

Lp(a) accumulates in the intima of arteries and the aortic valve leaflets. It is found throughout arteries, not just in atherosclerotic lesions as LDL and ApoB. The particle size of Lp(a), BP and arterial wall permeability impacts the deposit of Lp(a).[178] Uptake of Lp(a) by macrophages thus advances the development of atherosclerotic lesions.[178] There are multiple mechanisms through which Lp(a) contributes to the development of atherosclerosis:[174,179,180]

1. The expression of inflammatory cytokines such as IL-1β, IL-6, IL-8 and TNFα.
2. The expression of adhesion molecules on the endothelial cell surface such as vascular cell adhesion protein 1, intracellular adhesion molecule 1, E-selectin and P-selectin.
3. The stimulation of monocyte chemotactic protein and activation of nuclear factor κB causing monocyte chemotaxis.
4. The binding and transportation of oxidized phospholipids.

Therefore, Lp(a) is involved in the vulnerability and destabilization of atherosclerotic plaques as well as in promoting inflammatory state in the arteries. Patients with high Lp(a) levels have detectable ruptures and healings of atherosclerotic plaques which is an indication of higher-risk of CVD events.[177] Especially, in the younger population the risk is more evident than in elderly which could enable the recognition of the young high-risk individuals better than risk scores.[177,181]

Even with normal traditional lipid levels, an individual may have elevated Lp(a) levels which are only minimally affected by dietary and environmental factors.[172,177] There are no cut-off values for Lp(a) level but Lp(a) over 20 mg/dL has been associated with 2-fold increase in developing CVD and Lp(a) at or over 50 mg/dL with even higher risk.[182] Concentration of over 180 mg/dL correlates with CVD events as much as familial hypercholesterolemia.[172] It seems that lipid-lowering medication, such as statins, further increases the CVD risk if Lp(a) level is elevated. With reduced LDL-C level, the Lp(a)-related risk is strongly enhanced. In contrast to LDL-C, the statin therapy does not lower the Lp(a) level.[183] The Lp(a) functions as an independent predictor of future CVD events and mortality both in the primary[184] and secondary prevention[185,186]. The elevated level of Lp(a) has also been associated with poorer outcome in patients with ischaemic stroke, peripheral arterial disease, and calcific aortic valve disease.[187,188] The reduction of Lp(a) levels has been successful particularly with PCSK9 (proprotein convertase subtilisin/kexin type 9) inhibitors and consequently in the reduction of CVD-related risk.[189–192]

Apolipoprotein B

The LDL, IDL, VLDL and Lp(a) particles each contain one molecule of ApoB, thus the ApoB levels reflects the amount of all of these in the circulation, and therefore the actual number of atherogenic lipid particles.[193]

The ApoB is found in the surface of lipoproteins and is essential in maintaining the structural stability of VLDL particles and its metabolites IDL and LDL particles. Also, mainly ApoB defines the characteristics of lipoproteins, and has multiple functions in the regulation of lipid metabolism and transportation.[194] The ApoB is expresses as two isoforms which are encoded by *apob* gene. The truncated form of ApoB48 consists of the N-terminal part of the full-length protein and is present in the intestines while the full-length ApoB is synthesized primarily in liver from where atherogenic lipoproteins originate.[195] In the arterial wall, ApoB binds to proteoglycans via glycosaminoglycans (GAGs). Due to the bound ApoB, lipoproteins containing ApoB are retained in the subendothelium, which leads to aggregation of these particles in the arterial wall.[194,196,197]

Since each atherogenic lipoprotein particle contains one ApoB molecule, it gives an accurate estimation of the portion of atherogenic particles in patient. Even though majority of ApoB is found in LDL particles, the levels of ApoB and LDL-C do not correlate, which is most likely due to the heterogeneity of LDL particles.[198] The increased plasma ApoB levels has been associated with the length of atherosclerotic lesion and the size of plaque and necrotic core evaluated with IVUS.[199] Therefore, ApoB is a potential marker of vulnerable atherosclerotic plaque. With statin medication, the levels of ApoB are not as affected as LDL-C levels, so ApoB may

function as more precise indicator of abnormal lipid levels in the patient.[200] The measurement of ApoB with immunoassays is, however, challenging, time-consuming, expensive and standardized methods are not available.[201]

Recently, it has been shown that ApoB predicts cardiovascular events with higher sensitivity and specificity than LDL-C. In stable CAD patients, the ApoB levels in circulation predicted future MI in both men and women, regardless of age.[202] Also, ApoB could predict the risk of major CVD events better than LDL-C due to the heterogenous nature of atherogenic lipoprotein particles.[194] Moreover, ApoB/ApoA1 ratio has shown promise as an accurate predictor of CVD risk. The simplified description of ApoA1 is that it is the opposite molecule of ApoB. ApoA1 has anti-atherogenic properties since it is involved in the transportation of cholesterol within HDL particles. The increased ratio of these two describes the circulating cholesterol in plasma and consequently the cholesterol deposited into the arterial wall.[203] The ApoB/ApoA1 ratio could especially identify the high-risk individuals irrespective of traditional risk factors such as age, diabetes status and LDL-C.[202,204,205] As an independent marker, the ApoA1 has shown promise in research setting but clinical proof of its functionality as a marker or atheroprotective particle is relatively weak.[206] Despite the challenges in the measurement, both the ApoB and the ratio of ApoB/ApoA1 could be used in evaluating CVD event risk as well as monitoring and targeting the treatment better than traditional cholesterol markers.[207]

Lipoprotein-associated phospholipase A2

Another lipid-based biomarker associated with CAD is Lp-PLA2. It is a part of phospholipase A2 superfamily which consists of 16 distinct groups.[208] The Lp-PLA2 is a 45 kDa protein and is mainly secreted by macrophages.[209] Usually hematopoietic cells are the origin of circulating Lp-PLA2 but to some extent also liver cells, aorta cells and adipocytes are the source of this protein.[210–212] In the circulation Lp-PLA2 is principally complexed with LDL particles but in smaller amounts with HDL particles too.[213] It can hydrolyse oxidized LDL to two bioactive products: lysophosphatidylcholine and oxidized nonesterified fatty acids. Out of these, the former one is more distinctively connected with inflammatory responses in atherogenesis than the latter.[214]

The concentration of Lp-PLA2 is higher in vulnerable atherosclerotic plaques, thus suggested as a marker of the vulnerable plaque. The Lp-PLA2 also has been suggested to have a causative role in the development and progression of atherosclerosis and therefore is considered as a therapeutic target which is supported by animal model studies.[215] However, in clinical studies targeting inhibition of Lp-PLA2 with darapladip in atherosclerotic patients, the drug did not function as

desired.[216,217] Still, darapladip has produced favourable results in patients with diabetic macular edema or Alzheimer's disease.[218,219]

Even though inhibition of Lp-PLA2 activity is not clearly beneficial in treatment of chronic CAD or prevention of acute CAD, it seems that Lp-PLA2 still functions as an independent risk marker. Several studies have shown significant correlation with CAD and the elevated risk of cardiovascular events or mortality in the general population as well as in the diseased ones.[220,221] With Lp-PLA2 the measurements of mass or activity in the plasma are used and depending on the procedure results may vary because these measuring methods have not been standardized.[222]

Ceramides

Ceramides are part of lipid class, and their metabolism has a pivotal role in CAD. A recent discovery of ceramides by lipidomic analyses has produced novel information on future cardiovascular risk of a patient beyond traditional cholesterol measurements.[223]

All cells in the human body can synthesize ceramides and the activity of six different ceramide synthases regulate the amount of different-size ceramides in tissues and during physiological and pathophysiological conditions. There are four different ceramides associated with CAD. These consist of sphingosine backbone and differ from each other due to a side chain comprised of fatty acid. The fatty acid side chains can be palmitate, stearate, lignocerate or nervonate.[224–226]

Ceramides are measured from plasma sample with liquid chromatography-tandem mass spectrometry (LC-MS/MS). Different ceramides have particular fragmentation spectrums so they can be identified from each other. The concentration of certain ceramide is determined by comparing the spectrum to control samples of known concentrations.[227]

Ceramides are mostly synthesized in liver where they attach to the membrane of lipoproteins secreted to circulation. Majority of ceramides are found in LDL particles but in some extent also in HDL and VLDL particles.[228,229] Ceramides have a pathophysiological role in atherogenesis and metabolic disorders related to it. Cytokines secreted by atherosclerotic plaque increase the amount of sphingomyelinase which enables ceramide synthesis. Also, due to transportation by LDL particles to arterial wall, ceramide amount increases which further activates local transcription factors resulting in advancement of inflammatory state and thus atherosclerosis.[230]

Increased plasma levels of three ceramides predict the elevated risk of cardiovascular mortality, while one ceramide indicates a favourable outcome.[231,232] Furthermore, ratios of the ceramides elevated in CAD with ceramide decreased in CAD were found to be even more significant indicators of cardiovascular death. The

three ceramide ratios were significant predictors of cardiovascular death during follow-up in both high- and low-risk (BECAC cohort, Bergen Coronary Angiography Cohort) patients as well as in chronic CAD patients (Corogene cohort). Similarly, ceramide ratios were highly predictive of cardiovascular death within 1-year after enrolled ACS incident based on SPUM-ACS cohort (Special Program University Medicine – Inflammation in Acute Coronary Syndromes).[226]

Based on ceramide ratios, a Coronary Event Risk Test (CERT) has been established, where the risk of future event is described as points much like in available risk scores (see section 2.3 Clinical risk scores for CAD). According to points, the risk is divided into four classes. Chronic CAD patients are given the risk of cardiovascular death within 5-years, while for ACS patients the 1-year risk is given.[226] The risk is compared to a general population level where separate risks of cardiovascular event and death are derived from FINRISK 2002 cohort.[233]

Measurement of ceramides could prove to be more precise in predicting the risk of cardiovascular events or death than merely LDL-C alone. By estimating the risk more accurately, the more effective treatment and prevention plans can be formulated for patients. Also, monitoring of the advancement of CAD could be possible with CERT. Using ceramides in the risk prediction is still a relatively novel procedure and massive leaps in the research area of lipidomics are expectable.[226]

2.4.2 Inflammatory markers

In atherosclerosis, chronic inflammation state in the arterial wall has a major role in the development of atherogenesis.[11] C-reactive protein (CRP), various cytokines, myeloperoxidase (MPO) and matrix metalloproteinases (MMPs) are suggested to be biomarkers of this inflammatory state. These are also used in the prediction of future cardiovascular events and thus could be useful in determining risk-reducing treatments and anti-inflammatory therapies.[222]

C-reactive protein

CRP is a widely used biomarker of chronic inflammation and levels in the circulation remain constant for a long time because of its long half-life and stable structure. Currently, there are multiple commercial assays available for measuring high-sensitivity CRP (hs-CRP) which allows detection of even slightest elevations.[234]

CRP is a protein with pentameric structure formed by five identical 23 kDa polypeptide subunits attached non-covalently. CRP belongs to pentraxins that are soluble proteins which recognise microbial structures and have a major role in innate immunity. Natural ligands of CRP are C-polysaccharides expressed by *Streptococcus pneumoniae* that are rich of lysophosphatidylcholine. Also,

phosphocoline on the cell surface of apoptotic cells binds CRP. Inflammatory or ischaemic tissue damage induces secretion of pro-inflammatory cytokines which promotes CRP production in the liver.[235]

As a predictive biomarker, CRP has been linked to CAD, ischaemic stroke, and cardiovascular death.[236] Several studies have shown its risk-predictive capability together with LDL-C in primary prevention[237–240]: regardless of the LDL-C concentration, high CRP level in circulation indicated higher risk of major coronary events. Even with low LDL-C, the risk of cardiovascular events remained high if CRP was elevated. With lipid-lowering statin medication, also CRP levels decreased which gave better prognosis. It was concluded that a therapy which lowers both LDL-C and CRP levels improves prognosis.

When studied as part of secondary prevention in chronic CAD, CRP has been associated with the risk of MI, the need for revascularization, stroke, heart failure (HF) and cardiovascular, cancer-related and total mortality.[241–247] CRP was found to be an independent predictor of such endpoints even without traditional risk factors such as high age, male sex and T2D status or the extent or severity of CAD.[242] Additionally, patients with LDL-C >1.8 mmol/L, baseline hs-CRP categories of <1, 1–3 and >3 mg/dL showed higher 3-year Kaplan-Meier rates for these endpoints.[247] Reduction in CRP levels also indicated a decrease in the progression of atherosclerotic plaques even if serum lipid levels remained unaltered. Still, the reduction of both CRP (to <2 mg/L) and LDL-C (to <1.8 mmol/L) levels slowed down the progression of atherosclerotic lesions and reduced the residual risk of cardiovascular events.[248]

Likewise, hs-CRP has also been used to predict recurrent cardiovascular events in ACS patients (NSTEMI or STEMI). These results are summarized by Arroyo-Espliguero et al.[249] In short, with UAP patients, the prognosis was poorer if CRP level was above 0.3 mg/dL. For STEMI patients if the ACS-induced rapid elevation of CRP remained high for a longer period of time, even weeks, the prognosis for recurrent incidents was higher. NSTEMI patients tended to have lower increase of CRP level than STEMI patients, which indicated lower level of inflammation after myocardial necrosis. The cTns are precise markers of myocardial damage through necrosis and do not reflect the inflammatory status, so expectedly there is only weak correlation between cTns and CRP. Still, with CRP measurement the inflammatory status after vascular damage could be predicted since the inflammatory system reacts to even small stimuli, which is measurable with hs-CRP assays. As CRP levels remain elevated especially after STEMI, the chronic inflammation in the coronary arteries might predict recurrent cardiovascular event and therefore higher risk of mortality.

Even though hs-CRP is considered a good biomarker for risk prediction in CAD patients (chronic or acute) in scientific literature, it is not routinely used in clinical

practise. Also, inflammation from other sources may interfere the result interpretation since CRP is not specific marker of inflammation in coronary arteries but gives general indication of inflammation in the body. Regarding SCORE index, ESC did not find it to be additive in the primary prevention.[250] AHA agreed hs-CRP to be useful for moderate risk patients for whom lipid-lowering medication would be started if hs-CRP level would be at least 2 mg/L.[5] For secondary prevention neither ESC nor AHA recommends using hs-CRP in the risk stratification because it adds only little value to current cardiovascular risk assessment methods.[251]

Cytokines

Tumour necrosis factor α (TNF-α) promotes inflammation in atherosclerosis and is produced by the activated macrophages which are stimulated by interferon γ . In mice models TNF-α promoted uptake oxidized LDL by macrophages and thus formation of foam cells.[252] In general, TNF-α causes endothelial dysfunction and enhances oxidative stress.[253] By advancing dyslipidemia and insulin resistance, TNF-α promotes atherosclerosis since it has a crucial role in the formation and destabilization of atherosclerotic plaques.[254,255] With anti-TNF-α therapy, the reduced TNF-α levels indicated improved endothelial functions in rheumatoid arthritis patients.[256]

Interleukins (ILs) are the main cytokines initiating inflammatory processes by developing inflammatory cells. Helper T lymphocytes synthesise majority of ILs and consequently ILs function as cell-signalling mediators between leukocytes.[257] IL-1α and IL-1β are involved in early development of inflammation and their balance with IL-1 receptors antagonist seems to determine the severity of inflammation prosess.[258] Especially, both increased IL-1α and IL-1β levels have been implicated with unstable CAD[259] but there is evidence that lacking only IL-1β decreases atherosclerosis severity in apoE-deficient mice.[260] IL-2 is produced by activated T-cells and it has shown to be proinflammatory cytokine both in animal models and clinical studies.[261] In patients with UAP or recent MI, the IL-2 levels are more elevated than in chronic CAD patients.[262] IL-6 regulates multiple immune response reactions in acute-phase and hematopoiesis.[263] It is produced in macrophages which are activated by interferone γ, IL-1 and TNF-α. IL-6 has proatherogenic properties both locally and on a systemic level. In the development of atherosclerotic plaque, IL-6 is involved in trans-signalling pathway by which leukocytes eventually gather to intima[264] and macrophages transform into foam cells.[265] Although contradictory studies are also available where IL-6 is not as potent proinflammatory cytokine[266] as described in other studies, IL-6 is still considered a potential risk marker for future cardiovascular events. The increased level of IL-6 serves as a predictor of future cardiovascular

mortality, MI and stroke.[267] Also, elevated level of IL-6 in individuals of over 60 years of age have increased risk of CVD-related and overall mortality.[268]

Monocyte chemoattractant protein 1 (MCP-1) is responsible for the migration of monocytes to inflammation site in the intima and is produced by smooth muscle and endothelial cells which are stimulated by oxidized LDL.[269] Based on animal studies, MCP-1 has role in the stabilization of atherosclerotic plaque: in mice with deleted LDL-receptors, the absence of MCP-1 showed reduced atherogenesis[270] and in apoE-deficient mice, which were given inhibitory antibody to MCP-1, more stable atherosclerotic plaques were formed.[271] Also, after MI MCP-1 is aiding in the healing process of myocytes and formation of scar tissue.[272] In a population based study, MCP-1 adjusted with traditional risk factors did not serve as a biomarker for atherosclerosis[273] but after ACS, in patients with increased level of MCP-1, it was independently associated with future risk of death or recurrent MI within 10 months.[274]

Myeloperoxidase

Myeloperoxidase (MPO) is a 146 kDa enzyme and it is present in neutrophils as well as in monocytes which are further differentiated into macrophages. MPO is involved in the progression of atherosclerotic plaques. Especially, macrophages expressing MPO are present in the advanced atheroma rather than in the early stages of atherosclerotic lesions.[275] The effects of MPO during development of atherosclerosis are based on the catalytic activity of MPO. The enzyme produces oxidant-hypochlorous acid (HOCl) which promotes the formation of oxidized LDL and foam cells. It also oxidises other molecules which are involved in creating oxidative stress specifically in vulnerable rupture-prone plaques.[257,276,277]

Zhang *et al.*[278] reported in 2001 for the first time the positive correlation between circulating MPO and CAD. In the study, in patients with previous MI, PCI or >50% stenosis, the 4th, 3rd and 2nd quartiles of MPO differentiated from the 1st, i.e., the lowest MPO quartile. Many have discovered similar findings in post-STEMI patients where MPO is elevated but in few cases also contradictory findings have been reported (reviewed by Teng *et al.*[279]). The contradicting results might be caused by the ELISA-method used to determine the MPO concentration or the handling of the blood sample itself since MPO is a very sensitive protein. Various studies suggest that MPO is related also to severity of CAD. In these, ACS patients have higher MPO levels than stable CAD patients or controls.[280–282] MPO correlated with the narrowing coronary artery indicating that MPO is related to CAD severity.[283,284]

MPO can be used as risk predictive marker as well. In a large prospective study of healthy patients, the MPO predicted future risk of CAD when adjusted with traditional risk factors.[285] MPO in plasma was also elevated in cTn-negative patients

with chest pain examined with angiography. The study by Rebeiz *et al.*[286] showed this in patients with >70% diameter coronary stenosis, coronary thrombus, and plaque erosion. It seems that MPO is not associated with coronary artery calcium since calcification is usually a sign of a more stable plaque.[287] However, while MPO is connected to vulnerable plaques with thin fibrous cap and large necrotic core, it still inversely correlates with spotty calcification.[288] MPO can likewise be used as predictive marker for ACS patients in regards of future MACEs even as short time frame as 72 hours but also in longer time frames of 30 days to 6 months and even up to 3 years (reviewed by Teng *et al.*[279]).

Matrix metalloproteinases

MMPs belong to the family of metalloproteinases which have various proteolytic functions in CVD. Mainly, due to activation by MPO, MMPs degrade extracellular matrix, leading to thinning of the fibrous cap and eventually risk of rupture of the atherosclerotic plaque.[289] Especially, MMP-9 is involved in these processes.[290] MMP-2 along with MMP-3, MMP-9 and MMP-13 has been reported to contribute to vascular calcification via transportation by macrophages.[289] There are 28 different MMPs out of which 23 are expressed in human tissue and 14 in veins and arteries. The MMPs are classified according to the organization of their structural domains and substrate specificity.[291] All MMPs contain catalytic metalloproteinase domain where Zn^{2+} is in the active site along with cysteine-rich switch which is crucial in the activation of MMPs.[292] Different microRNA (miRNA) molecules control the expression of MMPs and regulation by miRNAs is a key factor in atherosclerotic plaque destabilization and oxidative stress in cardiomyocytes.[293]

Because of elevated concentrations in the circulation, MMP-2 and MMP-9 might be markers of vulnerable plaque.[294] Also, MMP-8 concentration in the circulation may be elevated especially if there are unstable atherosclerotic plaques in comparison to stable ones.[295]

Patients with ACS have elevated levels of MMP-2 which are independently associated with all-cause and cardiovascular death.[296] MMP-9 might function as a predictor of cardiovascular mortality. Increased levels of MMP-9 are possibly associated with severity of CAD and in ACS patients this elevated concentration could be linked to active plaque rupture.[297] Likewise, elevated MMP-9 concentration in ACS patients was associated in one study with future cardiovascular events[297], in particular patients with carotid atherosclerosis have higher prevalence of stroke and cardiovascular events during 10-year follow-up period[298]. Additionally, circulating MMP-9 levels have been linked to first-time CHD events within 8-year follow-up.[299] In men without CVD, increase of MMP-8 by 20 µg/L in circulation within 1 year increased the CVD event risk up to 15%. Also, asymptomatic CVD patients in the

beginning of the study with elevated MMP-8 levels were in 3-fold higher risk of cardiovascular death.[300] T2D patients with elevated levels of MMP-7 and MMP-12 might have higher risk of more severe cardiovascular events.[301] It has been suggested that measurement of MMPs from the circulation could identify patients in high risk of cardiovascular events and monitor treatment protocols.

2.4.3 Markers of cardiac injury

Markers of injury in the myocardium have been used in the diagnosis of acute MI. Mostly used are cTns which are considered as the golden standard in the diagnosis of acute MI for over two decades now. Clinical performance of cardiac troponin T (cTnT) and I (cTnI) are superior in comparison to previously used markers such as creatine kinase, lactate dehydrogenase and myoglobin in regards of specificity and sensitivity.[302] The elevated level of cTnT and cTnI in the circulation is seen after even the slightest necrotic change in the cardiomyocytes. These proteins are very specific to cardiomyocytes[303] and development of assays has enabled rapid and sensitive measurement of the analyte[304].

There are three types of troponin proteins, TnC, TnT and TnI, which are involved in the muscle contraction and relaxation together with myosin and actin.[305] Only the cardiac-specific isoforms of TnT and TnI are expressed in the adult cardiomyocytes.[303] Both TnT and TnI are also expressed in fast and slow muscle cells but in different isoforms that are called skeletal TnI and TnT. The circulating skeletal Tns are elevated after skeletal muscle injury and in muscle-related diseases such as myopathies.[306]

Assays for cTnT and cTnI have evolved in quite similar manner where lengthy assays detected µg/L concentrations of the analyte in the circulation whilst currently very rapid hs-cTn assays detecting ng/L or even pg/L concentrations are available (reviewed by Westermann et al.[304]). The criteria for hs-cTn assays are[307]:

1. The 99th percentile of apparently healthy reference population needs to have coefficient of variation less than or equal to 10%.
2. Concentrations in the general population need to measurable for at least 50% of the population or even proportion of 80%.

The first hs-cTnT assay was published in 2009 which had a Limit of Detection (LoD) of 2 ng/L and the 99th percentile in the reference population was 14 ng/L.[308,309] To date, sensitivity of the assay is not the only thing considered, and thus other approaches have been created to diagnose MI more accurately. Algorithms have been introduced where serial measurements in different time points are utilized and used for either rule-in or rule-out for further treatment.[304] Additive to serial sampling,

Food and Drug Administration has proposed simple sex-specific cut-off values for easier clinical utilisation.[310]

In addition to setting of MI, cTns can be elevated in circulation in various diseases and not always merely cardiac-related conditions. Still, cTns are usable as risk predictive markers. This is especially achieved due to hs-assays since measurement of lower analyte concentrations is needed. Risk prediction with cTns has been shown in non-acute settings for CAD or HF patients and even for general population.[304]

In chronic CAD patients, elevated cTnT and cTnI were found as independent predictors of HF and death.[311,312] Also, diabetic chronic CAD patients had increased risk of cardiovascular events and death.[313] In patients with previous MI or UAP and raised LDL-C, 1-year after use of statin medication, the increased cTn levels were associated with elevated rate of cardiovascular events while decreased cTn levels showed reduced risk.[314]

Patients with chronic kidney disease or chronic HF often have increased cTn levels. Even without CVD, most patients with impaired renal function have detectable cTnT and it is associated with incident HF, increased left ventricular mass, age and sex.[315] Also, in haemodialysis patients, hs-cTnT over 24 ng/L predicted all-cause mortality within follow-up (median 46 months).[316] In stable HF patients, increased cTn levels were in association with worsening New York Heart Association (NYHA) class and worse cardiovascular outcomes[317,318] as well as with all-cause mortality[319].

In general population, measurement of hs-cTnI has proven to be beneficial. When predicting cardiovascular events within 10-years, cTnI was one of the studied markers along with N-terminal prohormone of brain-type natriuretic peptide (NT-proBNP) and CRP, out of which cTnI outperformed the traditional cardiovascular risk factors.[320] In a largest study to date, as part of BiomarCaRE consortium, hs-cTnI values have been measured in a cohort of over 70 000 individuals.[321] The development of CVD or high mortality rate was observed in individuals with highest cTnI concentrations. Clinical relevance of hs-cTn-measurements in apparently healthy population remains uncertain and more research is required.[304]

2.4.4 Epigenetic markers

Epigenetic changes are modifications where genetic information changes without altering the nucleotide order in DNA. These non-coding molecules do not translate any protein but can be measurable in the circulation. The levels of small non-coding RNA molecules, micro RNAs (miRNAs), and long non-coding RNA molecules (lncRNA) are altered in CAD patients and can be used as risk-predictive markers of CVD events.

Micro RNAs

The miRNAs regulate gene expression by attaching to messenger RNA (mRNA). These 18–25 nucleotide long single-stranded miRNAs inactivate the target mRNA by mediating degradation of mRNA or repressing the post-transcriptional protein synthesis.[322] MiRNAs are mainly located intracellularly in vesicles and as attached to proteins but can also be functional in extracellular fluids such as plasma. The miRNA levels in circulation depend on the miRNA and its function. Several miRNAs have been associated with atherosclerosis. The atherosclerosis-associated miRNAs originate from cardiomyocytes, endothelial cells, arterial smooth muscle cells, and inflammatory cells. They are mostly found in extracellular exosomes and microvesicles, and in complex with lipoproteins, especially with HDL.[323–325] In CVDs, the miRNAs regulate myocardial remodelling and fibrosis, vascular inflammation, lipid processing, and electric remodelling.[326]

MiRNAs are involved in the differentiation of T cells, maturation of monocytes to macrophages and formation of foam cells. Up- or down-regulated expression of miRNAs has been also seen with activation of endothelial cells and phenotypic change of vascular smooth muscle cells. MiRNAs in the circulation may function as biomarkers of atherosclerosis.[327] Multiple miRNA profiles have been studied, where different patterns have been observed in patients with or without CAD (**Table 6**). Biomarker-miRNAs can be sensitively and specifically detected with quantitative reverse-transcriptase PCR method from various body liquids such as plasma, serum, urine, and cerebrospinal fluid.[328] However, there are still methodological limitations in the assessment of miRNAs. There is no adequate normalization available which makes data processing problematic.[329] Likewise, age, sex and ethnicity may have an effect to miRNA levels.[330]

Table 6 Micro RNA levels [increased (↑) or decreased (↓) as compared to controls] in the circulation of atherosclerotic patients.

Circulating level related to CAD		Associated miRNAs
Lipid metabolism	↑	miR-208b[331] miR-24, miR-33, miR-103a, miR-122[332,333] miR-17-5p, miR-92a, miR-93, miR-208a, miR-370, miR-486[334–336]
	↓	miR-17, miR-20a, miR-21, miR-27a, miR-92a, miR-126, miR-130a, miR-199a-5p, miR-221, let-7d[331]
Inflammation	↓	miR-10a[336–338], miR-22[339,340], miR-155[337,338]
Platelet activity	↑	miR-340*, miR-624*[341]
Cardiomyocyte injury	↑	miR-1, miR-133a, miR-208b, miR-499[342]

Abbreviations used in the table: CAD, coronary artery disease; miRNA: micro RNA.

Additionally, miRNA levels in circulation have been studied as predictive markers, especially in secondary prevention in CAD patients. The risk of CVD-related events or mortality increased roughly to 3-fold when miR-132, miR-140-3p and miR-210 were included in a model along with traditional risk factors, TnI, NT-proBNP and left ventricular EF.[343]

The circulating miRNAs are quite recent finding and there is a lot of unknown processes and links between different miRNAs. By progression of research and scientific methods, the number of discovered miRNAs associating with atherosclerosis will increase in the future.

Long-noncoding RNAs

Another regulatory RNA involved in the atherosclerotic process and development of CAD, is lncRNA. The lncRNAs are over 200 base pair long non-coding RNAs with the ability to influence on gene expression and genomic organization.[344,345] The lncRNAs are more like mRNA than miRNAs since they contain RNA polymerase II binding sites, 3' poly A tails and 5' caps.[346] LncRNAs can regulate immune responses, modify the function of endothelial and vascular smooth muscle cells, and alter lipid metabolism.

The H19-lncRNA increases the expression of transforming growth factor β1 (TGF-β1). TGF-β1 has many necessary protective functions in immune responses, cell proliferation and migration as well as in wound contraction, and it also triggers calcification in CAD patients.[347] Suppression of TGF-β1 in endothelial cells is achieved with CASC11-lncRNA. Its expression is decreased in CAD patients.[348] IFNG-AS1-lncRNA is overexpressed in CAD patients and the circulating levels correlate with inflammatory cytokines.[349] In endothelial cells, DQ485454 enhances transcription of ANRIL-lncRNA which is up-regulated in CAD patients. Furthermore, silencing DQ485454 resulted in changed expression of several CAD-related genes.[350] Down-regulation of NEXN-AS1-lncRNA suppresses nuclear factor κβ, decreases endothelial production of adhesion molecules and cytokines, and represses adhesion of monocytes to endothelial cells.[351] Another up-regulated lncRNA involved in endothelial proliferation, migration, and progression of cell cycle is FAL1. These functions are initiated when the PTEN/AKT signalling pathway is activated.[352] Similar to FAL1-lncRNA, LEF1-AS1-lncRNA modulates proliferation and migration of smooth muscle cells and is up-regulated in CAD patients.[353] LncRNAs partakes also in lipid metabolism. The CHROME-lncRNA inhibits HDL biosynthesis and cholesterol efflux by regulating the expression of several miRNAs.[354] In animal models, forced up-regulation of GAS5-lncRNA improved the state of hyperlipidemia, reduced myocardial damage, suppressed the

apoptosis of cardiomyocytes, and weakened oxidative stress. Accordingly, in CAD patients, GAS5-lncRNA is down-regulated.[355]

Multiple lncRNAs have been studied as diagnostic markers of CAD, and especially as prognostic markers. In risk prediction, the circulating levels of lncRNAs are mainly associated with poorer overall survival of CAD patients. For ANRIL-lncRNA[356,357] and LEF-AS1-lncRNA[353], the higher expression was linked to shorter survival of the patient. In contrast, low expression of CASC11-lncRNA correlated with reduced total survival of CAD patients.[348] In discrimination of CAD patients from controls, H19-[347], CoroMarker- (PPARδ-)[358], HULC-[359], DICER1-AS1-[359], and IFNG-AS1-lncRNA[349] were candidate biomarkers.

The lncRNAs have shown potential causative role in the development of atherosclerosis by regulating the expression of various target genes, especially miRNAs. They have shown promise as a disease marker of CAD and prognostic marker of survival and could possibly function as therapeutic targets as well.

2.5 Pregnancy-associated plasma protein A

2.5.1 Structure and function of PAPP-A

Pregnancy-associated plasma protein A (PAPP-A) was first discovered in the circulation of pregnant women. The protein was one of the four proteins identified in pregnancy plasma, but the function of PAPP-A remained unclear for two decades.[360] PAPP-A is mainly produced in the cytoplasm of syncytiotrophobalasts, but synthetization of PAPP-A is evident also in various reproductive and nonreproductive tissues.[361,362] Besides placenta, PAPP-A has been detected in e.g., adipose tissue[363], human osteoblasts[364], vascular smooth muscle cells (VSMCs)[365,366], fibroblasts[367], ascites[368], and pleura[369]. PAPP-A concentration in the circulation increases with gestational age until labor[370]. Low circulating PAPP-A concentration in the first trimester has been most predominantly associated with fetal Down syndrome[371,372], but also with pre-eclampsia, premature birth, and low birth weight of full-term babies[373–375].

PAPP-A belongs to the superfamily of metzincin metalloproteinases. Typical of these is the Zn^{2+} binding site and methionine (Met) residue located down-stream to the zinc-binding motif. The Met residue forms the so-called Met-turn motif.[376] The zinc-binding motif allows PAPP-A to be proteolytically active and the Met-turn motif directly interacts with it. Besides these characteristics, PAPP-A was not structurally similar to other protein classes in the family, and consequently was the first member of a newly formed group of pappalysins, pappalysin-1.[377] Other sequences important in the proteolytic domain of PAPP-A are the Lin-Notch repeats (LNR). LNR1 and LNR2 are located in the proteolytic domain while LNR3 is

located further at the C-terminal end of PAPP-A.[376] All of these motifs are required in the specific detection of substrate and enabling proteolytic activity. Up-stream of LNR3, there are five short consensus repeats (SCRs) also known as complement control protein modules which are involved in the binding of PAPP-A to cell surface. Especially, modules SCR3 and SCR4 are participating in the binding through heparan sulphate-like GAGs present on the cell surface.[378]

In PAPP-A protein one PAPP-A subunit of 200 kDa is bound with disulfide bonds to another PAPP-A subunit, resulting in 400 kDa sized protein. The disulfide bonds connect the two PAPP-A subunits antiparallelly thus allowing LNR1 and LNR2 to interact with LNR3. Largely, the PAPP-A in the circulation is in this form in apparently healthy individuals. The form in which PAPP-A is found predominantly in the circulation during pregnancy is a heterotetrameric 2:2 complex of two PAPP-A subunits and two subunits of proform of eosinophil major basic protein (proMBP). Thus, this form of PAPP-A is known as PAPP-A/proMBP complex.[379] The PAPP-A/proMBP complex is around 500 kDa in size and due to the complexation it is proteolytically inactive.[380,381]

The function of PAPP-A is to degrade insulin-like growth factor (IGF) binding proteins (IGFBPs) 2, 4 and 5.[382–385] The principal function of PAPP-A is to cleave IGFBP-4, which requires all the LNRs to be functional, while the cleavage of IGFBP-5 requires only LNR1 and LNR2 to be present. When IGFBP-4 is cleaved, it releases IGF-I and to some extent IGF-II, which is then able to bind to its receptor on the cell surface, type 1 IGF receptor (IGF-R1).[386] This initiates the IGF signalling pathways which have multiple effects both in normal physiology and in disease.[378] The proteolytical function of PAPP-A is more efficient when it is attached to cell surface and in close proximity to IGF-R1 similarly present on the cell surface.[387] Along with the irreversible binding with proMBP, stanniocalcin 2 (ST2) can inhibit the proteolytic activity of PAPP-A towards IGFBP-4 by covalently binding to the proteolytic domain of PAPP-A. Stanniocalcin 1 is not as efficient in inhibiting PAPP-A activity, since it cannot bind covalently to PAPP-A.[388,389] The role of PAPP-A in the IGF signalling axis is shown in **Figure 6**.

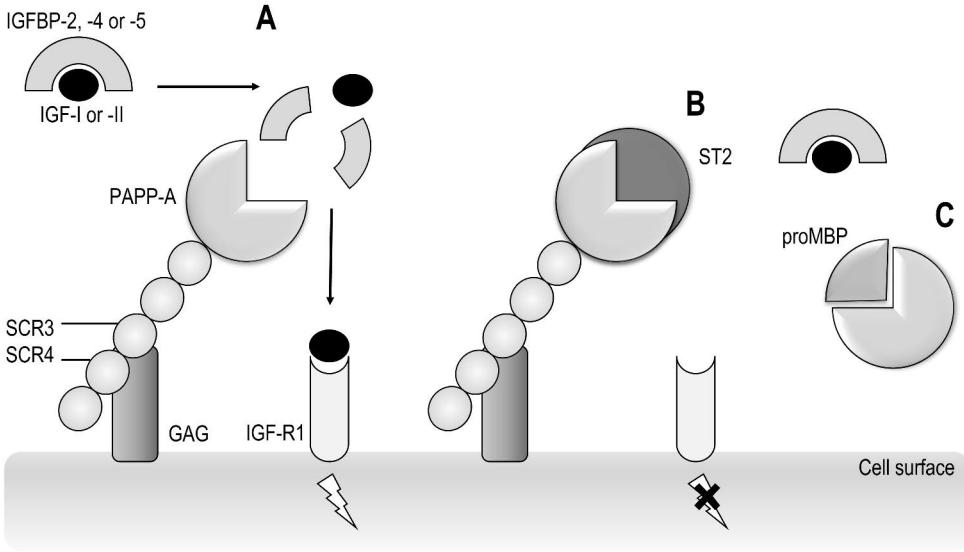

Figure 6 PAPP-A in the IGF signalling axis **A.** PAPP-A bound to cell surface via glycosaminoglycan (GAG) through short consensus repeats (SCR) 3 and 4 can cleave insulin-like growth factor binding proteins (IGFBPs) 2, 4 and 5, and thus release insulin-like growth factor (IGF) I or II. The free IGF is able to bind to type 1 IGF receptor (IGF-R1) on cell surface and activate a signalling pathway. **B.** In the presence of stanniocalcin 2 (ST2), the activity of PAPP-A is inhibited and thus the local IGF activity is inhibited. **C.** PAPP-A complexed with the proform of eosinophil major basic protein (proMBP) found predominantly in the circulation of pregnant women also inhibits the proteolytical activity of PAPP-A.

2.5.2 PAPP-A in atherosclerotic plaques

In 2001 Bayes-Genis *et al.* showed PAPP-A expression in ruptured and eroded atherosclerotic plaques with histological staining of tissue sections. Stable plaques of the coronary artery had none or minimal staining indicating presence of PAPP-A in vulnerable atherosclerotic plaques.[390] Since then, PAPP-A has been measured from the circulation of diverse CVD patients. PAPP-A seems to have a causal role in the development of atherosclerotic CVD as well. The association of PAPP-A with coronary atherosclerosis has been predominantly shown in animal models, especially in mouse models. Overexpression of PAPP-A in smooth muscle has lead to increase in the atherosclerotic lesion area while the number of lesions remained unaltered.[382] In contrast, apolipoprotein E (ApoE)-deficient mice on a high-fat diet were protected from atherosclerotic lesions when PAPP-A was genetically deleted.[391] Additionally, in a mouse model of atherosclerosis, progression of atherosclerotic plaques was halted when gene expression of PAPP-A was inactivated.[392] Likewise, the plaque burden reduced when PAPP-A activity was inhibited[393] The proatherosclerotic role of PAPP-A seems to depend on the ability to cleave IGFBP-4.[394] Thus, PAPP-A

inhibition could function as therapy for atherosclerosis-related diseases or as a preventive method.

PAPP-A is involved in multiple pathophysiological processes in atherogenesis. PAPP-A promotes lipid accumulation by contributing to the transformation of macrophages into foam cells. This occurs due to the PAPP-A activation of the IGF-1/PI3K/Akt pathway which leads to inhibition of cholesterol efflux in macrophages.[395] Also, in histological studies, PAPP-A has been colocalized with active macrophages in the unstable atherosclerotic plaque.[378]

The release of active IGF-I induces monocyte recruitment via intracellular adhesion molecule 1, vascular cellular adhesion molecule 1 and E-selectin which in turn triggers vascular inflammation. The mechanisms between IGF-I and atherosclerosis are still somewhat unclear but since PAPP-A contributes to the release of IGF-I, it possibly has a role in maintaining vascular inflammation.[396]

PAPP-A accelerates endothelial dysfunction by diminishing nitric oxide (NO) levels and promoting endothelin 1.[397] The normal endothelial function is achieved with the balance of vasodilative NO and vasoconstrictive endothelin 1. Decreased production of NO and increased synthesis of endothelin 1 are contributors of endothelial dysfunction which is a precursor for the formation of atherosclerotic lesions.[398,399]

PAPP-A partakes in the proliferation and migration of VSMCs by stimulating the proliferative capacity and migration from media to intima.[400] In mice, the opposite effect has been observed when PAPP-A has been genetically removed. There, the proliferation, and migration of VSMCs was inhibited, hence protecting against neointimal hyperplasia which precedes vascular injury.[401]

As originally shown by histological staining, PAPP-A is predominantly present in vulnerable plaques.[390] Additionally, elevated circulating PAPP-A was associated with TCFAs detected with IVUS, describing the higher plaque burden and tendency to rupture of the plaque.[402] In ApoE-deficient mice, the deletion of PAPP-A lead to more stable phenotype of atherosclerotic plaque.[392] Thus, PAPP-A may also be involved in the atherothrombus formation.

PAPP-A increases the tissue factor expression and its pro-coagulant activity in human umbilical vein endothelial cells which further activates the Akt/nuclear factor κB signalling pathway.[403] After plaque rupture, the expression of tissue factor induces thrombosis.[404]

In mouse models, inhibiting the IGFBP-4 proteolytic activity of PAPP-A by overexpressing ST2 has reduced the PAPP-A activity and consequently decreased the atherosclerotic lesion area by 47%.[405] Also ST1 can inhibit PAPP-A activity even though it is non-covalently bound to PAPP-A. ST1 reduces production of pro-inflammatory mediators, migration of aortic smooth muscle cells and inhibition of macrophage transformation to foam cells.[406]

2.5.3 Heparin-induced release of PAPP-A to circulation

Heparin is a very powerful anticoagulant and is widely used in any condition where blood clotting is undesired. Heparin medication can be in the form of either low molecular weight heparin (LMWH) or unfractionated heparin (UFH) and can be administrated intravenously (i.v.) or subcutaneously (s.c.). According to guideline of treating ACS in Finland, the dose of LMWH and UFH in STEMI is ≤0.6 mg/kg (i.v.) and 70–100 IU/kg (i.v.), respectively, while in NSTEMI the doses are 1 mg/kg (s.c.) and 70–100 IU/kg (i.v.) for LMWH and UFH, respectively.[407]

Heparin administered as an i.v. bolus elicits a very rapid increase of PAPP-A in the circulation. This phenomenon was first discovered by Terkelsen *et al.* in 2009 when STEMI patients were treated with UFH. PAPP-A elevation was not seen in patients who were not treated with heparin. Also, in mice receiving heparin PAPP-A rose rapidly and re-injection induced a new increase of PAPP-A concentration.[408] Similar findings were observed by Hájek *et al.* who also studied the dose-dependent release of i.v. administration and the clearance of the PAPP-A level. They discovered that the PAPP-A increase was related to dosage, and it remained elevated 1–2 hours after administration and reached baseline levels within 12 hours. PAPP-A concentration did not increase in the circulation of patients who underwent coronary angiogram without heparin medication and the PAPP-A level was not elevated in patients without observed coronary atherosclerosis.[409] In healthy, non-pregnant individuals, who were given i.v. UFH , a similar elevation of PAPP-A concentration was elicited even after repeated injections.[410] Tertti *et al.* measured both the complexed (with proMBP) and non-complexed forms of PAPP-A and found that the increase after heparin administration was evident with non-complexed PAPP-A, but not with complexed PAPP-A. Additionally, heparin was added after blood sampling to blood collection tube, and it did not increase either PAPP-A concentrations, indicating biological reason for this elevation.[411]

Heparin-induced PAPP-A release was extensively studied in various patient groups by Wittfooth *et al.* in 2011. All patients received either i.v. or s.c. administrated heparin and release of non-complexed PAPP-A occurred in regardless of the patient group: coronary angiography, PCI, haemodialysis and intensive care patients, as well as patients undergoing carotid endarterectomy and abdominal aortic aneurysm surgeries. Though, the original source of the PAPP-A release is still unclear. Much slower increase was obtained with s.c. administration of LMWH in intensive care patients in which the elevation of PAPP-A concentration could last up 2 hours. In haemodialysis patients who received i.v. LMWH bolus PAPP-A peaked at 5 minutes and also decreased rapidly. In addition, PAPP-A increase was lower, only median 50% from the baseline with s.c. administration of heparin, while i.v.-administrated heparin induced median 33-fold increase compared to baseline. Moreover, another anticoagulant, bivalirudin, was tested with patients undergoing

coronary angiography and PCI, and in contrast to heparin, no PAPP-A elevation was observed. Thus, the release mechanism of PAPP-A is related to interaction between PAPP-A and heparin. Likewise, PAPP-A extracted from carotid plaque tissue and abdominal aortic aneurysm plaque tissue was enhanced with LMWF-containing buffer and virtually all of the extracted PAPP-A was in non-complexed form. Further analysis of the heparin-PAPP-A interaction was conducted with gel filtration, and it revealed that the in the presence of heparin, the non-complexed PAPP-A has higher apparent molecular weight than without heparin. This strengthens the assumption of the interaction between the two and it cannot be explained by the PAPP-A complexation with proMBP since released PAPP-A is vastly in non-complexed form. Possibly, after heparin administration the PAPP-A is released in circulation with heparin attached to it..[412]

PAPP-A is bound to a GAG of a cell surface via the GAG binding site of PAPP-A that is located in the SCR3 and SCR4 modules of the PAPP-A molecule (see section 2.5.1 Structure and function of PAPP-A). However, this binding can be reversed with the addition of heparan sulphate or heparin GAGs.[378] Therefore, the assumed mechanism for the heparin-induced release of PAPP-A is that the heparin, LMWH or UFH, functions as s a GAG and binds to GAG binding site on PAPP-A whilst releasing PAPP-A from binding with cell surface GAG. This results in the detachment of PAPP-A from the cell surface.

Levels of IGFBP-4 are not similarly affected by heparin administration, so clinical utilization of IGFBP-4 fragments formed due to PAPP-A activity are studied as an equivalent biomarker to PAPP-A. The indirect measurement of PAPP-A activity is based on immunoassays of IGFBP-4, C-terminal end of IGFBP-4 (CT-IGFBP-4) and N-terminal end of IGFBP-4 (NT-IGFBP-4).[413] Both CT-IGFBP-4 and NT-IGFBP-4 have shown promise as a risk-predictive marker of MACE in patients with ischemia[414] or STEMI patients treated with PCI[413,415].

2.5.4 PAPP-A as a biomarker in cardiac conditions

PAPP-A assays

Most commercial assays measure all forms of PAPP-A together (i.e., total PAPP-A, tPAPP-A) and many are intended to be used in prenatal screening. In this setting, low detection limit is not relevant because concentrations are clearly elevated even in Down syndrome pregnancies as compared to amounts discovered in cardiac-related states or in apparently healthy individuals. The tPAPP-A assays measure PAPP-A whether it is complexed with proMBP or not, and the forms cannot be differentiated from each other.[416] In apparently healthy individuals, PAPP-A is mainly in complexed form (cPAPP-A), while in cardiac conditions PAPP-A is in

non-complexed, free form (fPAPP-A). Changes in individuals mostly occur below the stated detection limit of tPAPP-A assays and thus these are not able to reliably measure the fPAPP-A changes between individuals.[417,418] There are two methods to indirectly measure the fPAPP-A concentration. The first one uses two separate immunoassays targeting tPAPP-A and cPAPP-A. The fPAPP-A concentration is calculated as a difference of these results.[418] Another method is to measure IGFBP-4 fragments, NT-IGFBP-4 and CT-IGFBP-4, which reflect the amount of active fPAPP-A.[413]

As described in section 2.5.2, the atherosclerotic role of PAPP-A is mainly dependent on the cleavage of IGFBP-4, so the measurement of fPAPP-A form is at the essence when using PAPP-A as a cardiac-related marker. As a part of this thesis, the first direct fPAPP-A immunoassay was developed which was able to sensitively measure these low fPAPP-A concentrations observed in cardiac conditions.[419]

There was interest in the early 2000s to study PAPP-A in cardiac conditions, but contradictive results were obtained which possibly were influenced by the use of tPAPP-A assays as the measurement method and samples of patients who had received heparin when the heparin-effect was still unknown. Also, since standardized reference material for PAPP-A is not available, comparing results between assays was difficult. Some assays inform PAPP-A concentration as ng/mL while others use mIU/L as the unit. Roughly 1 mIU/L corresponds to 4.5 ng/mL, but clear conversion factor is not easy to generate due to heterogenous assay methodologies and existing different molecular forms that can be detected differently by different assays. Nevertheless, studies regarding the atherosclerotic role of PAPP-A/IGF/ST2 axis have remained as a topic of interest. The potential of fPAPP-A as a cardiac marker is still evident and with the advanced measurement technologies i.e., direct fPAPP-A assay, and indirect measurement of fPAPP-A activity through IGFBP-4 fragments, the interest in fPAPP-A hopefully gains more attention in upcoming years.

PAPP-A as a marker of acute coronary syndromes

Differences in circulating PAPP-A levels was first studied by Bayes-Genis *et al.* and found that UAP and MI patients had significantly higher concentration of PAPP-A than healthy control subjects or suspected chronic CAD patients. In the beginning of cardiac-related PAPP-A research, the biomarker was suggested as a diagnostic marker in ACS patients. The assumption was that since PAPP-A was found in vulnerable and thus in more unstable plaques, it could perform as diagnostic marker present in circulation earlier than necrosis-associated cTns.[390] Despite of the heparin-effect to PAPP-A molecule, several studies have found differences of PAPP-A concentration in the circulation of ACS patients compared to controls. Additionally,

prognostic capability of circulating PAPP-A has been evaluated in ACS patients. Most studies have linked high PAPP-A concentration with poorer outcome when assessing both short- and long-term risk. Diagnostic and prognostic studies of ACS patients involving circulating PAPP-A are presented in **Table 7** (page 65). Only studies where reportedly no heparin treatment was used, or the use was unlikely are included in the table.

PAPP-A as a marker of chronic coronary artery disease

Chronic CAD patients have been a study subject as well in regards of circulating PAPP-A concentration. Mainly, studies where PAPP-A is evaluated as a prognostic marker have been performed but, in few cases, also PAPP-A concentration has differed with diseased patients and controls. These studies are summarized in

Table 8 (page 67). Based on these clinical studies, elevated circulating PAPP-A concentration predicts poorer outcome in chronic CAD patients.

PAPP-A has been associated with imaging findings of CAD. In a study by Wu *et al.* in 2016, 3-vessel virtual histology (VH)-IVUS was used to study TCFA burden in CAD patients.[402] In total, 154 samples from stable angina or NSTE-ACS patients directed for PCI were analysed. Based on PAPP-A concentration, the patients were divided into tertiles. Patients in the highest PAPP-A tertile had significantly higher necrotic area at MLA site, necrotic core volume at culprit vessel and total (3-vessel) necrotic core volume than patients in the other two tertiles. Also, PAPP-A concentration correlated with the number of TCFAs. Patients in the highest PAPP-A tertile had the lowest cumulative event-free survival of MACE within 1-year follow-up period. Guven *et al.* (2017) studied the circulating PAPP-A association with CACS and carotid intima-media thickness (CIMT) in patients with elective CT due suspicion of subclinical atherosclerosis.[420] In 99 patients, CACS was evaluated with CT and CIMT with carotid ultrasound. PAPP-A, CACS and CIMT were significantly higher in CAD patients (i.e., patients with at least one coronary artery plaque), and PAPP-A strongly correlated with CACS (r=0.805) and moderately with CIMT (r=0.532). PAPP-A cut-off concentration of 2.35 ng/mL indicated the presence of vascular lesions.

Table 7 PAPP-A as a diagnostic and prognostic marker of acute coronary syndromes.

Diagnostic			
Study	**Study population**	**Controls**	**Outcome**
Heeschen *et al.* (2005)[421]	NSTE-ACS (N=323)	Stable angina (N=105) and no CHD (N=197)	Higher PAPP-A concentration in ACS patients than in both control groups (p=0.007 and p<0.001, respectively)
Elesber *et al.* (2007)[422]	ACS (N=19)	Non-cardiac chest pain (N=40)	Higher PAPP-A concentration in ACS patients (p=0.002)
McCann *et al.* (2008)[423]	STEMI (N=73) and NSTEMI (N=125), combined (N=198)	Unstable angina (N=124) and non-cardiac chest pain (N=93), combined (N=217)	Higher PAPP-A concentration in combined group of MI patients (p=0.044)
Iversen *et al.* (2009)[424]	High-risk ACS (N=415)	Low-risk ACS (N=123)	In high-risk ACS samples detectable PAPP-A (>4 mIU/L) in more samples than in low-risk ACS samples (p<0.001)
Body *et al.* (2011)[425]	MI (N=127)	Non-MI (N=586)	Higher PAPP-A concentration in MI patients (p=0.005)
Hajek *et al.* (2012)[426]	STE-ACS (N=18) and NSTE-ACS (N=27)	Non-ACS (N=22)	Higher PAPP-A concentration in ACS patients (p=0.006)
Schaub *et al.* (2012)[427]	MI (N=76)	Non-MI (N=322)	Higher PAPP-A concentration in MI patients (p<0.001)
Wlazeł *et al.* (2013)[428]	cTnI-positive patients with first MI (N=40)	No history with CVDs (N=38)	Higher PAPP-A concentration with MI patients (p=0.003), PAPP-A AUC=0.72 for ACS presentation
Mehrpooya *et al.* (2020)[429]	NSTEMI (N=25)	Unstable angina (N=68)	Higher PAPP-A concentration in NSTEMI patients (p=0.003)
Prognostic			
Study	**Study population**	**Endpoint**	**Outcome**
Heeschen *et al.* (2005)[421]	NSTE-ACS (N=323)	Death or non-fatal MI, follow up time 30 days	PAPP-A cut-off concentration >12.6 mIU/L independent predictor of the endpoint. Better prediction in patients with TnT concentration >0.1 µg/mL and PAPP-A cut-off concentration >7.0 mIU/L.

Table 7 continues			
Kavsak *et al.* (2009)[430]	Symptoms of cardiac ischaemia at admission (N=320), 3rd (highest) PAPP-A tertile (N=108)	All-cause mortality, follow-up time 2 years or 10 years	In highest PAPP-A tertile (>1.62 mIU/L), mortality within 2 years (p=0.03) or 10 years (p=0.05)
Iversen *et al.* (2009)[431]	High-risk NSTE-ACS (N=123), 4th (highest) PAPP-A quartile (N not reported)	Death or non-fatal MI, median follow-up time 2.95 years	In highest PAPP-A quartile (>15.5 mIU/L) vs other quartiles combined, greatest risk of death (p=0.003) or death and non-fatal MI combined (p=0.002). Highest PAPP-A quartile independent predictor of death.
Iversen *et al.* (2010)[432]	Low-risk NSTE-ACS (N=415), 4th (highest) PAPP-A quartile (N=103)	All-cause mortality or non-fatal MI, median follow-up time 3.4 years	In highest PAPP-A quartile (>12.4 mIU/L) greater risk of the endpoint after 3 months or 1 year. PAPP-A AUC=0.76 for death within 3 months.
Lund *et al.* (2010)[433]	NSTEMI (N=267), analysed with 2-assay fPAPP-A method and tPAPP-A assay[418], 3rd (highest) PAPP-A tertile (N=89)	All-cause mortality and non-fatal MI, follow-up time 1 year	Lowest event-free survival in highest fPAPP-A tertile (>1.74 mIU/L), highest tPAPP-A tertile (>2.99 mIU/L) not significant. The fPAPP-A independent predictor and in combination with elevated cTnI (>0.03 µg/L).
Table 7 continues			
Bonaca *et al.* (2012)[434]	NSTE-ACS (N=3 782), part of MERLIN-TIMI 36 Trial	CVD-related death or recurrent ischaemic event, median follow-up time 348 days	Short- (30 days) and long-term (1 year) prediction of CVD-related death or recurrent ischaemic event with PAPP-A cut-off concentration ≥6.0 µIU/mL. Lowest evenr-free survival if PAPP-A ≥6.0 µIU/mL and cTnI >0.04 µg/L)
von Haehling *et al.* (2013)[435]	ACS (N=1 229) and stable angina (N=1 339)	CVD-related death, MI, ischaemic stroke, or stent thrombosis, follow-up time 90 days	Independent predictor of CVD-related death, MI, ischaemic stroke, or stent thrombosis within 90 days with PAPP-A cut-off concentration 34.6 mIU/L

Abbreviations used in the table: NSTE-ACS, non-ST-elevation acute coronary syndrome; CHD, coronary heart disease; PAPP-A, pregnancy-associated plasma protein A; ACS, acute coronary syndrome; STEMI, ST-elevation myocardial infarction, NSTEMI, non-ST-elevation myocardial infarction; MI, myocardial infarction; STE-ACS, ST-elevation ACS; cTnI, cardiac troponin I; CVD, cardiovascular disease; AUC, area under the curve; TnT, troponin T; fPAPP-A, free PAPP-A; tPAPP-A, total PAPP-A.

Table 8 PAPP-A as a diagnostic and prognostic marker of chronic or stable coronary artery disease.

Diagnostic			
Study	**Study population**	**Controls**	**Outcome**
Cosin-Sales *et al.* (2005)[436]	Chronic stable angina pectoris (N=546) divided to single-vessel disease (N=127) and multi-vessel disease (N=419)	No CAD (N=97)	Higher PAPP-A concentration in patients with single-vessel (p=0.012) or multi-vessel disease (p<0.001) compared to controls. Higher PAPP-A concentration in patients with multi-vessel disease compared to single-vessel disease (p<0.001). PAPP-A AUC=0.75 for presence of CAD.
Mueller *et al.* (2006)[437]	Peripheral artery disease (N=433), 4th (highest) PAPP-A quartile (N=216)	Controls (N=433) matched with sex, age (±2 years) and diabetes status	Higher PAPP-A concentration in peripheral artery disease patients than in controls without CAD (p<0.001). The highest PAPP-A quartile (>1.163 mIU/L) independent predictor of symptomatic peripheral artery disease and when adjusted with clinical risk factors.
Heider *et al.* (2010)[438]	Symptomatic carotid stenosis (N=37)	Asymptomatic carotid stenosis (N=29)	Higher PAPP-A concentration in patients with unstable plaques (p=0.047) and in asymptomatic patients (p=0.025).
Prognostic			
Study	**Study population**	**Endpoint**	**Outcome**
Elesber *et al.* (2006)[439]	Chronic CAD (N=103)	Death, ACS and revascularization, median follow-up time 4.9 years	Highest PAPP-A quartile (>4.8 mIU/L) had lowest survival of all-cause mortality or ACS
Consuegra-Sanchez *et al.* (2008)[440]	Chronic stable angina (N=663)	All-cause mortality, median follow-up time 8.8 years	Poorer survival rate if PAPP-A concentration >4.6 mIU/L, independent predictor with PAPP-A cut-off concentration 4.8 mIU/L
Iversen *et al.* (2011)[441]	Chronic CAD (N=4 372), CLARICOR Trial	MI, all-cause mortality or both, median follow-up time 2.8 years	Elevated PAPP-A concentration (>4 mIU/L) associated with increased risk of endpoints

Table 8 continues			
Schulz *et al.* (2011)[442]	Chronic CAD (N=228)	All-cause mortality, cardiovascular death or all-cause mortality/non-fatal MI/ hospitalization, median follow-up time 1108 days	PAPP-A cut-off concentration >2.7 mIU/L associated with all endpoints
Zengin *et al.* (2015)[443]	CAD (N=927)	Cardiovascular death, median follow-up time 5.0 years	Patients with subacute MI, unstable angina, NSTEMI or STEMI had higher PAPP-A concentration than stable angina patients or patients without CAD. Poorer cumulative event-free survival in patients with PAPP-A concentration >11.40 IU/L.
Nilsson *et al.* (2020)[444]	Chronic CHD (N=1 996), placebo group of CLARICOR study	First occurrence of cardiovascular event or death, median follow-up time 10 years	Elevated PAPP-A levels (>4 mIU/L) associated with increased long-term mortality in chronic CAD patients

Abbreviations used in the table: CAD, coronary artery disease; PAPP-A, pregnancy-associated plasma protein A; AUC, area under the curve; ACS, acute coronary syndrome; MI, myocardial infarction; NSTEMI, non-ST-elevation MI; STEMI, ST-elevation MI; CHD, coronary heart disease.

PAPP-A as a marker of other cardiac-related conditions

Elevated circulating PAPP-A concentration has been additionally observed in HF patients. Often, destabilization of coronary plaques or plaque ruptures contribute to the development of HF, because of the continuous inflammatory state in the arteries. Traditionally, NT-proBNP has been used as a biomarker for HF and it has gained fundamental status in clinical practice. However, certain conditions such as obesity and renal dysfunction or the use of concomitant medication may affect to the NT-proBNP concentration in circulation.[445] In HF, sudden change in the disease state is possible which makes the monitoring and risk prediction difficult. Therefore, alternative biomarkers, especially reflecting the clinically silent inflammation process in atherosclerotic plaques, would be ideal.[446] In 2017, Dembic *et al.* studied the risk of death in 683 HF patients. The mean follow-up time of the patients was 7 years and in the analysis PAPP-A concentration was divided into quartiles. Kapplan-Meier analysis revealed that the highest PAPP-A quartile (>13.51 mIU/L) had lowest event-free survival rate and the risk of death was significantly increased [hazard ratio (HR) =1.42].[447] Similarly, Konev *et al.* (2020) showed that with the measurement of CT-IGFBP-4, which indirectly reflects the amount of active PAPP-A, the risk of all-cause mortality in acute HF patients was increased. They followed 156 acute HF patients for a 1 year. Surviving patients had significantly lower circulating CT-IGFBP-4 levels and the concentration independently predicted the all-cause mortality (AUC=0.727 and HR=3.26). The risk prediction of mortality within 1 year was further enhanced when CT-IGFBP-4 was combined with NT-proBNP and CRP (AUC=0.788 and HR=10.04 adjusted with clinical risk factors).[448] Also, PAPP-A has been found as a biomarker correlating with reduced coronary flow reserve in HF patients with preserved EF.[449] More particularly, in a recent study by Chandramouli *et al.* (2022), proteomic differences between sexes was studied in similar cohort of HF patients with preserved EF. Coronary microvascular dysfunction was classified if coronary flow reserve was <2.5. In men, PAPP-A was discovered as one of the biomarkers significantly associated with low coronary flow reserve, which in contrast was not observed in females.[450] Thus, circulating PAPP-A could be a possible marker in monitoring and risk stratification of HF patients.

Maternal circulating PAPP-A concentration is measured in the first trimester mainly in the screening purpose of Down syndrome pregnancies or risk of developing pre-eclampsia. However, in recent studies of maternal first trimester PAPP-A has been associated with fetal congenital heart defects.[451] This is a severe condition where defects are fatal in nature or require intervention in early years or at least long-term follow-up.[452] One risk factor for congenital heart defect is the increased measurement of nuchal translucency but alone the sensitivity is poor.[453] Alanen *at al.* (2019) studied 31 144 pregnancies out of which 71 were diagnosed with severe congenital heart defect. PAPP-A and free beta human chorionic

gonadotropin (fβ-hCG) were measured from maternal serum in the first trimester. In general, detection of congenital heart defects with serum biomarkers outperformed the mere measurement of nuchal translucency and sensitivities were further improved when adding prior risk and nuchal translucency measurement to these biochemical markers. Even with normal nuchal translucency measurement, the low levels of PAPP-A and fβ-hCG could indicate the presence of severe congenital heart defect.[454] Similar results were obtained by Hematian *et al.* (2021) where lower PAPP-A levels and increased nuchal translucency measurement were linked to greater risk of congenital heart defects. Especially, in the critical type of congenital heart defect, both the PAPP-A and fβ-hCG levels were decreased compared to controls.[455] Naturally, further validation of PAPP-A use in this setting is required but it is a promising biomarker in detecting severe congenital heart defect from maternal first trimester serum.

A novel target in using PAPP-A as a biomarker is the severe acute respiratory syndrome coronavirus 2 (SARS-CoV-2). Even though SARS-CoV-2 infection mainly affects to respiratory system, the prevalence of CVD in infected individuals is roughly 8–12%.[456] The infection can cause myocardial damage and arrhythmia due to systemic inflammation in the body. Many patients with clinically observed cardiovascular changes, also have enhanced cytokine response.[457,458] Additionally, destabilization of atherosclerotic plaques and hypoxia may contribute to the cardiovascular damage during SARS-CoV-2 infection.[458] Sanchez *et al.* published in 2021 findings where PAPP-A and ischemia-modified albumin were evaluated as early markers of SARS-CoV-2 infection. Both markers were elevated during early and acute phases of infection, but especially in the early phase these markers alone (PAPP-A AUC=0.801 and ischemia-modified albumin AUC=0.941) proved to be sensitive predictors of the infection and in combination even more accurate (AUC=0.947). Interestingly, PAPP-A was elevated in PCR-positive SARS-CoV-2 infected individuals who did not yet have measurable IgG response which empowers the role of PAPP-A as early marker of the infection.[459] In regards to pregnant women and SARS-CoV-2 infection, Trilla *et al.* (2022) discovered that PAPP-A levels were elevated in symptomatic individuals but the prevalence of obstetric complications, such as pre-eclampsia, was not increased.[460] However, in a previous meta-analysis by Di Mascio *et al.* (2020), pre-eclampsia was more common in SARS-CoV-2 infected pregnant mothers than in uninfected ones.[461] Altogether, SARS-CoV-2 infection could advance the thrombotic episodes and inflammatory processes during infection and for which PAPP-A could function as a biomarker.

3 Aims of the study

The overall aim of this study was to develop an immunoassay for the direct measurement of non-complexed form of PAPP-A, i.e., fPAPP-A and evaluate its clinical performance as a cardiac-related risk-predictive marker in ACS patients as well as its association with coronary atherosclerotic burden in patients with suspected obstructive CAD. Also, the aim was to study the heparin-induced release of fPAPP-A in relation to coronary atherosclerotic findings.

The aims, described in detail, were:

I: To develop an immunoassay for the direct detection of fPAPP-A and determine the analytical performance characteristics according to the relevant guidelines of the Clinical and Laboratory Standards Institute (CLSI). The clinical performance of fPAPP-A as a cardiac-risk predictive marker was assessed with survival analysis of ACS patients classified based on their plasma fPAPP-A concentration. The clinical performance was also compared to tPAPP-A assay as well as to fPAPP-A measured with an indirect method as a difference of separate assays measuring tPAPP-A and cPAPP-A (i.e., 2-assay fPAPP-A).

II: To study the relation of the heparin-induced release of fPAPP-A to the athrerosclerotic burden in patients with suspected obstructive CAD. The presence of obstructive CAD and coronary atherosclerotic burden were evaluated with hybrid coronary CTA and PET-MPI. The released concentration of fPAPP-A was compared to imaging findings.

III: To evaluate the fPAPP-A concentration in relation to coronary atherosclerotic findings in coronary CTA and PET-MPI of patients with suspected obstructive CAD. Thorough analysis of imaging findings was performed for each patient, which were then classified based on the severity of CAD.

4 Summary of Materials and Methods

A summary of materials and methods used in this study with some supplemental information is presented here. The complete descriptions of the materials and methods for each individual study can be found in the original publications **I–II** and manuscript **III**.

4.1 Direct free PAPP-A assay

4.1.1 Free PAPP-A assay design

The developed direct fPAPP-A assay is a sandwich-type immunoassay utilizing a lanthanide chelate label as a tracer. The capture antibody was labelled with biotin which was immobilized onto streptavidin surface. The developed assay was used in publications **I-III**.

The assay principle in short: Biotinylated monoclonal Ab (mAb) specific for fPAPP-A was bound to streptavidin-coated microtiter-well which allowed binding of fPAPP-A in the sample or recombinantly produced non-complexed PAPP-A (rPAPP-A) in calibrators. The mAb that was used as tracer recognizes PAPP-A whether or not it is in complex with proMBP. Time-resolved fluorescence was measured from the bottom of the well using a multilabel counter. The specific assay protocol is presented in **Table 9**.

Table 9 Protocol of developed direct free pregnancy-associated plasma protein A (fPAPP-A) immunoassay.

Solid phase		
Microtiter plate	Streptavidin-coated 96-well plate, Kaivogen Oy, Finland	
Capture immobilization		
Capture	Biotinylated in house fPAPP-A recognizing mAb	200 ng/well
Capture diluted to	Buffer Solution RED, Kaivogen Oy	25 µL/well
Incubation	Plate shaker, PerkinElmer/Wallac, Finland	1 h, room temperature, slow shaking
1st wash		
Washing solution	Wash Concentrate 25x, Kaivogen Oy	Diluted to 1-fold with mQ-water
Washing	Plate washer, PerkinElmer/Wallac	2 times/well
Sample and tracer addition		
Calibrator or sample	7.5% BSA-TSA ± rPAPP-A **OR** undiluted serum/heparinized plasma	30 µL
Tracer	tPAPP-A recognizing mAb 3C8, HyTest Ltd, Finland, labelled with Eu^{3+}	100 ng/well
Tracer diluted to	PAPP-A Assay Buffer: 0.05 mol/L Tris-HCl, pH 7.75, 0.1 g/L Tween 40, 0.5 g/L bovine-γ-globulin, 20 µmol/L DTPA, 5 g/L BSA, 0.01 g/L native mouse IgG, 0.005 g/L denaturated mouse IgG, 0.6 mol/L NaCl, 0.1 mol/L $CaCl_2$, 7.5 g/L CHAPS, 0.5 g/L NaN_3	10 µL/well
Incubation	iEMS incubator/shaker, Thermo Electron Corporation/Labsystems, Finland	1.5 h, +36°C, 900 rpm
2nd wash (washing solution and washer same as in 1st wash but each well washed 6 times)		
Drying		
Dryer	Hot air blower	5 min, +60°C
Measurement		
Time-resolved fluorometer	Victor®X4 Multilabel counter, PerkinElmer/Wallac λ_{Ex} 340 nm, λ_{Em} 615 nm, measurement delay 250 µs, measurement window 750 µs	

Abbreviations used in the table: mAb, monoclonal antibody; BSA-TSA, bovine serum albumin in tris-saline-azide; rPAPP-A, recombinantly produced non-complexed PAPP-A; tPAPP-A, total PAPP-A; DTPA, diethylenetriaminepentaacetic acid; IgG, immunoglobulin G; CHAPS, 3-[(3-cholamidopropyl)dimethylammonio]-1-propanesulfonate hydrate.

4.1.2 Recombinantly produced PAPP-A

The rPAPP-A was used as the calibrator in the immunoassay (used in publications **I-III**). Desired concentration of rPAPP-A was diluted into tris-buffered saline with azide (TSA) and bovine serum albumin (BSA) [50 mmol/L Tris-HCl, pH 7.75, 150 mmol/L NaCl, 0.5 g/L NaN3, 60 g/L BSA (Bioreba AG, Switzerland)]. Pre-prepared calibration series was stored at -20°C until use.

The rPAPP-A was produced in HEK293T cells and purified with heparin and anti-FLAG columns.[412,462] The FLAG-tagged full-length PAPP-A expression plasmid was a gift from Prof. Xuezhong Qin from Loma Linda University.

4.1.3 Antibodies

Antibodies binding exclusively the free form of PAPP-A were produced in-house by traditional hybridoma technique. Three BALB/c mice were immunized with three doses of purified rPAPP-A. Spleen cells were extracted and hybridized with SP2/0 cells. Produced hybridomas were screened for positive binding to Eu-labelled rPAPP-A and negative binding to Eu-labelled cPAPP-A.

The cPAPP-A used in the screening was purified from 3rd trimester pregnancy serum. For the purification, the serum was diluted in 10-fold into TSA and filtered with 0.22 µm pore size filter. Diluted serum was bound to proMBP-binding immunoaffinity column which contained pro-MBP-specific mAb 234-10 (Statens Serum Institute, Denmark) bound to Sepharose 4B matrix. TSA was used for washing and TSA supplemented with 1 M NaCl was used for the elution of cPAPP-A. Collected fractions containing cPAPP-A were pooled and concentrated with 30 kDa Amicon Ultra centrifugal filter device (Merck, USA) into 150 mM NaCl.

The purified cPAPP-A and rPAPP-A were labelled with europium (Eu-)N1 chelate [N1-(4-isothiocyanatobenzyl)diethylenetriamine-N1,N2,N3,N4-tetracis(acetic acid)]. For cPAPP-A 100-fold molar excess of the chelate was used while with rPAPP-A a 250-fold molar excess was used. The labelling reaction occurred at room temperature (RT) in 50 mM carbonate buffer solution (pH 9.6) during overnight incubation in the dark. After incubation, the labelled PAPP-A was purified with NAP-5 and NAP-10 columns (GE Healthcare, USA) using TSA for column equilibration, wash, and elution. The labelling degree was determined against an Eu-standard. Both the labelled PAPP-A and the Eu-standard were diluted into Europium Fluorescence Intensifier (EFI, Kaivogen Oy, Finland) and the measured time-resolved fluorescence signal from these was compared to each other.

The hybridoma cell lines were screened for fPAPP-A antibody production by testing the cell culture medium in a sandwich-type immunoassay. First, 50 µl of cell culture medium and 100 µl of red assay buffer (Kaivogen Oy) were added to anti-mouse antibody coated 96-well plate well (Kaivogen Oy). The well was incubated

at RT for 2 h in slow shaking and washed two times. Then, 10 ng of Eu-N1 labelled rPAPP-A or cPAPP-A was added to the well. The well was again incubated for 2 h at RT with slow shaking. After, the well was washed twice and 200 µl of EFI was added. After 10-minute incubation, the fluorescence signal was measured in time-resolved mode. The cell lines with culture medium producing high signals with labelled rPAPP-A but low signals with labelled cPAPP-A were chosen for subcloning and further immunoassay testing.

The produced fPAPP-A antibodies were purified with protein G columns and labelled with Eu^{3+}-chelate (protocol described below). The antibodies were tested extensively in sandwich-type immunoassays in combinations with each other and with tPAPP-A recognizing antibodies developed in the same process or with those that were kindly received from HyTest (Finland) to find optimal antibody combinations for the direct fPAPP-A immunoassay.

Labelling of antibodies

The capture antibodies for the immunoassay were labelled with 10- to 20-fold molar excess of biotin isothiocyanate (synthesized in-house) and tracer antibodies with 20- to 40-fold molar excess of intrinsically fluorescent [2,2′,2″,2‴-{[2-(4-isothiocyanatophenyl)ethylimino]bis-(methylene)bis{4-{[4-(alfa-galactopyranoxy) phenyl]ethynyl}pyridine-6,2-diyl}bis(methylenenitrilo)}tetrakis(acetato)] Eu^{3+}-chelate (synthesized in-house)[463], as described previously[464]. Labelled antibodies were stored at +4 °C.

4.1.4 Assessment of analytical assay performance

Determination of analytical limits included the Limit of Blank (LoB), LoD and Limit of Quantitation (LoQ). These were performed according to CLSI guidelines, EP17-A2[465] for LoB and LoD, and EP5-A2[466] and EP17-A2[465] for LoQ. The LoB and LoD were determined according to Classical Approach where 5 batches of BSA-TSA was used as zero calibrators (blank samples) and 7 serum sample pools as the low-level samples. The fPAPP-A concentration was targeted at 1–5×LoB, here concentrations of 0.3–0.9 mIU/L were used. The assay was repeated on 4 consecutive days, and each sample was measured in 4 replicates. Parametric data analysis approach was used. The determined LoQ described the within-laboratory precision. For this, fPAPP-A concentration in 8 serum sample pools (0.3–8.5 mIU/L of endogenous fPAPP-A) were measured on 20 consecutive days in 4 replicates, and results were calculated as indicated in the CLSI guidelines with 20%CV as the accuracy goal for the developed assay.

Matrix effect in the developed assay was estimated by studying matched serum, lithium heparin (LiH) plasma, and EDTA plasma samples from healthy donors (N=12). In the samples 30 mIU/L of rPAPP-A was added and measured concentrations were compared with similarly supplemented BSA-TSA for calculating recoveries.

Dilution linearity was assessed by measuring serial dilutions up to 1/243 of 3 endogenous fPAPP-A serum samples and a healthy serum pool where varying amounts of rPAPP-A was added. One serum sample containing rPAPP-A and one endogenous serum sample were diluted in both BSA-TSA and healthy serum pool (0.6 mIU/L of endogenous fPAPP-A). Two additional endogenous serum samples were diluted in TSA-BSA. Undiluted concentrations of the samples were 33.6–233.5 mIU/L.

Interference of cPAPP-A in the assay was assessed by adding 3rd trimester pregnancy serum into patient samples (N=2; 7.7 or 52.3 mIU/L) or into rPAPP-A–supplemented (0.3 or 30 mIU/L) healthy sera (N=3). The concentration of the supplemented cPAPP-A in samples was either 100 or 1 000 mIU/L.

Comparison of methods was performed by analyzing admission serum samples of 389 patients who were hospitalized due to suspected ACS. The developed fPAPP-A assay was evaluated against the previously published 2-assay fPAPP-A detection method[418]. In this reference method, the measured cPAPP-A concentration was subtracted from the measured tPAPP-A concentration. The analytical detection limits (zero calibrator+3SD) in the 2-assay fPAPP-A method were 0.18 and 0.23 mIU/L for total and complexed assays, respectively. Functional detection limits (imprecision <20%) were 0.27 and 0.70 mIU/L for total and complexed assays, respectively. For direct fPAPP-A assay, only samples that had concentration >LoD and concentration CV% <20 were included; for the 2-assay fPAPP-A method, only such samples in which concentrations of both assays were above the analytical detection limit and concentration CV% <20 were included. In total, 312 samples met these criteria.

fPAPP-A concentration in the reference population was determined with samples from 147 healthy individuals. Results of 14 samples (10%) were rejected due to high CV% (>20) and insufficient volume to repeat the measurement. Concentrations <LoD (10%) were included in the data analysis but as a concentration of LoD/2. In this reference panel, 62 (47%) individuals were men and the median age (25th–75th percentile) was 56 (50–71) years.

Stability of rPAPP-A and endogenous fPAPP-A was studied by storing aliquoted samples at +4°C, RT, or +37°C for 1 or 7 days or by subjecting aliquots to 1, 3, or 5 freeze–thaw cycles. rPAPP-A concentrations of 1, 10, and 100 mIU/L were added to buffer and 2 healthy sera. Additionally, 2 patient samples with endogenous fPAPP-A (6.4 and 73.2 mIU/L) were included in the experiment.

Clinical performance of the developed fPAPP-A assay was assessed by studying fPAPP-A concentrations in suspected ACS patients (N=389). Available serum samples from non-heparinized patients diagnosed with NST-ACS upon hospitalization were included in the study (N=197)[433]. Patients were divided into 2 groups based on the presentation of a predetermined end point. The end point included MI or death and was met during the 1-year follow-up period by 46 (23%) patients. Median age (25^{th}–75^{th} percentile) and number (percentage) of men in the groups were 76 (64–81) years and 29 (63%) for patients who met the end point and 69 (58 –77) years and 90 (60%) for those who did not. For survival analysis, the same patients were divided into tertiles based on the direct fPAPP-A concentrations or the previously determined 2-assay fPAPP-A and tPAPP-A concentrations and also to cTnI positive and negative groups (cTnI ≥30 µg/L or <30 µg/L).

4.2 Clinical samples

The study protocols for the collection of blood samples were approved by the local ethics committees, and the studies were conducted in accordance with the Declaration of Helsinki as revised in 2013. All samples were collected after informed consent of the participants.

Study **I**: Samples of known endogenous fPAPP-A concentration were collected at the Hospital District of Helsinki and Uusimaa during carotid endarterectomy or abdominal aortic aneurysm surgeries and appropriate permits were acquired upon collection. In the preparation of LoD and LoQ samples, these samples were diluted with healthy serum pool from volunteer donors. In order to achieve samples with desired concentration, also samples containing endogenous fPAPP-A were pooled, if necessary. Similarly, these samples containing varying amounts of endogenous fPAPP-A were used in the linearity and cPAPP-A interference studies together with pooled healthy sera. In addition, the samples were utilized when studying accelerated stability of endogenous fPAPP-A as well as endurance in repeated freeze-thaw cycles. Pooled serum sample of 3^{rd} trimester pregnancy was collected from healthy volunteers and used in the cPAPP-A interference study. A patient panel representing the reference population was purchased from Labquality, Finland. Samples from ACS patients were collected at the Turku University Central Hospital, and appropriate permits were granted at the time of collection. These samples were used in predicting the 1-year risk of MI or death with direct fPAPP-A assay, 2-assay fPAPP-A and tPAPP-A assay. Samples from only affirmatively non-heparinized patients were included in the study.

Study **II**: Patients scheduled for coronary CTA were given a single i.v. dose (0.2 mg/kg) of LMWH (enoxaparin, Klexane®, Sanofi Oy, Finland). In the first part of the study, blood sample was collected from eight patients at baseline and 3, 5 and

10 minutes after heparin injection. The peak fPAPP-A release was observed at 5 minutes for the majority of the patients. Therefore, in rest of the patients, blood samples were drawn at baseline and at 5 minutes after administration of heparin. The samples were collected at Turku University Central Hospital and ethical approval was granted prior collection.

Study **III**: The collection at the Turku University Central Hospital of serum from patients with suspected obstructive CAD undergoing coronary CTA and PET-MPI continued without the administration of heparin. Samples were collected between March 2016 and January 2019. In total, 252 samples were collected out of which 30 were excluded (previous CAD N=3, previous MI or obstructive CAD documented as ≥50% diameter stenosis by ICA or anomalous coronary anatomy N=2, severe valvular heart disease N=3, error in blood sampling N=1, strongly hemolyzed blood sample N=10, failure to perform scan due to contra-indications N=3, or non-diagnostic image quality N=8). Thus, the final study population consisted of 222 patients without previous history of CAD. Routine practice at Turku University Central Hospital is that patients initially undergo coronary CTA using a hybrid PET-CT scanner, and immediately after the coronary CTA, the attending physician performs initial assessment of the CTA scan and decides whether a PET-MPI study is needed. If obstructive CAD was excluded by coronary CTA no further imaging procedure was needed. In the presence of any suspected obstructive lesions (typically ≥50% diameter stenosis), PET-MPI was performed using ^{15}O-water during adenosine stress to assess the hemodynamic significance of the stenosis. Here, 143 patients underwent PET-MPI, whereas 9 patients with obstructive CAD on CTA were directly referred for ICA due to a contra-indication to MPI study (N=6) or logistic reasons (N=3).

Patient samples used in studies **I-III** are listed in **Table 10**. All samples were stored at -70°C until analysis. Blood from apparently healthy volunteer donors were collected in either serum, LiH plasma or EDTA plasma blood collection tubes and stored at -20°C. After blood collection, the tubes were kept at RT approximately 30 minutes. Tubes were then centrifuged with 1810 *g* at +20°C for 15 minutes. When pooling samples from multiple donors, the sera were combined and let to stand for 30 minutes to allow biochemical reactions between serum from different individuals occur. Then, possibly formed aggregates were filtered out with 0.45 µm pore size filter. Pooled serum samples were stored at -20°C.

Table 10 Patient samples used in the studies I-III.

	Sample matrix	N	Study
Apparently healthy non-pregnant individuals	Serum LiH plasma EDTA plasma Collected from volunteer donors	Multiple individuals and pool prepared from various donors	**I** LoD and LoQ Linearity cPAPP-A interference fPAPP-A stability
Samples with endogenous fPAPP-A	Serum Collected during carotid endarterectomy or abdominal aortic aneurysm surgery at Hospital district of Helsinki and Uusimaa	Multiple individuals and pool prepared from various donors	**I** LoD and LoQ Linearity cPAPP-A interference fPAPP-A stability
3rd trimester pregnancy sample	Serum Collected from volunteer donors	Pool prepared from various donors	**I** cPAPP-A interference
Reference population	Serum Purchased from Labquality	147	**I** fPAPP-A concentration in reference population
NSTE-ACS	Serum Collected from ACS patients at Turku University Central Hospital	389 out of which 197 were non-heparinized	**I** Risk prediction of MI or death within 1-year follow-up period
Suspected CAD patients	Serum Collected during scheduled coronary CTA at Turku University Central Hospital	49	**II** Heparin-induced release of fPAPP-A **III** Baseline samples used in the evaluation of atherosclerotic burden
		252 out of which 222 used in the study (this includes the 49 previously collected samples)	**III** Evaluation of atherosclerotic burden

Abbreviations used in the table: LiH, lithium heparin; EDTA, ethylenediaminetetraacetic acid; LoD, Limit of Detection; LoQ, Limit of Quantitation; cPAPP-A, complexed pregnancy-associated plasma protein A; fPAPP-A, free PAPP-A; NSTE-ACS, non-ST-elevated acute coronary syndrome; MI, myocardial infarction; CAD, coronary artery disease; CTA, computed tomography angiography.

4.3 Other laboratory analyses

The 2-assay fPAPP-A was measured with two assays and was used in publication **I**. In general, the assays had similar-type sandwich immunoassay as the developed direct fPAPP-A but both tPAPP-A and cPAPP-A assays were performed separately.

The result from the cPAPP-A assay was subtracted from measured tPAPP-A concentration, thus resulting in indirect concentration measurement of fPAPP-A.[418]

In publication **I**, the cTnI concentration was measured with contemporary 2nd generation assay, Innotrac AiO! cTnI assay (by Radiometer/Innotrac Diagnostics, Finland).[433] In publication **III**, the cTnI was measured with an assay developed in-house. From the perspective of sensitivity, the assay was in high-sensitivity range but since only 18% of the reference population had measurable cTnI concentration, the assay could not be classified as hs-cTnI assay.[467]

The LDL-C concentration used in the publication **III** was calculated with the Friedewald formula (see section 2.4.1 Lipid profile). The TC and TG were measured with enzymatic assays of Roche Diagnostics GmbH (Germany). The HDL-C in the formula was measured with phosphotungstate-$MgCl_2$ -precipitation method.[468]

4.4 Coronary CTA and PET image acquisition and interpretation

Coronary CTA was performed with 64-row hybrid PET-CT scanner (GE Discovery VCT, GE D690, 166 or GE Discovery MI, General Electric Medical Systems, Waukesha, WI, USA) as previously described.[469,470] Collimation was set at 64×0.625 mm, gantry rotation time was 350 ms, tube current 600 to 750 mA, and voltage 100 to 120 kV, depending on patient size. Before coronary CTA, metoprolol (up to 30 mg, if needed) was given intravenously to achieve a target heart rate of <60 beats/min. Isosorbide dinitrate aerosol (1.25 mg) was administered to obtain vasodilation. Coronary artery calcium scan was performed before coronary CTA. Coronary CTA was performed using intravenously administered low-osmolal iodine contrast agent (60-80 ml; 320-400 mg iodine/ml; injection velocity 4-5 ml/s) followed by saline flush. Prospectively ECG-triggered acquisition was applied whenever feasible.

Based on the initial evaluation of coronary CTA findings, a dynamic ^{15}O-water PET scan was carried out during adenosine stress using a hybrid PET-CT scanner in the same imaging session, as previously described.[469,471] Scans were performed after overnight fast. Patients were instructed to abstain from alcohol and caffeine for 24 h before the study. In some patients, PET was performed in a separate session due to logistic reasons or caffeine use. Adenosine infusion was started 2 min before the stress PET scan and continued at a rate of 140 µg/kg/min until the scan was complete. ^{15}O-water (Radiowater Generator, Hidex Oy, Turku, Finland) was injected as an intravenous bolus (injected activity target 500 MBq or 1000 MBq depending on scanner used) over 15 seconds and dynamic PET acquisition was performed (14×5 s, 3×10 s, 3×20 s, and 4×30 s).

Coronary CTA images were analyzed according to the 17-segment vessel system using GE ADW 4.4 Workstation software (General Electric Medical Systems, Waukesha, Wisconsin). The presence of coronary atherosclerosis and stenosis was evaluated in all coronary segments. A previously validated CTA risk score was also calculated by taking into account the plaque burden (number of coronary segments with atherosclerosis), severity (the presence of stenosis), location (a weight factor based on the Leaman score) and composition (calcified, non-calcified or mixed).[116] The Agatston CAC score was measured (N=221) in the non-enhanced scan.

The PET data were analyzed quantitatively using Carimas software (Turku, Finland).[472] Absolute stress MBF (ml/g/min) was quantified individually for each of the standard 17 myocardial segments. Stress MBF of ≤2.3 mL/g/min in at least 1 of the 17 myocardial segments was considered abnormal reflecting hemodynamically significant obstructive CAD based on a previous validation study.[473] The analysis was performed by an experienced physician and recorded in a standardized reporting system.

In study **III**, obstructive CAD was defined as atherosclerotic lesion on CTA associated with abnormal stress MBF or ≥70% stenosis on ICA. In study **II**, ≥50% stenosis determined was used as the definition of obstructive since at the time of data analysis PET-MPI data was unavailable. Other patients were classified as having normal coronary arteries (no atherosclerosis) or non-obstructive coronary atherosclerosis depending on CTA findings.

4.5 Statistical analyses

Analyses were performed with IBM® SPSS® Statistics (versions 23, 24 and 27, IBM, USA) and Analyse-it® for Microsoft Excel (version 3.76.5 Method Validation Edition, Analyse-it® Software Ltd, USA). In general, 2-tailed p-values were noted, and all p-values <0.05 were considered statistically significant. Normality of the distribution of continuous variables was determined by the Shapiro–Wilk's test and visual examination.

Assay performance

Linear regression analysis was used in the assessment of linearity in diluted fPAPP-A/rPAPP-A samples. Comparison of methods used weighted Deming regression and Pearson's correlation when studying association between two methods. Pearson's correlation was also utilized when analysing fPAPP-A concentration and age in the reference population. In addition, independent-samples t-test and one-way ANOVA were used in testing difference between fPAPP-A concentration in sex and age groups, respectively, in the reference population.

Clinical performance of the direct fPAPP-A assay was assessed as meeting the predetermined end point (MI or death within 1 year) or not. Univariate analysis was used when testing differences in the clinical data, and the follow-up data of meeting the endpoint were adjusted by sex and age. The fPAPP-A concentrations were log-transformed to enable parametric statistical testing. After testing, the log-concentrations were transformed back, and model-adjusted concentrations were reported. Survival curve analysis with direct fPAPP-A, 2-assay fPAPP-A, and tPAPP-A tertiles was performed with the Kaplan–Meier method. Differences between curves were tested with log-rank test. Cox's proportional hazards model was used in the calculation of risk ratios (RRs).

Heparin-induced release of fPAPP-A

Differences between groups were tested with independent samples t-test or one-way ANOVA. Pearson's correlation was used when studying relationship between numerical variables. Presented data is described as the mean (SD).

Coronary atherosclerotic changes in suspected stable CAD patients

Frequencies of categorical variables are reported as counts (%). Continuous variables are expressed as median (25^{th}–75^{th} percentile). Due to non-gaussian distribution of the continuous variables, nonparametric Mann-Whitney U-test and Kruskall-Wallis H-test were used when comparing continuous variables in groups. Post-hoc comparisons in Kruskall-Wallis H-test were Bonferroni-corrected. Pearson's and Spearman's correlation were utilized when studying the relationship between continuous variables (correlation coefficient r and r_s, respectively). ROC curves were constructed with presence of any atherosclerosis and obstructive CAD as state variables. The probability of falling into state variable class was presented as AUC with 95% confidence intervals (CI). Same variables were used in binary logistic regression analysis as dependent variables. In logistic regression model, sex, age, and fPAPP-A concentration were tested as predictors of the dependent variable and the risk was described as odds ratios (OR) with 95% CI.

5 Results and discussion

5.1 Analytical performance of free PAPP-A assay

In most clinical studies including PAPP-A measurement, assays which measure both complexed and non-complexed forms of PAPP-A together, i.e., tPAPP-A assays, are generally used.[416] However, fPAPP-A has been suggested to be more precise in cardiac-related events, but a sensitive direct measurement method for fPAPP-A has been lacking.[433] As part of this thesis, the first direct immunoassay towards fPAPP-A was created.

In the production of fPAPP-A antibodies by traditional hybridoma method, 30 mAbs were created which exclusively bound the free form of PAPP-A. In a relative epitope mapping it was discovered that produced antibodies divided into 5 epitope clusters. These fPAPP-A epitope clusters were available probably due to the missing complexation with proMBP leaving the epitopes accessible or due to different conformation when the binding of proMBP subunits is missing. It was possible to create only a relative epitope map of the produced antibodies since the exact epitope targets of the fPAPP-A antibodies are unknown and the tertiary structure of PAPP-A is unsolved. The detection of rPAPP-A was better in many produced antibodies than the detection of endogenous fPAPP-A in patient samples. Also, in some antibbodies there was high interference of cPAPP-A which indicated crossreactivity with complexed form of PAPP-A. In addition, certain antibody combinations generated high serum-based background signal which decreased the sensitivity. Despite these difficulties in assay development, extensive testing of different mAb combinations and optimization of assay conditions and buffers yielded an optimal assay where a fPAPP-A recognizing in house mAb was used as the capture and a commercial tPAPP-A mAb 3C8 from HyTest as the tracer.

The developed fPAPP-A assay had a wide dynamic range. The calibration curve ($y=588x+828$) was linear at least up to 1 000 mIU/L ($R^2=0.999$) (**Figure 7**) and no high-dose hook effect was observed even at 3 000 mIU/L (unpublished data). The determined concentrations for LoB and LoD were 0.25 and 0.40 mIU/L, respectively. A 20% CV accuracy goal resulted in LoQ concentration of 1.30 mIU/L. The within-laboratory precision profile is shown in **Figure 8**. The low LoB and LoD concentrations ensured a sensitive measurement of blood samples. This is later shown with the sensitive analysis of reference population panel, where 90% of the

samples had measurable fPAPP-A concentration, i.e., >LoD concentration. The predetermined accuracy goal of 20% CV was set, and it was based on previous guidelines on imprecision levels of developed assays[474]. Regarding the imprecision requirement, the achieved LoQ concentration appears adequate when considering patients with potentially increased concentrations of fPAPP-A.

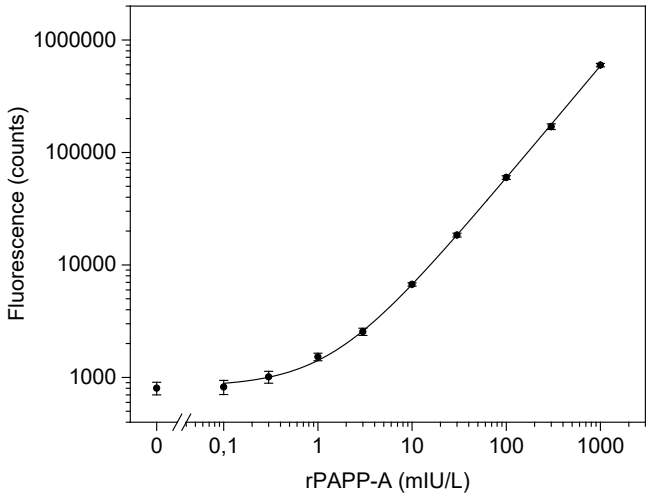

Figure 7 The calibration curve of fPAPP-A assay. Fluorescence signals of PAPP-A concentrations are illustrated as means of 14–16 replicates. Error bars indicate the standard deviation in each concentration point.

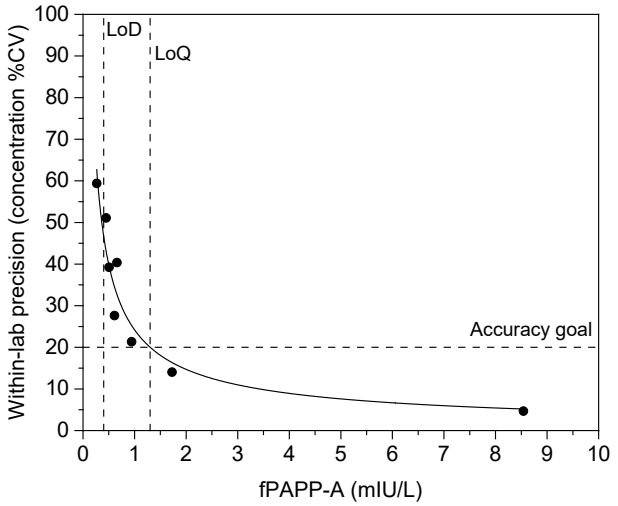

Figure 8 Precision profile of fPAPP-A assay. Within-laboratory precision as CV% was determined according to Clinical and Laboratory Standards Institute guidelines EP5-A2 and EP17-A2 by using 8 serum sample pools containing varying concentrations of endogenous fPAPP-A (filled circles) fitted with power function model. LoD (0.4 mIU/L) and LoQ (1.3 mIU/L) concentrations are illustrated as dashed vertical lines and 20 CV% accuracy goal as dashed horizontal line.

There are no certified reference materials or methods for fPAPP-A measurement available, so recovery study of different blood sample matrices was performed to reflect the accuracy of the developed assay. In general, 80%–120% recoveries have been deemed acceptable[475]. Three different blood sample matrices were tested. These were serum, LiH plasma and EDTA plasma. Only EDTA plasma was not suitable for the developed assay. Median recoveries (25^{th}–75^{th} percentiles) in 12 individuals were 82% (76%–90%), 73% (67%–77%), and 49% (45%–54%) for serum, LiH, and EDTA plasma, respectively. Serum was seemingly the best sample matrix and the only one which yielded recoveries within the acceptable range. Still, LiH plasma could also be an acceptable option since the recoveries were adequate. The explanation of the unsuitability of blood collection tubes with EDTA as an anticoagulant is based on the biochemical structure of PAPP-A. EDTA can chelate the zinc found in the zinc-binding motif of PAPP-A and consequently may alter the PAPP-A conformation, which may lead to decreased detection of PAPP-A[377].

Linearity of rPAPP-A or endogenous fPAPP-A containing samples was assessed by diluting in BSA-TSA buffer or in healthy serum pool. Only results from dilutions which exceeded the LoQ concentration were included in the linear regression analysis. In samples diluted in healthy serum pool, the baseline fPAPP-A was subtracted. Samples containing supplemented rPAPP-A diluted in either healthy serum pool or BSA-TSA resulted in a linear response (R^2=0.997) across the measurement range (2.3–233.5 mIU/L, **Figure 9**). The linearity of samples containing endogenous fPAPP-A was similarly excellent (R^2=0.990–1.000, **Figure 9**). Hence, the linearities of patient samples and rPAPP-A -supplemented serum samples were good, and this confirms the assumption that the developed assay reliably measures fPAPP-A. Also, the interference of biological components in serum do not affect the measurement. Based on linearity study, it appears that the binding characteristics of both the endogenous fPAPP-A and rPAPP-A in serum are similar in the developed assay.

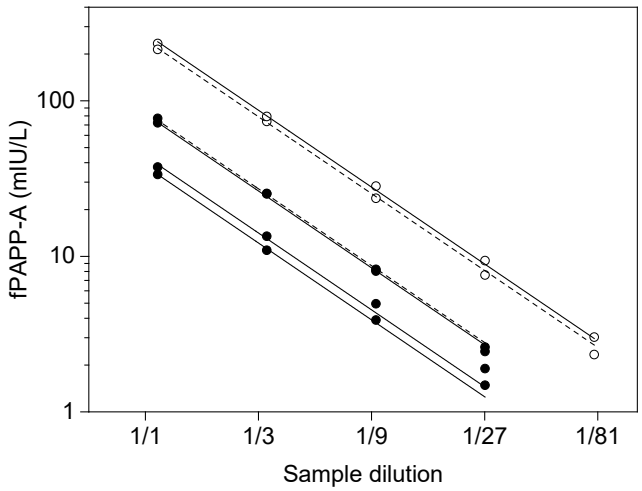

Figure 9 Dilution linearity of fPAPP-A assay. Linearity was determined with rPAPP-A spiked healthy serum pool (N=2, open circles) and samples containing endogenous fPAPP-A (N=4, filled circles). Diluents were BSA-TSA (solid line) and healthy serum pool (dashed line). With linear regression analysis, adjusted R^2 values for rPAPP-A spiked serum samples were 0.997 and for endogenous fPAPP-A serum samples 0.990–1.000.

Interference of cPAPP-A in the developed fPAPP-A assay was studied by adding known amounts of 3rd trimester pregnancy serum to samples containing either endogenous fPAPP-A or rPAPP-A in healthy serum. On average (SD) the developed assay detected 1.5% (0.6%) of the added 3rd trimester pregnancy serum tPAPP-A. Towards delivery, the PAPP-A in serum is mostly (>99%) present in the complexed form[476]. Still, due to detection of enzymatically active PAPP-A indicate that some of the PAPP-A in late pregnancy is in fact in free form[476]. The observed interference with the developed assay may truly represent this fPAPP-A concentration in pregnancy serum. If not, still the detected cPAPP-A interference is not clinically relevant as proportion in the measured concentration is so little that presumably it would not affect to the interpretation of the result.

Method comparison was performed between the developed direct fPAPP-A assay and previously published 2-assay fPAPP-A method[418]. The weighted Deming regression yielded a slope (95% CIs) of 0.781 (0.451–1.110) and y-intercept of -0.091 (-0.630 to 0.447) mIU/L ($S_{y|x}$=2.157 mIU/L) (**Figure 10**). The two methods had clear but not very strong correlation between them (r=0.819, p<0.001). The assays use different antibodies, different calibrators, and different approaches, which most likely justifies the deviations between the methods. The calibrators in the 2-assay fPAPP-A methods are based on pregnancy serum for both tPAPP-A and cPAPP-A assays while the developed direct fPAPP-A assay used rPAPP-A-based calibrators which are in non-complexed form. The different calibration principle may

explain the difference in the slope of the correlation. Also, since the 2-assay fPAPP-A method uses two separate assays with their own imprecision, this cumulatively increases the total variation of fPAPP-A concentrations determined with this method.[433] For this reason, the 2-assay fPAPP-A method has higher imprecision especially at lower concentration range which thereby weakens the correlation. Thus, the weak correlation, especially at the low concentration range, may be because of the higher imprecision of the 2-assay method. The affinities of the antibodies and calibrator material may vary as well as the detection of endogenous fPAPP-A. Therefore, the observed discrepancies could clarify certain outliers.

In the reference population, the median fPAPP-A concentration (25^{th}–75^{th} percentile) in the whole cohort was 1.0 (0.7–1.4) mIU/L. The rate of rejection of high CV% samples (10%) from this analysis was reasonable given the low concentrations in these samples in relation to the LoD and LoQ of the assay. There was no statistically significant difference in fPAPP-A concentration between sexes (p=0.935). The fPAPP-A concentration weakly correlated with age (r=0.175, p=0.043).

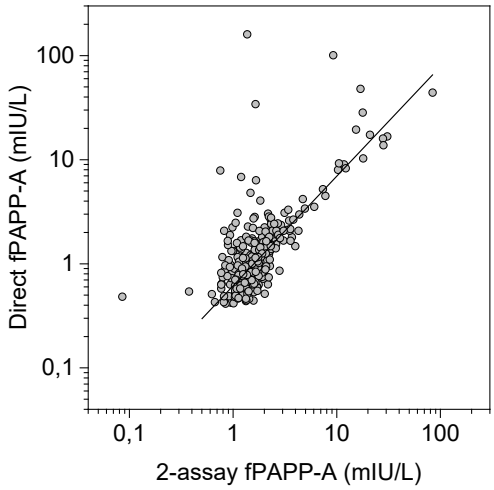

Figure 10 Comparison of 2 fPAPP-A assays with suspected acute coronary syndrome patient samples (N=312). Results are shown as means of 2 replicates (gray circles). Weighted Deming regression resulted in an equation of y=-0.091+0.781x and Pearson's regression coefficient of 0.819 (p<0.001).

The endurance of the analyte, rPAPP-A in TSA-BSA and rPAPP-A in serum and endogenous fPAPP-A in patient serum samples, was investigated in stability study where the samples were stressed either with temperature or by repeating multiple freeze-thaw cycles. Both rPAPP-A (in buffer and serum) and endogenous fPAPP-A endured at least 5 freeze-thaw cycles (**Table 11**). The endogenous fPAPP-A was

stable in all stored temperatures and with the maximum storing time (**Table 11**). The rPAPP-A in buffer and serum were relatively stable the maximum storing time in both +4°C and RT, but in +37°C the stability clearly declined (**Table 11**). Since the stability of endogenous fPAPP-A in serum is very good, it enables e.g., prolonged waiting until analysis or changes in the temperature during possible sample transport. The rPAPP-A used in calibrators could be aliquoted and always fresh batch could be used safely in the assay. The determination of in-use time of the rPAPP-A calibrators would need further testing.

Table 11 Stability of rPAPP-A and endogenous fPAPP-A [% of untreated sample results as medians (25^{th}–75^{th} percentile)]. Samples were stored at +4°C, RT or +37°C for 1 and 7 days and 1, 3 or 5 freeze-thaw cycles were tested.

	Median (25^{th}–75^{th} percentile) % of untreated sample		
	rPAPP-A	**rPAPP-A**	**Endogenous fPAPP-A**
	Buffer (N=3)	**Serum (N=6)**	**Serum (N=2)**
1x freeze-thaw	138 (126–139)	115 (114–117)	120 (118–122)
3x freeze-thaw	116 (108–117)	108 (101–112)	128 (122–135)
5x freeze-thaw	112 (111–124)	112 (111–120)	136 (131–142)
+4°C, 1 day	117 (115–118)	114 (113–115)	114 (114–115)
+4°C, 7 days	115 (108–118)	107 (102–109)	124 (120–127)
RT, 1 day	110 (105–112)	105 (102–123)	114 (110–118)
RT, 7 days	119 (113–125)	87 (83–89)	123 (122–125)
+37°C, 1 day	65 (64–66)	65 (64–77)	111 (110–113)
+37°C, 7 days	21 (20–23)	23 (20–44)	91 (91–92)

Abbreviations used in the table: rPAPP-A, recombinantly produced pregnancy-associated plasma protein A; fPAPP-A, free PAPP-A; RT, room temperature.

5.2 Clinical performance of free PAPP-A assay

5.2.1 Outcome after acute coronary syndrome

Clinical performance of the developed direct fPAPP-A assay was tested with NST-ACS patients who were followed for one year. The endpoint was defined as all-cause mortality or having MI. Besides the developed assay, analysis was likewise performed for tPAPP-A assay and 2-assay fPAPP-A method. A statistical model was created where patients meeting the endpoint or not were compared to each other. The model was adjusted by age and sex, and the difference between the two groups was statistically significant (p=0.008). The model-adjusted fPAPP-A concentrations significantly differed between sexes and in meeting the endpoint. The concentration

was higher in men (p=0.021) and if the endpoint was met (p=0.037). Age in the model did not correlate with fPAPP-A concentration (r=0.009, p=0.124). Patients who met the endpoint had on average (95% CI) adjusted fPAPP-A concentration of 1.13 (0.87–1.47) mIU/L and those who did not 0.82 (0.71–0.95) mIU/L (**Figure 11**). Model-adjusted fPAPP-A concentrations in men and women were 1.13 (0.95–1.35) mIU/L and 0.82 (0.66–1.03) mIU/L, respectively.

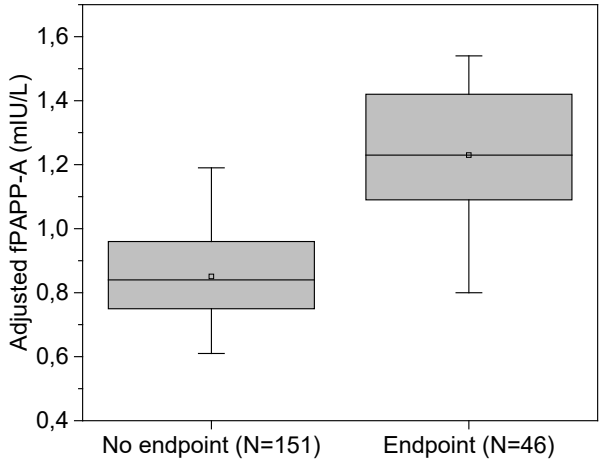

Figure 11 Direct fPAPP-A in admission samples of non-ST elevation acute coronary syndrome patients who did or did not meet the predetermined end point (MI or death) during 1-year follow-up (p=0.008). Model-adjusted concentrations are reported. The box represents interquartile range, and median is illustrated as a horizontal line. Mean is marked as a square inside the box. Whiskers indicate 10th and the 90th percentiles.

In the survival analysis, the patients were divided into tertiles on the basis of direct fPAPP-A (<0.74, 0.74–1.24, >1.24 mIU/L), 2-assay fPAPP-A (<1.26, 1.26–1.74, >1.74 mIU/L) and tPAPP-A (<1.97, 1.97–2.98, >2.98 mIU/L). Differences between tertiles was significant with fPAPP-A measured directly or with 2-assay method, while with tPAPP-A assay the survival of the endpoint within 1-year follow-up was not statistically significant (p-values 0.014, 0.015, and 0.31, respectively) (**Figure 12**).

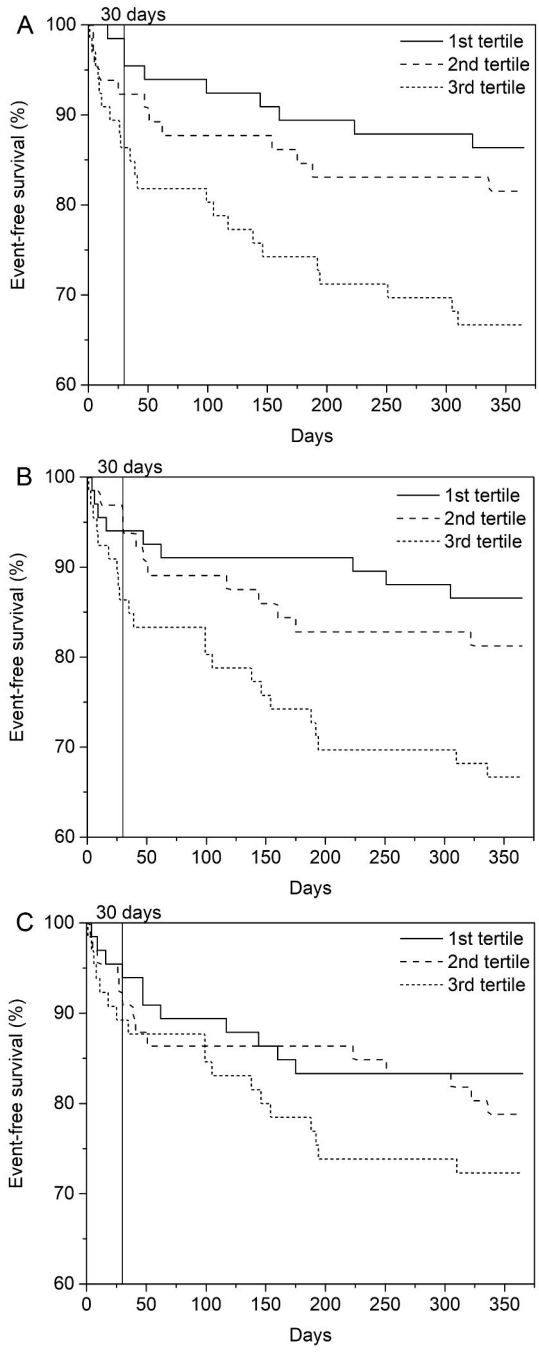

Figure 12 Kaplan–Meier curves of event-free survival for non-ST elevation acute coronary syndrome patients encountering MI or death within 1 year according to direct fPAPP-A (**A**), 2-assay fPAPP-A method (**B**), and tPAPP-A (**C**) tertiles (1st solid line, 2nd dashed line, 3rd dotted line). Differences between tertiles were statistically significant with direct and 2-assay fPAPP-A but not with tPAPP-A (p-values 0.014, 0.015, and 0.31, respectively).

Similar risks of death or MI within 1-year were obtained with both fPAPP-A methods: Patients in the 3rd tertile had 2.8-fold (95% CI, 1.3–6.3; p=0.007) higher risk than patients in the 1st tertile and 2.0-fold (95% CI, 1.0–4.2; p=0.05) higher risk than patients in the 2nd tertile. However, with a shorter follow-up period of 30 days, direct fPAPP-A provided better risk prediction than 2-assay fPAPP-A. The risk (95% CI; p-value) of meeting the endpoint between the 3rd and 1st tertiles was 4.8-fold (1.2–31.4; 0.022) greater with directly measured fPAPP-A, while with 2-assay fPAPP-A method, the risk was 2.4-fold (0.8–8.7; 0.14) and not statistically significant. The RR (95% CI; p-value) was not significant between 3rd and 2nd tertiles with either fPAPP-A methods: 1.8 (0.6 –5.9; 0.28) and 3.1 (0.9 –13.8; 0.07) for direct and 2-assay fPAPP-A methods, respectively. With tPAPP-A assay, the difference of the risk (RR; 95% CI; p-value) between 3rd and 1st tertile were not significant with neither 1-year or 30-day follow-up period: 1.8 RR (0.8–3.9; 0.13) or 2.5 RR (0.7–11.4; 0.17). The ability of direct fPAPP-A to predict the risk of adverse cardiac events was studied in conjunction with contemporary measurement of cTnI (**Figure 13**). Seemingly, PAPP-A provides additional prognostic information with cTnI result. Directly measured fPAPP-A enabled enhanced risk prediction in combination with cTnI [cTnI-negative patient in the 1st fPAPP-A tertile vs. cTnI-positive patient in the 3rd fPAPP-A tertile with 1-year RR, 95% CI (7.4; 2.4–23.3) than tPAPP-A (3.1; 1.0–9.3) or 2-assay fPAPP-A method (3.4; 1.4–10.8)] (**Table 12**). On average, 36.4% (SD 5.4%) of the patients were cTnI-positive in each tertile group, and there was no significant difference in this respect between groups.

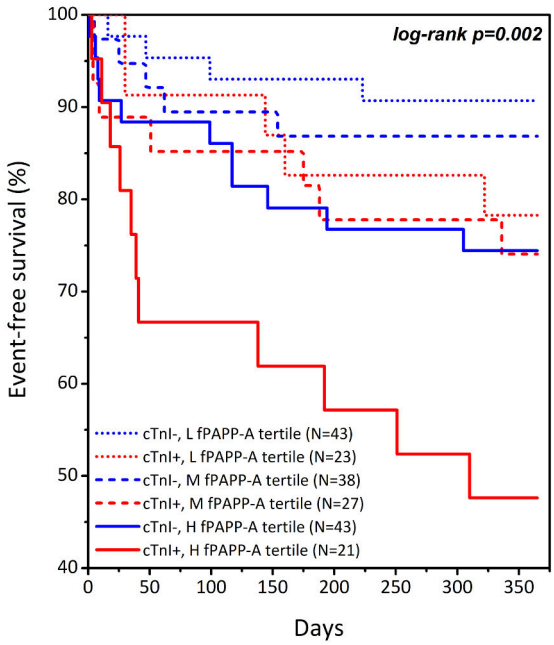

Figure 13 Kaplan–Meier curves of event-free survival for non-ST elevation acute coronary syndrome patients encountering MI or death within 1 year when combining direct fPAPP-A and contemporary cTnI results. Patients were divided based on fPAPP-A tertile [lowest (L) dotted line, middle (M) dashed line and highest (H) solid line) and cTnI positivity (cTnI+ red and cTnI- blue). A cTnI positive patient in the highest fPAPP-A tertile had 7.4-fold higher risk of MI or death than a patient in the cTnI negative patient in the lowest fPAPP-A tertile ($p<0.05$).

Table 12 Risk of cardiac event or death (compared to cTnI negative, 1st PAPP-A tertile).

Tertile	cTnI-negative[a]: RR (95% CI)			cTnI-positive[a]: RR (95% CI)		
	Direct fPAPP-A	2-assay fPAPP-A	tPAPP-A	Direct fPAPP-A	2-assay fPAPP-A	tPAPP-A
1-year follow-up						
1st	-			2.4 (0.7–9.1)	1.4 (0.4–5.7)	2.4 (0.8–8.0)
2nd	1.5 (0.4–5.5)	0.5[b] (0.1–2.2)	1.0 (0.3–3.5)	3.1 (0.9–10.5)	3.2[c] (1.2–8.8)	3.8[c] (1.3–11.5)
3rd	3.1[c] (1.0–9.6)	2.8[c] (1.1–7.5)	2.5 (0.9–7.3)	7.4[c] (2.4–23.3)	3.9[c] (1.4–10.8)	3.1[c] (1.0–9.3)
30-day follow-up						
1st	-			0.0[b] (−)	2.9 (0.4–20.3)	3.9 (0.4–43.1)
2nd	2.3 (0.2–25.3)	0.0[b] (−)	3.1 (0.3–29.4)	5.1 (0.5–49.1)	1.7 (0.2–12.2)	3.9 (0.4–42.7)
3rd	5.3 (0.6–45.2)	3.9 (0.8–19.2)	4.8 (0.5–42.8)	8.8[c] (1.0–78.4)	3.2 (0.5–18.9)	5.4 (0.6–52.0)

Abbreviations used in the table: PAPP-A, pregnancy-associated plasma protein A; cTnI, cardiac troponin I; RR, risk ratio; fPAPP-A, free PAPP-A; tPAPP-A, total PAPP-A.
[a]cTnI concentration ≥0.03 µg/L was considered positive.
[b]Higher risk in the reference group (cTnI negative, 1st PAPP-A tertile) if RR<1.0.
[c]Statistically significant ($p<0.05$) difference in risk compared to cTnI negative, 1st PAPP-A tertile.

After NST-ACS diagnosis, patients who had MI or death within 1 year had statistically significantly higher fPAPP-A concentration than patients who did not meet the endpoint. As previous studies have shown, PAPP-A is a candidate risk marker of cardiac-related events and death[426,433–435,443,447,477–480]. Same was demonstrated with the developed direct fPAPP-A assay. With 1-year follow-up, the performance of directly measured fPAPP-A was comparable to that of the 2-assay fPAPP-A method. But, with early follow-up time of 30-days, the developed direct assay could predict adverse outcomes better than the 2-assay fPAPP-A method. When considered in conjunction with cTnI results of the same sample, the prognostic performance of directly measured fPAPP-A was even further enhanced. It was clearly shown that at least in this setting and patient population, the directly measured fPAPP-A outperformed fPAPP-A measured with a 2-assay approach or tPAPP-A assay. These patients who are at greater risk of adverse cardiac events or death possibly have severe atherosclerotic lesions or numerous vulnerable plaques. Therefore, these patients need to be identified as early as possible to enable better care.

5.2.2 Chronic coronary artery disease

Median (25^{th}–75^{th} percentile) age of patients with suspected chronic CAD (N=222) was 63 (55–71) years and 44% of the patients were males. Majority of the patients (68%) had either atypical chest pain or dyspnea as the primary symptom. Baseline characteristics of the patients are presented in **Table 13**. Based on CAD status, the patients were classified into three main groups (**Figure 14**). Regarding coronary CTA, in total 129 patients (58%) had detectable coronary atherosclerosis while the rest 93 patients (42%) did not. According to hybrid PET-CT or ICA, non-obstructive atherosclerosis was diagnosed in 101 patients (45%), whereas 28 patients (13%) patients had obstructive CAD (24 had abnormal stress MBF and 4 had ≥70% stenosis by ICA). Out of the patients with obstructive CAD, 14 had single-vessel, 4 had 2-vessel, and 10 had 3-vessel disease.

Table 13 Characteristics of the study population.

	Number (%) / Total
Age, median (25^{th}–75^{th} percentile)	63 (55–71) / 222
Male	98 (44%) / 222
Risk factors for CAD	
Current smoking	29 (14%) / 202
Previous smoking	35 (17%) / 202
Diabetes	34 (17%) / 200
Hypertension	120 (60%) / 200
Dyslipidemia	102 (52%) / 195
BMI, median (25^{th}–75^{th} percentile)	28 (25–31) / 149
Family history of CAD	89 (50%) / 179
Primary symptoms	
Typical AP	38 (17%) / 222
Atypical AP or dyspnea	151 (68%) / 222
Other	33 (15%) / 222
Positive exercise ECG	49 (37%) / 131
LVEF <40%	6 (5%) / 111
Medication	
Beta-blocker	80 (39%) / 205
Lipid-lowering drug	76 (37%) / 206
Antiplatelet drug	57 (28%) / 206
Anticoagulant	20 (10%) / 202
Long-acting nitrate	20 (10%) / 203
Diuretic	44 (22%) / 202
ACEi or ARB	90 (44%) / 204
Calcium-channel blocker	27 (13%) / 202
Antiarrhythmic agent	5 (3%) / 202

Abbreviations used in the table: CAD, coronary artery disease; BMI, body mass index; AP, angina pectoris; ECG, electrocardiogram; LVEF, left ventricular ejection fraction; ACEi, angiotensin converting enzyme inhibitor; ARB, angiotensin receptor blocker.

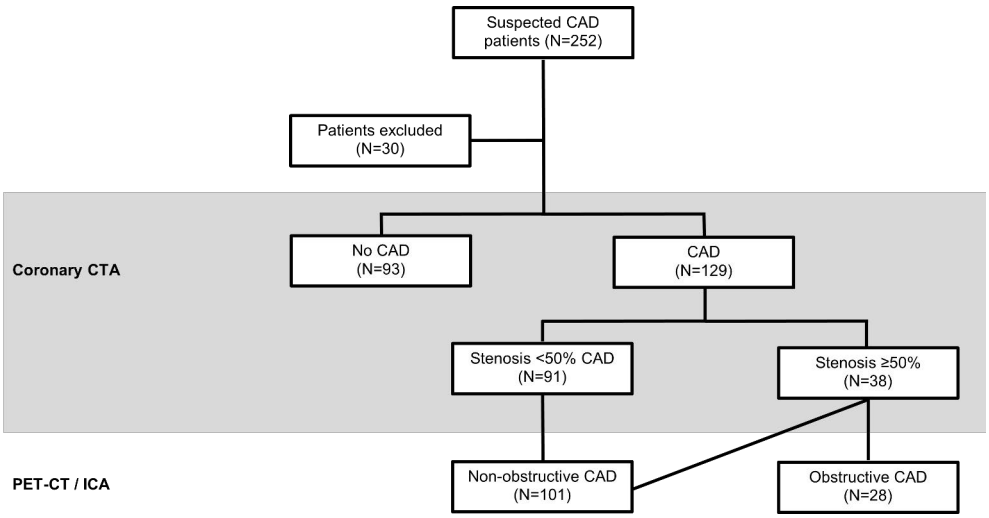

Figure 14 Classification of coronary artery disease (CAD) in the study. Based on coronary computed tomography angiography (CTA), patients were classified as having no coronary atherosclerosis or any CAD (atherosclerotic plaque in at least one coronary segment). All patients with suspected obstructive CAD based on coronary CTA had either positron emission tomography (PET) or invasive coronary angiography (ICA) to confirm obstructive CAD (abnormal stress myocardial blood flow or ≥70% stenosis by ICA). Thirty patients were excluded from the study.

The concentration of fPAPP-A was associated with the presence and severity of CAD and results are summarized in **Table 14** and **Table 15**. The concentration of fPAPP-A was higher in patients with any coronary atherosclerosis (N=129) than those with normal (N=93) coronary arteries [1.0 (0.6–1.3) mIU/L vs. 0.8 (0.5–273 1.1) mIU/L, p=0.021]. Furthermore, both patients with non-obstructive or obstructive CAD had higher fPAPP-A concentrations than those with normal coronary arteries [0.9 (0.6–1.2) mIU/L, p=0.012 or 1.2 (1.0–1.5) mIU/L, p<0.003 vs. 0.8 (0.5–1.1) mIU/L]. No statistically significant difference of fPAPP-A concentration was observed between patients with non-obstructive atherosclerosis and those with normal coronary arteries (p=0.72). The fPAPP-A concentration weakly but significantly correlated with CAC score (r_s=0.157, p=0.019) and CTA risk score (r_s=0.198, p=0.003) which are used measures in evaluating the extent of coronary artery calcification or coronary atherosclerosis with CTA imaging. Males had higher fPAPP-A concentration than females [1.0 (0.7–1.3) mIU/L vs. 0.8 (0.5–1.2) mIU/L, p=0.008]. Also, the circulating fPAPP-A was elevated in patients without family history of CAD compared to those who did have [1.0 (0.7–1.3) mIU/L vs. 0.8 (0.5–1.1) mIU/L, p=0.021]. Anticoagulation medication resulted in higher fPAPP-A concentration than in non-anticoagulated patients [1.2 (0.8–1.6) mIU/L vs. 0.9 (0.6–1.2) mIU/L, p=0.033]. Statistically significant correlation

between fPAPP-A concentration and age (r=0.155, p=0.020) was observed, although the correlation was relatively weak.

In the ROC analysis it was discovered, that circulating fPAPP-A concentration predicted better the presence of obstructive CAD than merely any atherosclerosis (**Figure 15**). More detailed comparisons between the extent of atherosclerosis and fPAPP-A concentrations are shown in **Table 14**. If there was atherosclerosis in ≥4 segments, the fPAPP-A concentration was higher than in those with normal coronary arteries [1.1 (0.9-1.4) mIU/L vs. 0.8 (0.5–1.1) mIU/L, p=0.003]. An atherosclerotic plaque in the LM coronary artery or in all 3 main coronary arteries had elevated fPAPP-A concentrations (p=0.026) compared to those patients who did not. Patients with non-calcified plaques, the concentration of fPAPP-A was not statistically significantly higher. An example of a patient with obstructive CAD and elevated fPAPP-A concentration is shown in **Figure 16**.

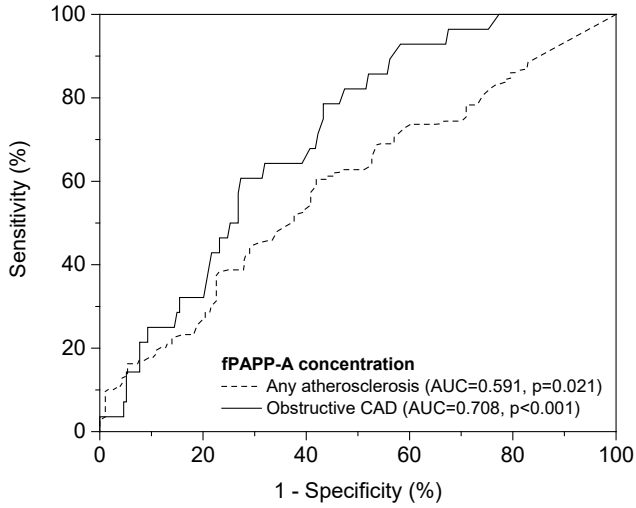

Figure 15 ROC curves of fPAPP-A concentration for the detection of any coronary atherosclerosis (dashed line) and obstructive CAD (solid line).

Table 14 The concentration of fPAPP-A [median (25^{th}–75^{th} percentile) mIU/L] in relation to imaging findings.

		Presence			Total number of affected segments			
		No	**Yes**	**p-value**	**0**	**1–3**	**≥4**	**p-value**
Atherosclerotic plaque	N (%)	93 (42%)	129 (58%)	0.021	93 (42%)	84 (38%)	45 (20%)	0.006[a]
	fPAPP-A	0.8 (0.5–1.1)	1.0 (0.6–1.3)		0.8 (0.5–1.1)	0.9 (0.6–1.2)	1.1 (0.9–1.4)	
Calcified of mixed plaque	N (%)	105 (47%)	117 (53%)	0.047	105 (47%)	74 (33%)	43 (20%)	0.005[b]
	fPAPP-A	0.8 (0.6–1.1)	1.0 (0.6–1.3)		0.8 (0.6–1.1)	0.9 (0.6–1.4)	1.1 (0.5–1.4)	
Non-calcified or mixed plaque	N (%)	159 (72%)	63 (28%)	0.12	159 (72%)	58 (26%)	5 (2%)	0.093
	fPAPP-A	0.9 (0.6–1.2)	1.0 (0.8–1.3)		0.9 (0.6–1.2)	1.0 (0.8–1.3)	0.7 (0.4–1.0)	
3-vessel or LM plaque	N (%)	179 (81%)	43 (19%)	0.026				
	fPAPP-A	0.9 (0.6–1.2)	1.0 (0.8–1.4)					
Obstructive CAD	N (%)	194 (87%)	28 (13%)	0.001				
	fPAPP-A	0.9 (0.6–1.2)	1.2 (1.0–1.5)					
ALL	N (%)	222 (100%)						
	fPAPP-A	0.9 (0.6–1.3)						

Abbreviations used in the table: fPAPP-A, free pregnancy-associated plasma protein A; LM, left main coronary artery; CAD, coronary artery disease.
[a]Pairwise comparisons: 0 vs. 1–3 segments, p=0.83; 0 vs. ≥4 segments, p=0.003; 1–3 vs ≥4 segments, p=0.11
[b]Pairwise comparisons: 0 vs. 1–3 segments, p=1.0; 0 vs. ≥4 segments, p=0.003; 1–3 vs ≥4 segments, p=0.066

Table 15 The median (25th–75th percentile) concentration of fPAPP-A, biomarkers, and clinical risk factors in predicting likelihood of non-obstructive and obstructive CAD.

	Correlation to fPAPP-A		PET-CTA / ICA CAD status				ROC: Obstructive CAD	
			No	Non-obstructive	Obstructive	p-value	AUC (95% CI)	p-value
fPAPP-A		N (%) mIU/L	93 (42%) 0.8 (0.5–1.1)	101 (45%) 0.9 (0.6–1.2)	28 (13%) 1.2 (1.0–1.5)	<0.001[a]	0.708 (0.677–0.871)	<0.001
LDL-C	r=-0.104 p=0.13	N (%) mmol/L	88 (42%) 3.9 (3.1–4.7)	95 (45%) 3.7 (3.0–4.3)	28 (13%) 3.3 (2.7–3.8)	0.059	0.373 (0.263–0.484)	0.031
cTnI	r_s=0.023 p=0.73	N (%) ng/L	91 (41%) 1.5 (1.5–1.5)	101 (46%) 1.5 (1.5–1.5)	28 (13%) 1.5 (1.5–1.5)	0.99	0.497 (0.382–0.612)	0.96
10-year FRS CHD	r=0.055 p=0.49	N (%) %	66 (40%) 15 (11–21)	77 (46%) 22 (14–32)	23 (14%) 22 (18–33)	<0.001[b]	0.635 (0.511–0.759)	0.038
CAC score	r_s=0.157 p=0.019	N (%)	92 (42%) 0 (0–0)	101 (45%) 64 (20–238)	28 (13%) 572 (211–1 448)	<0.001[c]	0.858 (0.775–0.941)	<0.001
CTA risk score	r_s=0.198 p=0.003	N (%)	93 (42%) 0.0 (0.0–0.0)	101 (45%) 6.0 (4.2–10.2)	28 (13%) 19.4 (11.5–26.2)	<0.001[d]	0.908 (0.856–0.960)	<0.001

Abbreviations used in the table: fPAPP-A, free pregnancy-associated plasma protein A; PET-CTA, positron emission tomography-computed tomography angiography; ICA, invasive coronary angiography; CAD, coronary artery disease; ROC, receiver operator characteristics; AUC, area under the curve; CI, confidence interval; LDL-C, low-density lipoprotein cholesterol; cTnI, cardiac troponin I; FRS, Framingham Risk Score; CHD, coronary heart disease; CAC, coronary artery calcium.

[a]Pairwise comparisons: No vs. Non-obstructive, p=0.72; No vs. Obstructive, p<0.003; Non-obstructive vs Obstructive, p=0.012

[b]Pairwise comparisons: No vs. Non-obstructive, p=<0.003; No vs. Obstructive, p=0.003; Non-obstructive vs Obstructive, p=1.00

[c]Pairwise comparisons: No vs. Non-obstructive, p<0.003; No vs. Obstructive, p<0.003; Non-obstructive vs Obstructive, p<0.003

[d]Pairwise comparisons: No vs. Non-obstructive, p<0.003; No vs. Obstructive, p<0.003; Non-obstructive vs Obstructive, p<0.003

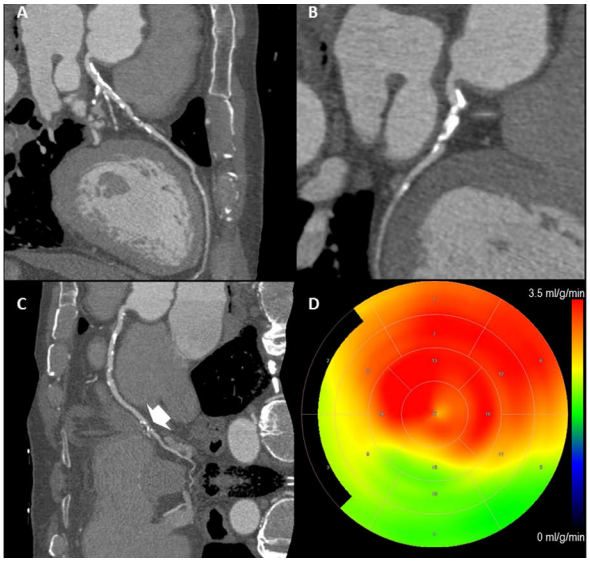

Figure 16 An example of a patient with elevated fPAPP-A concentration (1.4 mIU/L), extensive coronary atherosclerosis (coronary artery calcium score 2 982) and an obstructive lesion (arrow in panel C) in the right coronary artery. Figure shows coronary computed tomography angiography images of the left anterior descending (**A**), left circumflex (**B**) and the right coronary artery (**C**). Polar map (**D**) shows reduced stress myocardial blood flow by radiowater positron emission tomography in the right coronary artery territory (green color).

The levels of LDL-C and cTnI did not differ in patients with normal coronary arteries, non-obstructive atherosclerosis or obstructive CAD (**Table 15**). Particularly, in this cohort of suspected stable CAD patients, the cTnI was above the LoD in only 33 individuals (15%). The FRS significantly differed in patients with non-obstructive atherosclerosis or obstructive CAD when compared to patients with normal coronary arteries ($p=0.003$ and $p<0.003$, respectively). Though, the FRS was statistically similar between patients with obstructive CAD and those with non-obstructive atherosclerosis. Since the fPAPP-A concentration had dependency on sex and age, these were included with fPAPP-A in multivariable logistic regression models where the prediction of the presence of any coronary atherosclerosis and obstructive CAD was evaluated. In both models of any atherosclerosis and obstructive CAD, sex and age were significant predictors, but fPAPP-A concentration predicted only obstructive CAD (**Table 16**). The odds (95% CI) of obstructive CAD increased by 62% (105%–251%) with each unit increase of fPAPP-A concentration. In predicting obstructive CAD, the model which included fPAPP-A, age, and sex [AUC (95% CI): 0.774 (0.677–0.871), $p<0.001$] performed better than fPAPP-A alone [AUC (95% CI): 0.708 (0.622–0.795), $p<0.001$] (**Figure 15**,

Figure 17 and **Table 16**). The fPAPP-A concentration alone as well as the model containing fPAPP-A, age, and sex outperformed FRS in predicting obstructive CAD in ROC analysis (**Table 15**, **Figure 17**). However, CAC and CTA risk scores were superior in predicting the presence of obstructive CAD than clinical risk factors and circulating biomarkers including fPAPP-A (**Table 15**, **Figure 17**). The prediction of obstructive CAD was improved by logistic regression model combining sex, age, and fPAPP-A concentration closer to the performance of CAC and CTA risk scores (**Table 15**, **Figure 17**).

Table 16 Sex, age, and fPAPP-A in predicting any coronary atherosclerosis or obstructive CAD based on logistic regression analysis.

		OR (95% CI)	p-value
Any atherosclerosis	Male sex	2.61 (1.37–4.97)	0.003
	Age (years)	1.07 (1.04–1.10)	<0.001
	fPAPP-A (mIU/L)	1.48 (0.93–2.36)	0.097
Obstructive CAD	Male sex	6.28 (2.36–16.94)	<0.001
	Age (years)	1.06 (1.02–1.10)	0.008
	fPAPP-A (mIU/L)	1.62 (1.05–2.51)	0.030

Abbreviations used in the table: fPAPP-A, free pregnancy-associated plasma protein A; CAD, coronary artery disease; OR, odds ratio; CI, confidence interval.

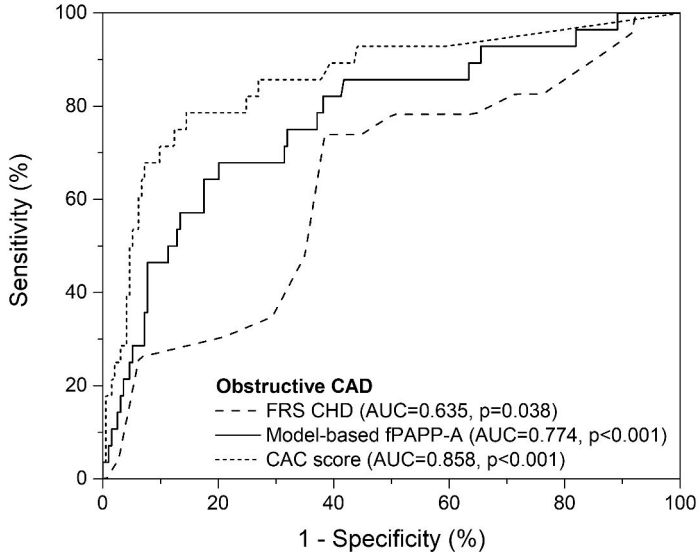

Figure 17 ROC curves of 10-year coronary heart disease risk by Framingham Risk Score (FRS CHD, dotted line), coronary artery calcium score (CACS, dashed line), and combination of fPAPP-A, age, and sex (Model-based fPAPP-A, solid line) in the prediction of obstructive CAD.

The obtained results of fPAPP-A concentration in patients with suspected chronic CAD indicated that fPAPP-A is a potential biomarker of CAD. The fPAPP-A concentration was evidently increased in the presence of coronary atherosclerosis and especially in patients with obstructive CAD. The elevated fPAPP-A levels alone or in combination with age and sex outperformed either clinical risk factors or cTnI for predicting obstructive CAD.

Even though LDL-C and cTnI are widely used in risk assessment[481–483], in this cohort the biomarkers did not perform well in predicting coronary atherosclerosis or obstructive CAD. Yet, atherosclerosis can be present even at very low LDL-C concentration[484], which is in line with findings of this study. Though, in this cohort 37% of the patients were on statin medication and nearly half of the patients with obstructive CAD used statins and had the lowest LDL-C levels which could have confounded the observed results and thus weaken the predictive value of LDL-C. In regards of poor performance of cTnI, the assay used here cannot be classified as a high-sensitivity assay, as it reportedly detects <50% of apparently healthy individuals. In the study cohort only 15% had detectable cTnI concentration. Additionally, in biochemical perspective the cTnI and fPAPP-A most likely measure different aspects of coronary damage. Traditionally, cTnI is used to reflect ischemia-related injury of the cardiac muscle cells, while fPAPP-A may have function in the remodelling of the atherosclerotic plaques.[390] Therefore, fPAPP-A perhaps is associated with atherosclerotic changes regardless of dynamic changes observed in ischemia status. Moreover, based on previous research[419,433,485], fPAPP-A and cTnI concentration do not correlate, but fPAPP-A might be additive to cTnI[419].

Clinical practise guidelines recommend the use of the 10-year CHD risk by FRS which is a well-established way to assess the risk of having CAD.[29,486] In this cohort, as expected, the FRS was clearly higher in coronary atherosclerotic patients, but the risk score could not discriminate patients with non-obstructive atherosclerosis and obstructive CAD from each other. As shown with ROC analysis, the fPAPP-A levels outperformed FRS in predicting the presence of obstructive CAD. This suggests that direct fPAPP-A measurement could be more beneficial than determining traditional clinical risk factors in predicting obstructive CAD.

With different imaging modalities, the determination of CAC score is a widely used method to estimate the extent of coronary atherosclerosis. The likelihood of obstructive CAD can be effectively ruled out with determination of CAC score[487] and especially, the absence of coronary calcium is linked with low likelihood of obstructive CAD and consequently good outcome[6]. The CAC score clearly differentiated patients with normal coronary arteries, non-obstructive CAD, and obstructive CAD from each other. Also, in the ROC analysis, CAC score had better AUC for the identification of obstructive CAD than fPAPP-A. Still, fPAPP-A weakly correlated with CAC score as well as with the CTA risk score which are

known to accurately reflect the extent of coronary atherosclerosis. Besides in this cohort, the extensive calcification has been previously connected with fPAPP-A.[420]

Most reports studying PAPP-A in cardiac setting are using tPAPP-A assays. Since the method used in this cohort measures directly the non-complexed form of PAPP-A, fPAPP-A, the contradictive results of PAPP-A association with chronic CAD could be at least partly explained by the difference in the detected form of PAPP-A.[442,443] In these studies, the coronary stenosis was detected angiographically, which is an ineffective predictor of myocardial ischemia[6,488]. In comparison, this study incorporates extremely detailed characterization of atherosclerotic burden by coronary CTA as well as haemodynamically significant coronary stenosis by quantitative PET-MPI. Still, due to the small size of the cohort, exact conclusions cannot be made and obtained results merely describe the potential role of fPAPP-A as a cardiac-related risk marker. For this reason, larger populations need to be evaluated in order to demonstrate the clinical value of fPAPP-A in assessing the likelihood of obstructive CAD. Nevertheless, as many previous studies have shown, the association of elevated PAPP-A with the extent and severity of CAD is evident since measured tPAPP-A can act as an independent predictor of MACE and mortality.[439–441,444]

5.3 Heparin-induced release of free PAPP-A to circulation

Based on the preliminary study (N=8) of timing the blood sample collection, it was concluded that the highest fPAPP-A concentration increase is achieved 5 minutes after heparin administration (**Figure 18**). According to coronary CTA, coronary atherosclerosis was detected in 31 (63%) individuals. Out of these, 7 patients had obstructive CAD and the rest 24 patients had non-obstructive atherosclerosis. In this study, obstructive CAD was defined as having ≥50% diameter stenosis in at least one coronary segment (classification of segments by Uusitalo *et al.*[116]). Patients with coronary atherosclerosis had plaques in 1 to 12 coronary segments, and there were 8 patients who had a plaque in 4 or more segments. Plaques were classified as calcified, non-calcified or mixed and these were present at least in one coronary segment in 23, 10 and 11 patients, respectively. Based on coronary CTA, 5 patients had 3-vessel coronary atherosclerosis. Median (25^{th}–75^{th} percentile) CAC score was 50 (10–149) in atherosclerotic patients and the previously validated coronary CTA-derived risk score[116] was 7.2 (4.2–8.7).

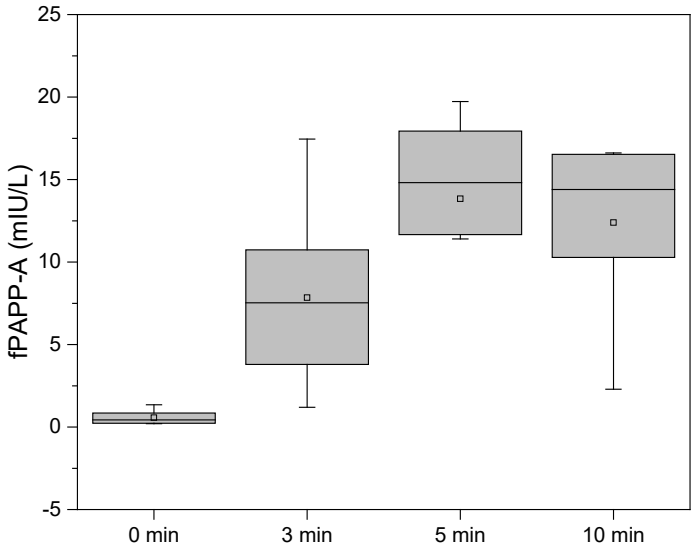

Figure 18 The fPAPP-A concentration after heparin administration. In a preliminary study of 8 patients, venous blood samples were collected at baseline and 3, 5 and 10 minutes after heparin administration. On average, the highest fPAPP-A increase was achieved at 5 minutes after heparin injection.

In the whole patient cohort (N=49), the average fPAPP-A concentration was 0.7 (0.4) mIU/L before and 12.1 (5.6) mIU/L after heparin administration ($p<0.001$) (**Figure 19**). The fPAPP-A increase after the heparin injection was on average (SD) 24 (19)-fold. The fPAPP-A concentration after heparin administration was higher in men than in women [14.6 (4.5) vs. 10.7 (5.8) mIU/L, $p=0.020$], in smokers (N=10) than in non-smokers [15.5 (5.5) vs. 10.1 (5.3) mIU/L, $p=0.022$] and in patients with atypical (N=22) than typical angina pectoris [14.1 (5.1) vs. 7.2 (4.8) mIU/L, $p=0.027$]. The released fPAPP-A after heparin administration was inversely related with age ($r=-0.282$, $p=0.05$). The total amount of injected heparin was 9.6–24.6 mg depending on the patient's weight, and it did not correlate with heparin-induced fPAPP-A concentration ($r=0.123$, $p=0.4$). Also, there was a weak but non-significant correlation between fPAPP-A before and after heparin administration ($r=0.242$, $p=0.093$).

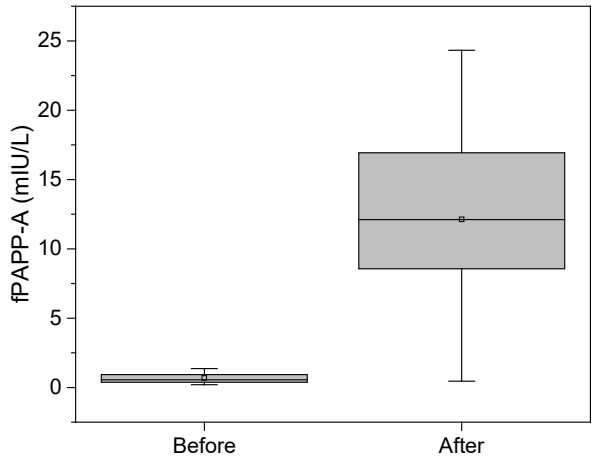

Figure 19 fPAPP-A concentration before and after heparin administration in suspected chronic CAD patients (N=49). Before heparin administration the mean (SD) fPAPP-A concentration was 0.7 (0.4) mIU/L and after 12.1 (5.6) mIU/L and the difference was statistically significant (p<0.001). The box represents interquartile range and median is illustrated as a horizontal line. Mean is marked as a square inside the box. Whiskers indicate 10th and the 90th percentiles.

In the coronary CTA, the fPAPP-A concentration after heparin administration did not correlate with the presence and extent of coronary atherosclerosis. The concentration did not differ in patients without any atherosclerosis, with non-obstructive CAD or with obstructive disease [11.8 (6.8) mIU/L vs. 12.5 (5.5) mIU/L vs. 11.6 (2.7) mIU/L, p=0.89] (**Figure 20**). As a measure of the extent of coronary atherosclerosis, there was no difference between patients with atherosclerosis involving none, <4 or ≥4 coronary segments [11.8 (6.8) vs. 12.0 (5.3) vs. 13.2 (4.2) mIU/L, p=0.84). The CAC score did not correlate with the released fPAPP-A concentration (r=0.057, p=0.71) nor correlated the coronary CTA-derived risk score (r=0.012, p=0.94). The released fPAPP-A was not differing in patients with 3-vessel obstructive CAD from other patients [12.7 (1.6) mIU/L vs. 12.1 (5.9) mIU/L, p=0.56]. The fold-change of heparin-induced fPAPP-A neither had any significant association with coronary atherosclerosis.

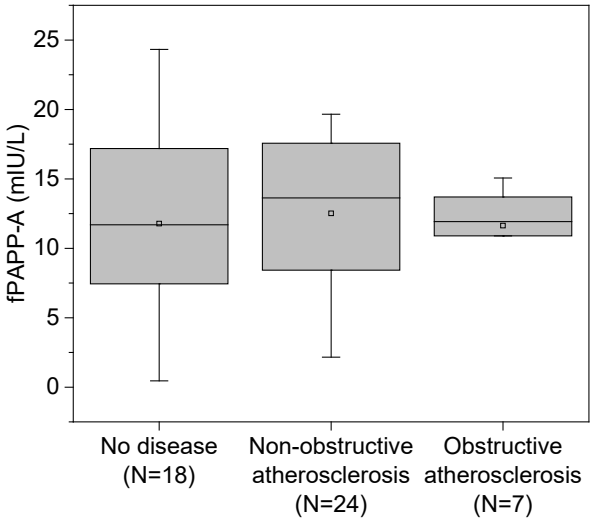

Figure 20 The fPAPP-A concentration after heparin administration in suspected chronic coronary artery disease (CAD) patients (N=49) categorized according to the coronary computed tomography angiography (CTA) findings. The fPAPP-A concentrations were similar among the 3 groups (p=0.89). The box represents interquartile range and median is illustrated as a horizontal line. Mean is marked as a square inside the box. Whiskers indicate 10th and the 90th percentiles.

The original hypothesis of the study was that the fPAPP-A released into the circulation after i.v. heparin administration would have originated from the vascular endothelium. It was assumed that the fPAPP-A reservoir in the vascular endothelium would represent the processes involved in coronary atherosclerosis. Such processes would include active remodelling and vascular healing present in the progressive and high-risk coronary atherosclerotic plaques. Then, these could be associated with the extent of atherosclerosis. However, the obtained results are not supporting this hypothesis. There can be multiple reasons for this. Firstly, the heparin-induced release of fPAPP-A to the circulation may originate from some other source than the vascular endothelium. Also, the fPAPP-A reservoir released to circulation may have been derived from other atherosclerotic lesions in the vascular system and not merely from coronary-based atherosclerotic lesions. Based on research on PAPP-A, it has been proven that PAPP-A is present in many tissues, especially in the placenta but also in other tissues such as tumours, reproductive organs, and healing tissues (summarized by Hjortebjerg *et al.*[489]). These may well be the source of fPAPP-A release after i.v. administration of heparin. Secondly, since circulating PAPP-A has been associated with vulnerable atherosclerotic plaques, it may not show as high lumen stenosis degree or in the number of coronary segments affected by atherosclerotic plaques, which were the main atherosclerotic characteristics investigated with CTA. Lastly, the timing of the blood sample collection is

complicated and may result in error thus increasing the patient-to-patient variation. After heparin administration the release of fPAPP-A concentration is very rapid and maximum values are reached within 5 minutes. Then, the clearance of fPAPP-A occurs also quite fast and thus the kinetics of fPAPP-A release after heparin administration are swift.[412] Accurate timing of sampling is crucial and yet difficult so the individual difference in kinetics, this might misperceive the results.

6 Conclusions

The CVDs are major sosioeconomical challenge faced throughout the world. These affect all people regardless of sex, age or ethnicity. Though clinical presentation of CVD is more apparent with increasing age, the mechanism of atherosclerosis behind CVDs starts to progress during adolescence. There is a need to identify the high-risk patients as early as possible to ensure better care of the disease in order to prevent MACE of occuring.

To date, many approaches are available to assess the risk of developing CAD or MACE. Multiple biomarkers have been identified which have prognostic capability to detect future cardiovascular events. When adding known clinical risk factors such as age, sex, and BP information to certain biomarker results, usually cholesterol measurements, easy-to-use risk scores have been generated. These scores give individual risk of future cardiovascular events or mortality. The most accurate method to evaluate the extent and severity of atherosclerotic burden is obtained with different imaging modalities. Currently, coronary CTA combined with PET-MPI gives the most precise estimation on the state of coronary arteries and the heamodynamical stress caused by atherosclerosis. This combination of imaging technologies is powerful in ruling-out atherosclerosis but also functions as a prognostic tool to determine the risk of future cardiovascular events or death.

In this thesis, the first immunoassay directly measuring circulating fPAPP-A was developed. PAPP-A has shown promise as a cardiac-related marker in acute and chronic settings as well as in predicting CVD-based risk. As stated in previous studies, the fPAPP-A is more accurate than tPAPP-A when measuring PAPP-A in cardiac conditions, but thus far sensitive and reliable methodology has been lacking. Also, the usability of PAPP-A as a biomarker has been questioned due to the heparin-induced release to circulation.

The main conclusions based on the original publications are:

I. The developed direct fPAPP-A immunoassay sensitively measures circulating fPAPP-A in serum. Based on the extensive evaluation of analytical characteristics of the assay, it can be concluded that the developed assay can be used in reliable measurement of non-complexed form of PAPP-

A, the fPAPP-A. The clinical performance of directly measured fPAPP-A outperformed tPAPP-A assay and 2-assay fPAPP-A method in predicting the risk of MI or death within 1-year after NSTE-ACS. The fPAPP-A functioned as an independent and additive marker in relation to cTnI in assessing future risk of cardiac-related events.

II. In contrast to the study hypothesis, the amount of released fPAPP-A to circulation after i.v. administration of LMWH cannot be used as measure of atherosclerotic burden. There was no association between heparin-induced release of fPAPP-A to circulation and coronary atherosclerosis. Thus, studies where heparin was administrated to patients may confound the achieved results and conclusions should be evaluated cautiously.

III. The elevated concentration of fPAPP-A was associated with the extent and severity of coronary atherosclerosis in patients with suspected obstructive CAD. The circulating fPAPP-A outperformed traditional risk factors and other evaluated biomarkers in the detection of obstructive CAD. The ability of fPAPP-A to predict obstructive CAD was further enhanced when in conjunction with age and sex.

Thorough clinical validation of the developed fPAPP-A assay is required for the usage of this promising biomarker. The fPAPP-A could be used in assessing atherosclerosis in different settings, such as pre-screening patients for preventive therapies, diagnosing obstructive CAD or evaluating the future risk of MACE or death. There is a need to evaluate the clinical likelihood of obstructive CAD prior to diagnostic testing[6,490] and for this fPAPP-A could be a potential biomarker. Also, in HF patients with preserved EF, PAPP-A is suggested as biomarker of reduced coronary flow reserve.[449]

Traditionally, PAPP-A is used in prenatal screening of Down syndrome pregnancies. However, in early stages of pregnancy, 15%–40% of PAPP-A is in non-complexed free form, while during late pregnancy the portion of fPAPP-A is remarkedly reduced (<1%).[491] Therefore, fPAPP-A (or fPAPP-A/tPAPP-A ratio) in maternal serum would be interesting research target for chromosomal defects beside Down syndrome, pregnancy complications or cardiovascular risk of the neonate.

Acknowledgements

This research was carried out during 2013–2022 at the Biotechnology Unit, University of Turku in collaboration with Turku University Central Hospital Heart Center and Turku PET Centre. Financial support from Doctoral Programme in Clinical Reaserch (DPCR), Turku University Foundation and Wallac Oy are gratefully ackowledged.

I wish to thank Professor Emeritus Kim Pettersson, Professor Tero Soukka, Professor Urpo Lamminmäki and Assisstant Professor Saara Wittfooth for creating inspiring place to study and do reaserch. You have given me opportunity to do my thesis work in high-quality environment, the Biotechnology Unit.

I want to express my deepest gratitude to my principal supervisor Assisstant Professor Saara Wittfooth and supervisor Professor Antti Saraste. During these years you have been nothing but supportive towards my studies. I wish to thank Antti for opening a whole new world for "immunoassay developer". Imaging coronary arteries has brought invaluable content to my thesis work. I appriciate you Saara for passing on your vast knowledge on immunoassay development and especially of PAPP-A to me while also giving me responsibilities and room to grow and challenge myself as a researcher. Beside being my professional mentor, I consider you as friend also, so thank you for being so kind and trusting me as your PhD student.

I am extremely grateful for my esteemed pre-examiners Adjunct Professor Päivi Laitinen and Professor Jari Laukkanen for reviewing this thesis and giving me valuable feedback.

This work would have not been possible without the contribution from all of my co-authors Dr. Juha Lund, Dr. Joanna Danielsson, Pirjo Pietilä, Veikko Wahlroos, Keira Pudge, Isto Leinonen, Dr. Pekka Porela, Dr. Tuomo Ilva, Dr. Mauri Lepäntalo, Professor Kari Pulkki, Dr. Liisa-Maria Voipio-Pulkki, Dr. Teemu Maaniitty, Professor Juhani Knuuti and Dr. Wail Nammas. You are sincerely thanked for the vital input.

Since I first started working at the Biotechnology Unit in 2005, I have had the chance to work with many wonderful people throughout the years. There are so many that it is impossible to list you here, but all of you are equally appreciated. Teija Luotohaara, Pirjo Pietilä, Pirjo Laaksonen, Mirja Jaala, Marja Maula, Martti

Sointusalo, Jani Koskinen and Sanna Laitinen are thanked for keeping the day-to-day operations smooth both at the laboratory and at the Biotechnology Unit.

I would also like to thank my current employee Wallac Oy and especially the head of R&D Janne Seppälä, for granting me study leave to finish my thesis work. I am grateful for my wonderful supervisor Joonas Siivonen for believing in my ability to finish my studies even when I have not been so certain of it. The personnel at Wallac Oy are fantastic and working there has further developed my skills as a specialist in the field of diagnostics.

I would have not been able to achieve this sometimes-stressful PhD project without keeping "mental health days" with my dear friends. The group of Toimiston Tytsyt is going stronger than ever and no words are enough to describe how I feel towards all of you: Katriina, Minna, Henna, Erica, Anni and Sandra. Even though we are no longer located in the same office, we continue to share ups and downs of our lives almost daily. I am fortunate to still have high school friends Katri, Nina, Heidi and Paula in my life. We have known each other for over two decades and every time we meet, laughter-therapy is warranted. We have grown up together and hopefully continue to grow old together. Thank you for being part of my life.

I am endlessly thankful for my parents Ritva and Markku for always encouraging me to educate. You have been proud of all my achievements whether in work, or personal life. Without your support I would have not been able to "go to school" so long. You are also the best grandparents my daughters could have. My sister Riina and her son, my godson, Henrik, are very dear to me. Thank you for understanding my geeky nature and for all the wonderful memories we have made together.

I want to express my love and gratitude for my fiancée Ville. You understand me better than anyone else and without your support (or threats to throw my computer of the terrace into forest when I have been too tired), I would have not been able to finish this project. You balance me and always know how to cheer me up. Through Ville, I have also gained another family. Ville's children Venla, Lotta and Eetu, parents Eija and Jasse and sister Virpi are thanked for including me into your life.

Finally, my dearest daughters Matilda and Aino, you are the light of my life. It has been wonderful to see you grow into fine young ladies. Thank you for understanding, even at a such young age, my passion towards my work and that "mommy works a lot". I hope I have made you as proud of me as I am of you.

Turku, August 2022

Emilia Tuunainen

List of References

1. Roth, G. A. *et al.* Demographic and epidemiologic drivers of global cardiovascular mortality. *N. Engl. J. Med.* **372**, 1333–1341 (2015).
2. Benjamin, E. J. *et al.* Heart Disease and Stroke Statistics-2019 Update: A Report From the American Heart Association. *Circulation* **139**, e56–e528 (2019).
3. Global, regional, and national incidence, prevalence, and years lived with disability for 310 diseases and injuries, 1990-2015: a systematic analysis for the Global Burden of Disease Study 2015. *Lancet (London, England)* **388**, 1545–1602 (2016).
4. *Atherosclerosis: Clinical Perspectives Through Imaging*. (Springer-Verlag London, 2013). doi:10.1007/978-1-4471-4288-1
5. Arnett, D. K. *et al.* 2019 ACC/AHA Guideline on the Primary Prevention of Cardiovascular Disease: A Report of the American College of Cardiology/American Heart Association Task Force on Clinical Practice Guidelines. *Circulation* **140**, e596–e646 (2019).
6. Knuuti, J. *et al.* 2019 ESC Guidelines for the diagnosis and management of chronic coronary syndromes. *Eur. Heart J.* **41**, 407–477 (2020).
7. Grundy, S. M., Pasternak, R., Greenland, P., Smith, S. J. & Fuster, V. AHA/ACC scientific statement: Assessment of cardiovascular risk by use of multiple-risk-factor assessment equations: a statement for healthcare professionals from the American Heart Association and the American College of Cardiology. *J. Am. Coll. Cardiol.* **34**, 1348–1359 (1999).
8. Fruchart, J.-C. *et al.* The Residual Risk Reduction Initiative: a call to action to reduce residual vascular risk in patients with dyslipidemia. *Am. J. Cardiol.* **102**, 1K-34K (2008).
9. Budoff, M. J. & Gul, K. M. Expert review on coronary calcium. *Vasc. Health Risk Manag.* **4**, 315–324 (2008).
10. Burke, A. P. *et al.* Morphologic findings of coronary atherosclerotic plaques in diabetics: a postmortem study. *Arterioscler. Thromb. Vasc. Biol.* **24**, 1266–1271 (2004).
11. Libby, P. *et al.* Atherosclerosis. *Nat. Rev. Dis. Prim.* **5**, 56 (2019).
12. Fan, J. & Watanabe, T. Inflammatory reactions in the pathogenesis of atherosclerosis. *J. Atheroscler. Thromb.* **10**, 63–71 (2003).
13. Glaser, R. *et al.* Clinical progression of incidental, asymptomatic lesions discovered during culprit vessel coronary intervention. *Circulation* **111**, 143–149 (2005).
14. Kolodgie, F. D. *et al.* The thin-cap fibroatheroma: a type of vulnerable plaque: the major precursor lesion to acute coronary syndromes. *Curr. Opin. Cardiol.* **16**, 285–292 (2001).
15. Mann, J. & Davies, M. J. Mechanisms of progression in native coronary artery disease: role of healed plaque disruption. *Heart* **82**, 265–268 (1999).
16. Rosenfeld, M. E., Averill, M. M., Bennett, B. J. & Schwartz, S. M. Progression and disruption of advanced atherosclerotic plaques in murine models. *Curr. Drug Targets* **9**, 210–216 (2008).
17. Shiomi, M. & Fan, J. Unstable coronary plaques and cardiac events in myocardial infarction-prone Watanabe heritable hyperlipidemic rabbits: questions and quandaries. *Current opinion in lipidology* **19**, 631–636 (2008).
18. Stary, H. C. *et al.* A definition of advanced types of atherosclerotic lesions and a histological classification of atherosclerosis. A report from the Committee on Vascular Lesions of the Council

on Arteriosclerosis, American Heart Association. *Arterioscler. Thromb. Vasc. Biol.* **15**, 1512–1531 (1995).
19. Stary, H. C. *et al.* A definition of initial, fatty streak, and intermediate lesions of atherosclerosis. A report from the Committee on Vascular Lesions of the Council on Arteriosclerosis, American Heart Association. *Arterioscler. Thromb. a J. Vasc. Biol.* **14**, 840–856 (1994).
20. Virmani, R. *et al.* Atherosclerotic plaque progression and vulnerability to rupture: angiogenesis as a source of intraplaque hemorrhage. *Arterioscler. Thromb. Vasc. Biol.* **25**, 2054–2061 (2005).
21. Wang, T. J. *et al.* C-reactive protein is associated with subclinical epicardial coronary calcification in men and women: the Framingham Heart Study. *Circulation* **106**, 1189–1191 (2002).
22. Yusuf, S. *et al.* Effect of potentially modifiable risk factors associated with myocardial infarction in 52 countries (the INTERHEART study): case-control study. *Lancet (London, England)* **364**, 937–952 (2004).
23. Keil, U. & Kuulasmaa, K. WHO MONICA Project: risk factors. *Int. J. Epidemiol.* **18**, S46-55 (1989).
24. Margolis, J. R., Gillum, R. F., Feinleib, M., Brasch, R. & Fabsitz, R. Community surveillance for coronary heart disease: the Framingham Cardiovascular Disease survey. Comparisons with the Framingham Heart Study and previous short-term studies. *Am. J. Cardiol.* **37**, 61–67 (1976).
25. Rigotti, N. A. & Clair, C. Managing tobacco use: the neglected cardiovascular disease risk factor. *Eur. Heart J.* **34**, 3259–3267 (2013).
26. Critchley, J. A. & Capewell, S. Mortality risk reduction associated with smoking cessation in patients with coronary heart disease: a systematic review. *JAMA* **290**, 86–97 (2003).
27. Chobanian, A. V *et al.* The Seventh Report of the Joint National Committee on Prevention, Detection, Evaluation, and Treatment of High Blood Pressure: the JNC 7 report. *JAMA* **289**, 2560–2572 (2003).
28. Stamler, J., Wentworth, D. & Neaton, J. D. Is relationship between serum cholesterol and risk of premature death from coronary heart disease continuous and graded? Findings in 356,222 primary screenees of the Multiple Risk Factor Intervention Trial (MRFIT). *JAMA* **256**, 2823–2828 (1986).
29. Wilson, P. W. *et al.* Prediction of coronary heart disease using risk factor categories. *Circulation* **97**, 1837–1847 (1998).
30. Roger, V. L. *et al.* Heart disease and stroke statistics--2011 update: a report from the American Heart Association. *Circulation* **123**, e18–e209 (2011).
31. Kannel, W. B. & McGee, D. L. Diabetes and glucose tolerance as risk factors for cardiovascular disease: the Framingham study. *Diabetes Care* **2**, 120–126 (1979).
32. Sperling, L. S. *et al.* The CardioMetabolic Health Alliance: Working Toward a New Care Model for the Metabolic Syndrome. *J. Am. Coll. Cardiol.* **66**, 1050–1067 (2015).
33. Lloyd-Jones, D. M. *et al.* Parental cardiovascular disease as a risk factor for cardiovascular disease in middle-aged adults: a prospective study of parents and offspring. *JAMA* **291**, 2204–2211 (2004).
34. Haskell, W. L. *et al.* Physical activity and public health: updated recommendation for adults from the American College of Sports Medicine and the American Heart Association. *Circulation* **116**, 1081–1093 (2007).
35. Conroy, R. M. *et al.* Estimation of ten-year risk of fatal cardiovascular disease in Europe: the SCORE project. *Eur. Heart J.* **24**, 987–1003 (2003).
36. Vartiainen, E. *et al.* Sydäninfarkti- ja aivohalvausriskin arviointi FINRISKI-tutkimuksessa. *Lääkärilehti* **62**, 4507–4513 (2007).
37. Gould, K. L., Lipscomb, K. & Hamilton, G. W. Physiologic basis for assessing critical coronary stenosis. Instantaneous flow response and regional distribution during coronary hyperemia as measures of coronary flow reserve. *Am. J. Cardiol.* **33**, 87–94 (1974).
38. Davies, M. J. The pathophysiology of acute coronary syndromes. *Heart* **83**, 361–366 (2000).
39. Virmani, R., Burke, A. P., Farb, A. & Kolodgie, F. D. Pathology of the vulnerable plaque. *J. Am. Coll. Cardiol.* **47**, C13-8 (2006).

40. Cannon, C. P. *et al.* The electrocardiogram predicts one-year outcome of patients with unstable angina and non-Q wave myocardial infarction: results of the TIMI III Registry ECG Ancillary Study. Thrombolysis in Myocardial Ischemia. *J. Am. Coll. Cardiol.* **30**, 133–140 (1997).
41. Kushner, F. G. *et al.* 2009 focused updates: ACC/AHA guidelines for the management of patients with ST-elevation myocardial infarction (updating the 2004 guideline and 2007 focused update) and ACC/AHA/SCAI guidelines on percutaneous coronary intervention (updating the 2005 gui. *J. Am. Coll. Cardiol.* **54**, 2205–2241 (2009).
42. Anderson, J. L. *et al.* ACC/AHA 2007 guidelines for the management of patients with unstable angina/non-ST-Elevation myocardial infarction: a report of the American College of Cardiology/American Heart Association Task Force on Practice Guidelines (Writing Committee to Revise t. *J. Am. Coll. Cardiol.* **50**, e1–e157 (2007).
43. Leech, G. J., McCulloch, M. L. & Adams, D. Physical Principles of Ultrasound. in *Echocardiography* (eds. Nihoyannopoulos, P. & Kisslo, J.) 3–31 (Springer International Publishing, 2018). doi:10.1007/978-3-319-71617-6_1
44. Picano, E. Stress echocardiography. *Expert Rev. Cardiovasc. Ther.* **2**, 77–88 (2004).
45. Pálinkás, A. *et al.* The value of ECG and echocardiography during stress testing for identifying systemic endothelial dysfunction and epicardial artery stenosis. *Eur. Heart J.* **23**, 1587–1595 (2002).
46. Mazeika, P., Nihoyannopoulos, P., Joshi, J. & Oakley, C. M. Evaluation of dipyridamole-Doppler echocardiography for detection of myocardial ischemia and coronary artery disease. *Am. J. Cardiol.* **68**, 478–484 (1991).
47. Geleijnse, M. L., Fioretti, P. M. & Roelandt, J. R. Methodology, feasibility, safety and diagnostic accuracy of dobutamine stress echocardiography. *J. Am. Coll. Cardiol.* **30**, 595–606 (1997).
48. Picano, E. Stress echocardiography. From pathophysiological toy to diagnostic tool. *Circulation* **85**, 1604–1612 (1992).
49. Sicari, R. *et al.* Stress Echocardiography Expert Consensus Statement--Executive Summary: European Association of Echocardiography (EAE) (a registered branch of the ESC). *Eur. Heart J.* **30**, 278–289 (2009).
50. Knuuti, J. *et al.* The performance of non-invasive tests to rule-in and rule-out significant coronary artery stenosis in patients with stable angina: a meta-analysis focused on post-test disease probability. *Eur. Heart J.* **39**, 3322–3330 (2018).
51. Steurer, J., Fischer, J. E., Bachmann, L. M., Koller, M. & ter Riet, G. Communicating accuracy of tests to general practitioners: a controlled study. *BMJ* **324**, 824–826 (2002).
52. Metz, L. D. *et al.* The prognostic value of normal exercise myocardial perfusion imaging and exercise echocardiography: a meta-analysis. *J. Am. Coll. Cardiol.* **49**, 227–237 (2007).
53. Fraker, T. D. J. *et al.* 2007 chronic angina focused update of the ACC/AHA 2002 guidelines for the management of patients with chronic stable angina: a report of the American College of Cardiology/American Heart Association Task Force on Practice Guidelines Writing Group to deve. *J. Am. Coll. Cardiol.* **50**, 2264–2274 (2007).
54. Antman, E. M. *et al.* 2007 focused update of the ACC/AHA 2004 guidelines for the management of patients with ST-elevation myocardial infarction: a report of the American College of Cardiology/American Heart Association Task Force on Practice Guidelines. *J. Am. Coll. Cardiol.* **51**, 210–247 (2008).
55. Seldinger, S. I. Catheter replacement of the needle in percutaneous arteriography; a new technique. *Acta radiol.* **39**, 368–376 (1953).
56. DeRouen, T. A., Murray, J. A. & Owen, W. Variability in the analysis of coronary arteriograms. *Circulation* **55**, 324–328 (1977).
57. Brown, B. G., Bolson, E., Frimer, M. & Dodge, H. T. Quantitative coronary arteriography: estimation of dimensions, hemodynamic resistance, and atheroma mass of coronary artery lesions using the arteriogram and digital computation. *Circulation* **55**, 329–337 (1977).

58. Serruys, P. W. *et al.* Percutaneous coronary intervention versus coronary-artery bypass grafting for severe coronary artery disease. *N. Engl. J. Med.* **360**, 961–972 (2009).
59. Mark, D. B. *et al.* Continuing evolution of therapy for coronary artery disease. Initial results from the era of coronary angioplasty. *Circulation* **89**, 2015–2025 (1994).
60. Nissen, S. E. & Yock, P. Intravascular ultrasound: novel pathophysiological insights and current clinical applications. *Circulation* **103**, 604–616 (2001).
61. Mintz, G. S. *et al.* American College of Cardiology Clinical Expert Consensus Document on Standards for Acquisition, Measurement and Reporting of Intravascular Ultrasound Studies (IVUS). A report of the American College of Cardiology Task Force on Clinical Expert Consensus D. *J. Am. Coll. Cardiol.* **37**, 1478–1492 (2001).
62. Fassa, A.-A. *et al.* Intravascular ultrasound-guided treatment for angiographically indeterminate left main coronary artery disease: a long-term follow-up study. *J. Am. Coll. Cardiol.* **45**, 204–211 (2005).
63. Abizaid, A. *et al.* Clinical, intravascular ultrasound, and quantitative angiographic determinants of the coronary flow reserve before and after percutaneous transluminal coronary angioplasty. *Am. J. Cardiol.* **82**, 423–428 (1998).
64. Takagi, A. *et al.* Clinical potential of intravascular ultrasound for physiological assessment of coronary stenosis: relationship between quantitative ultrasound tomography and pressure-derived fractional flow reserve. *Circulation* **100**, 250–255 (1999).
65. Albiero, R. *et al.* Comparison of immediate and intermediate-term results of intravascular ultrasound versus angiography-guided Palmaz-Schatz stent implantation in matched lesions. *Circulation* **96**, 2997–3005 (1997).
66. Nissen, S. E. *et al.* Effect of antihypertensive agents on cardiovascular events in patients with coronary disease and normal blood pressure: the CAMELOT study: a randomized controlled trial. *JAMA* **292**, 2217–2225 (2004).
67. Nissen, S. E. *et al.* Effect of very high-intensity statin therapy on regression of coronary atherosclerosis: the ASTEROID trial. *JAMA* **295**, 1556–1565 (2006).
68. Nair, A., Margolis, M. P., Kuban, B. D. & Vince, D. G. Automated coronary plaque characterisation with intravascular ultrasound backscatter: ex vivo validation. *EuroIntervention J. Eur. Collab. with Work. Gr. Interv. Cardiol. Eur. Soc. Cardiol.* **3**, 113–120 (2007).
69. Nasu, K. *et al.* Accuracy of in vivo coronary plaque morphology assessment: a validation study of in vivo virtual histology compared with in vitro histopathology. *J. Am. Coll. Cardiol.* **47**, 2405–2412 (2006).
70. Stone, G. W. *et al.* A prospective natural-history study of coronary atherosclerosis. *N. Engl. J. Med.* **364**, 226–235 (2011).
71. Regar, E., Schaar, J. A., Mont, E., Virmani, R. & Serruys, P. W. Optical coherence tomography. *Cardiovasc. Radiat. Med.* **4**, 198–204 (2003).
72. Jang, I.-K. *et al.* Visualization of coronary atherosclerotic plaques in patients using optical coherence tomography: comparison with intravascular ultrasound. *J. Am. Coll. Cardiol.* **39**, 604–609 (2002).
73. Caplan, J. D., Waxman, S., Nesto, R. W. & Muller, J. E. Near-infrared spectroscopy for the detection of vulnerable coronary artery plaques. *J. Am. Coll. Cardiol.* **47**, C92-6 (2006).
74. Gardner, C. M. *et al.* Detection of lipid core coronary plaques in autopsy specimens with a novel catheter-based near-infrared spectroscopy system. *JACC. Cardiovasc. Imaging* **1**, 638–648 (2008).
75. Porto, I., Selvanayagam, J., Ashar, V., Neubauer, S. & Banning, A. P. Safety of magnetic resonance imaging one to three days after bare metal and drug-eluting stent implantation. *Am. J. Cardiol.* **96**, 366–368 (2005).
76. Manning, W. J. *et al.* Coronary magnetic resonance imaging. *Cardiol. Clin.* **25**, 141–70, vi (2007).
77. Sakuma, H. *et al.* Detection of coronary artery stenosis with whole-heart coronary magnetic resonance angiography. *J. Am. Coll. Cardiol.* **48**, 1946–1950 (2006).

78. Schuetz, G. M., Zacharopoulou, N. M., Schlattmann, P. & Dewey, M. Meta-analysis: noninvasive coronary angiography using computed tomography versus magnetic resonance imaging. *Ann. Intern. Med.* **152**, 167–177 (2010).
79. Langer, C. *et al.* Noninvasive coronary angiography focusing on calcification: multislice computed tomography compared with magnetic resonance imaging. *J. Comput. Assist. Tomogr.* **33**, 179–185 (2009).
80. Kuijpers, D., Ho, K. Y. J. A. M., van Dijkman, P. R. M., Vliegenthart, R. & Oudkerk, M. Dobutamine cardiovascular magnetic resonance for the detection of myocardial ischemia with the use of myocardial tagging. *Circulation* **107**, 1592–1597 (2003).
81. Lubbers, D. D. *et al.* The additional value of first pass myocardial perfusion imaging during peak dose of dobutamine stress cardiac MRI for the detection of myocardial ischemia. *Int. J. Cardiovasc. Imaging* **24**, 69–76 (2008).
82. Vancraeynest, D., Pasquet, A., Roelants, V., Gerber, B. L. & Vanoverschelde, J.-L. J. Imaging the vulnerable plaque. *J. Am. Coll. Cardiol.* **57**, 1961–1979 (2011).
83. Briley-Saebo, K. C. *et al.* Targeted molecular probes for imaging atherosclerotic lesions with magnetic resonance using antibodies that recognize oxidation-specific epitopes. *Circulation* **117**, 3206–3215 (2008).
84. Fayad, Z. A. *et al.* Noninvasive in vivo human coronary artery lumen and wall imaging using black-blood magnetic resonance imaging. *Circulation* **102**, 506–510 (2000).
85. Schneiderman, J. *et al.* Diagnosis of thin-cap fibroatheromas by a self-contained intravascular magnetic resonance imaging probe in ex vivo human aortas and in situ coronary arteries. *J. Am. Coll. Cardiol.* **45**, 1961–1969 (2005).
86. Yuan, C. *et al.* In vivo accuracy of multispectral magnetic resonance imaging for identifying lipid-rich necrotic cores and intraplaque hemorrhage in advanced human carotid plaques. *Circulation* **104**, 2051–2056 (2001).
87. Lee, J. M. S. *et al.* Effects of high-dose modified-release nicotinic acid on atherosclerosis and vascular function: a randomized, placebo-controlled, magnetic resonance imaging study. *J. Am. Coll. Cardiol.* **54**, 1787–1794 (2009).
88. Tang, T. Y. *et al.* The ATHEROMA (Atorvastatin Therapy: Effects on Reduction of Macrophage Activity) Study. Evaluation using ultrasmall superparamagnetic iron oxide-enhanced magnetic resonance imaging in carotid disease. *J. Am. Coll. Cardiol.* **53**, 2039–2050 (2009).
89. West, A. M. *et al.* The effect of ezetimibe on peripheral arterial atherosclerosis depends upon statin use at baseline. *Atherosclerosis* **218**, 156–162 (2011).
90. Horiguchi, J. *et al.* Coronary artery calcium scoring using 16-MDCT and a retrospective ECG-gating reconstruction algorithm. *AJR. Am. J. Roentgenol.* **183**, 103–108 (2004).
91. Greenland, P. *et al.* ACCF/AHA 2007 clinical expert consensus document on coronary artery calcium scoring by computed tomography in global cardiovascular risk assessment and in evaluation of patients with chest pain: a report of the American College of Cardiology Foundation C. *J. Am. Coll. Cardiol.* **49**, 378–402 (2007).
92. The Multi-Ethnic Study of Atherosclerosis. MESA arterial age calculator. Available at: https://www.mesa-nhlbi.org/Calcium/ArterialAge.aspx.
93. Kronmal, R. A. *et al.* Risk factors for the progression of coronary artery calcification in asymptomatic subjects: results from the Multi-Ethnic Study of Atherosclerosis (MESA). *Circulation* **115**, 2722–2730 (2007).
94. Burke, A. P., Taylor, A., Farb, A., Malcom, G. T. & Virmani, R. Coronary calcification: insights from sudden coronary death victims. *Z. Kardiol.* **89 Suppl 2**, 49–53 (2000).
95. Taylor, A. J. *et al.* Community-based provision of statin and aspirin after the detection of coronary artery calcium within a community-based screening cohort. *J. Am. Coll. Cardiol.* **51**, 1337–1341 (2008).

96. Arad, Y., Spadaro, L. A., Roth, M., Newstein, D. & Guerci, A. D. Treatment of asymptomatic adults with elevated coronary calcium scores with atorvastatin, vitamin C, and vitamin E: the St. Francis Heart Study randomized clinical trial. *J. Am. Coll. Cardiol.* **46**, 166–172 (2005).
97. Voros, S. *et al.* Coronary atherosclerosis imaging by coronary CT angiography: current status, correlation with intravascular interrogation and meta-analysis. *JACC. Cardiovasc. Imaging* **4**, 537–548 (2011).
98. Bamberg, F. *et al.* Meta-analysis and systematic review of the long-term predictive value of assessment of coronary atherosclerosis by contrast-enhanced coronary computed tomography angiography. *J. Am. Coll. Cardiol.* **57**, 2426–2436 (2011).
99. Ostrom, M. P. *et al.* Mortality incidence and the severity of coronary atherosclerosis assessed by computed tomography angiography. *J. Am. Coll. Cardiol.* **52**, 1335–1343 (2008).
100. van der Wal, A. C., Becker, A. E., van der Loos, C. M. & Das, P. K. Site of intimal rupture or erosion of thrombosed coronary atherosclerotic plaques is characterized by an inflammatory process irrespective of the dominant plaque morphology. *Circulation* **89**, 36–44 (1994).
101. Pelberg, R. *Cardiac CT Angiography Manual*. (Springer-Verlag London, 2015). doi:10.1007/978-1-4471-6690-0
102. Abbara, S. *et al.* SCCT guidelines for the performance and acquisition of coronary computed tomographic angiography: A report of the society of Cardiovascular Computed Tomography Guidelines Committee: Endorsed by the North American Society for Cardiovascular Imaging (NASCI. *J. Cardiovasc. Comput. Tomogr.* **10**, 435–449 (2016).
103. Halliburton, S. S. *et al.* SCCT guidelines on radiation dose and dose-optimization strategies in cardiovascular CT. *J. Cardiovasc. Comput. Tomogr.* **5**, 198–224 (2011).
104. Raff, G. L. *et al.* SCCT guidelines for the interpretation and reporting of coronary computed tomographic angiography. *J. Cardiovasc. Comput. Tomogr.* **3**, 122–136 (2009).
105. Taylor, A. J. *et al.* ACCF/SCCT/ACR/AHA/ASE/ASNC/NASCI/SCAI/SCMR 2010 Appropriate Use Criteria for Cardiac Computed Tomography. A Report of the American College of Cardiology Foundation Appropriate Use Criteria Task Force, the Society of Cardiovascular Computed Tomography, th. *J. Cardiovasc. Comput. Tomogr.* **4**, 407.e1–33 (2010).
106. Budoff, M. J. *et al.* ACCF/AHA clinical competence statement on cardiac imaging with computed tomography and magnetic resonance: a report of the American College of Cardiology Foundation/American Heart Association/American College of Physicians Task Force on Clinical Competen. *J. Am. Coll. Cardiol.* **46**, 383–402 (2005).
107. Weigold, W. G. *et al.* Standardized medical terminology for cardiac computed tomography: a report of the Society of Cardiovascular Computed Tomography. *J. Cardiovasc. Comput. Tomogr.* **5**, 136–144 (2011).
108. Meijboom, W. B. *et al.* Diagnostic accuracy of 64-slice computed tomography coronary angiography: a prospective, multicenter, multivendor study. *J. Am. Coll. Cardiol.* **52**, 2135–2144 (2008).
109. Miller, J. M. *et al.* Diagnostic performance of coronary angiography by 64-row CT. *N. Engl. J. Med.* **359**, 2324–2336 (2008).
110. Stein, P. D., Yaekoub, A. Y., Matta, F. & Sostman, H. D. 64-slice CT for diagnosis of coronary artery disease: a systematic review. *Am. J. Med.* **121**, 715–725 (2008).
111. Cheng, V. Y. *et al.* Reproducibility of coronary artery plaque volume and composition quantification by 64-detector row coronary computed tomographic angiography: an intraobserver, interobserver, and interscan variability study. *J. Cardiovasc. Comput. Tomogr.* **3**, 312–320 (2009).
112. Rinehart, S. *et al.* Quantitative measurements of coronary arterial stenosis, plaque geometry, and composition are highly reproducible with a standardized coronary arterial computed tomographic approach in high-quality CT datasets. *J. Cardiovasc. Comput. Tomogr.* **5**, 35–43 (2011).

113. Hulten, E. A., Carbonaro, S., Petrillo, S. P., Mitchell, J. D. & Villines, T. C. Prognostic value of cardiac computed tomography angiography: a systematic review and meta-analysis. *J. Am. Coll. Cardiol.* **57**, 1237–1247 (2011).
114. Lin, F. Y. *et al.* Mortality risk in symptomatic patients with nonobstructive coronary artery disease: a prospective 2-center study of 2,583 patients undergoing 64-detector row coronary computed tomographic angiography. *J. Am. Coll. Cardiol.* **58**, 510–519 (2011).
115. Min, J. K. *et al.* Prognostic value of multidetector coronary computed tomographic angiography for prediction of all-cause mortality. *J. Am. Coll. Cardiol.* **50**, 1161–1170 (2007).
116. Uusitalo, V. *et al.* Coronary computed tomography angiography derived risk score in predicting cardiac events. *J. Cardiovasc. Comput. Tomogr.* **11**, 274–280 (2017).
117. Garcia, E. V *et al.* Technical aspects of myocardial SPECT imaging with technetium-99m sestamibi. *Am. J. Cardiol.* **66**, 23E-31E (1990).
118. Taillefer, R. *et al.* Comparative diagnostic accuracy of Tl-201 and Tc-99m sestamibi SPECT imaging (perfusion and ECG-gated SPECT) in detecting coronary artery disease in women. *J. Am. Coll. Cardiol.* **29**, 69–77 (1997).
119. Watson, D. D. & Smith, W. H. Sestamibi and the issue of tissue crosstalk. *Journal of nuclear medicine : official publication, Society of Nuclear Medicine* **31**, 1409–1411 (1990).
120. Golzar, Y. & Doukky, R. Regadenoson use in patients with chronic obstructive pulmonary disease: the state of current knowledge. *Int. J. Chron. Obstruct. Pulmon. Dis.* **9**, 129–137 (2014).
121. Slomka, P. J., Patton, J. A., Berman, D. S. & Germano, G. Advances in technical aspects of myocardial perfusion SPECT imaging. *J. Nucl. Cardiol. Off. Publ. Am. Soc. Nucl. Cardiol.* **16**, 255–276 (2009).
122. Underwood, S. R. *et al.* Myocardial perfusion scintigraphy: the evidence. *Eur. J. Nucl. Med. Mol. Imaging* **31**, 261–291 (2004).
123. Berman, D. S. *et al.* Underestimation of extent of ischemia by gated SPECT myocardial perfusion imaging in patients with left main coronary artery disease. *J. Nucl. Cardiol. Off. Publ. Am. Soc. Nucl. Cardiol.* **14**, 521–528 (2007).
124. Melikian, N. *et al.* Fractional flow reserve and myocardial perfusion imaging in patients with angiographic multivessel coronary artery disease. *JACC. Cardiovasc. Interv.* **3**, 307–314 (2010).
125. Berger, B. C. *et al.* Redistribution of thallium at rest in patients with stable and unstable angina and the effect of coronary artery bypass surgery. *Circulation* **60**, 1114–1125 (1979).
126. Iskander, S. & Iskandrian, A. E. Risk assessment using single-photon emission computed tomographic technetium-99m sestamibi imaging. *J. Am. Coll. Cardiol.* **32**, 57–62 (1998).
127. Shaw, L. J. & Iskandrian, A. E. Prognostic value of gated myocardial perfusion SPECT. *J. Nucl. Cardiol. Off. Publ. Am. Soc. Nucl. Cardiol.* **11**, 171–185 (2004).
128. Rajagopalan, N., Miller, T. D., Hodge, D. O., Frye, R. L. & Gibbons, R. J. Identifying high-risk asymptomatic diabetic patients who are candidates for screening stress single-photon emission computed tomography imaging. *J. Am. Coll. Cardiol.* **45**, 43–49 (2005).
129. Travin, M. I. *et al.* The prognostic value of ECG-gated SPECT imaging in patients undergoing stress Tc-99m sestamibi myocardial perfusion imaging. *J. Nucl. Cardiol. Off. Publ. Am. Soc. Nucl. Cardiol.* **11**, 253–262 (2004).
130. Hachamovitch, R. *et al.* Determinants of risk and its temporal variation in patients with normal stress myocardial perfusion scans: what is the warranty period of a normal scan? *J. Am. Coll. Cardiol.* **41**, 1329–1340 (2003).
131. Maddahi, J. & Packard, R. R. S. Cardiac PET perfusion tracers: current status and future directions. *Semin. Nucl. Med.* **44**, 333–343 (2014).
132. Nammas, W., Maaniitty, T., Knuuti, J. & Saraste, A. Cardiac perfusion by positron emission tomography. *Clin. Physiol. Funct. Imaging* **41**, 385–400 (2021).
133. Chatal, J.-F. *et al.* Story of Rubidium-82 and Advantages for Myocardial Perfusion PET Imaging. *Front. Med.* **2**, 65 (2015).

134. Dorbala, S. *et al.* SNMMI/ASNC/SCCT guideline for cardiac SPECT/CT and PET/CT 1.0. *J. Nucl. Med.* **54**, 1485–1507 (2013).
135. Camici, P. G. & Rimoldi, O. E. The clinical value of myocardial blood flow measurement. *J. Nucl. Med.* **50**, 1076–1087 (2009).
136. Juneau, D. *et al.* Clinical PET Myocardial Perfusion Imaging and Flow Quantification. *Cardiol. Clin.* **34**, 69–85 (2016).
137. Nandalur, K. R. *et al.* Diagnostic performance of positron emission tomography in the detection of coronary artery disease: a meta-analysis. *Acad. Radiol.* **15**, 444–451 (2008).
138. Parker, M. W. *et al.* Diagnostic accuracy of cardiac positron emission tomography versus single photon emission computed tomography for coronary artery disease: a bivariate meta-analysis. *Circ. Cardiovasc. Imaging* **5**, 700–707 (2012).
139. Yoshinaga, K. *et al.* What is the prognostic value of myocardial perfusion imaging using rubidium-82 positron emission tomography? *J. Am. Coll. Cardiol.* **48**, 1029–1039 (2006).
140. Gerber, B. L. *et al.* Positron emission tomography using(18)F-fluoro-deoxyglucose and euglycaemic hyperinsulinaemic glucose clamp: optimal criteria for the prediction of recovery of post-ischaemic left ventricular dysfunction. Results from the European Community Concerted Act. *Eur. Heart J.* **22**, 1691–1701 (2001).
141. Anavekar, N. S., Chareonthaitawee, P., Narula, J. & Gersh, B. J. Revascularization in Patients With Severe Left Ventricular Dysfunction: Is the Assessment of Viability Still Viable? *J. Am. Coll. Cardiol.* **67**, 2874–2887 (2016).
142. A Project of the National Heart, Lung, and B. I. and B. U. History of the Framingham Heart Study. *Framingham Heart Study* (2017). Available at: http://www.framinghamheartstudy.org/about-fhs/history.php.
143. Framingham Heart Study. Participant Cohorts. (2019). Available at: https://framinghamheartstudy.org/participants/participant-cohorts/.
144. Schnabel, R. B. *et al.* Development of a risk score for atrial fibrillation (Framingham Heart Study): a community-based cohort study. *Lancet (London, England)* **373**, 739–745 (2009).
145. Schnabel, R. B. *et al.* Risk assessment for incident heart failure in individuals with atrial fibrillation. *Eur. J. Heart Fail.* **15**, 843–849 (2013).
146. D'Agostino, R. B. S. *et al.* General cardiovascular risk profile for use in primary care: the Framingham Heart Study. *Circulation* **117**, 743–753 (2008).
147. Pencina, M. J., D'Agostino, R. B. S., Larson, M. G., Massaro, J. M. & Vasan, R. S. Predicting the 30-year risk of cardiovascular disease: the framingham heart study. *Circulation* **119**, 3078–3084 (2009).
148. Kannel, W. B. *et al.* Profile for estimating risk of heart failure. *Arch. Intern. Med.* **159**, 1197–1204 (1999).
149. Executive Summary of The Third Report of The National Cholesterol Education Program (NCEP) Expert Panel on Detection, Evaluation, And Treatment of High Blood Cholesterol In Adults (Adult Treatment Panel III). *JAMA* **285**, 2486–2497 (2001).
150. D'Agostino, R. B. *et al.* Primary and subsequent coronary risk appraisal: new results from the Framingham study. *Am. Heart J.* **139**, 272–281 (2000).
151. Wilson, P. W. F. *et al.* Prediction of incident diabetes mellitus in middle-aged adults: the Framingham Offspring Study. *Arch. Intern. Med.* **167**, 1068–1074 (2007).
152. Long, M. T. *et al.* A simple clinical model predicts incident hepatic steatosis in a community-based cohort: The Framingham Heart Study. *Liver Int. Off. J. Int. Assoc. Study Liver* **38**, 1495–1503 (2018).
153. Parikh, N. I. *et al.* A risk score for predicting near-term incidence of hypertension: the Framingham Heart Study. *Ann. Intern. Med.* **148**, 102–110 (2008).
154. Murabito, J. M., D'Agostino, R. B., Silbershatz, H. & Wilson, W. F. Intermittent claudication. A risk profile from The Framingham Heart Study. *Circulation* **96**, 44–49 (1997).

155. D'Agostino, R. B., Wolf, P. A., Belanger, A. J. & Kannel, W. B. Stroke risk profile: adjustment for antihypertensive medication. The Framingham Study. *Stroke* **25**, 40–43 (1994).
156. Wang, T. J. *et al.* A risk score for predicting stroke or death in individuals with new-onset atrial fibrillation in the community: the Framingham Heart Study. *JAMA* **290**, 1049–1056 (2003).
157. Framingham Heart Study. About the Framingham Heart Study. Available at: https://framinghamheartstudy.org/fhs-about/.
158. SCORE2 risk prediction algorithms: new models to estimate 10-year risk of cardiovascular disease in Europe. *Eur. Heart J.* **42**, 2439–2454 (2021).
159. SCORE2-OP risk prediction algorithms: estimating incident cardiovascular event risk in older persons in four geographical risk regions. *Eur. Heart J.* **42**, 2455–2467 (2021).
160. Duodecim, T. FINRISK calculator. Available at: https://www.terveyskirjasto.fi/pgt00016#s3.
161. Vartiainen, E. *et al.* Sepelvaltimotaudin ja aivohalvauksen riskin arviointi FINRISKI 2.0 -laskurilla. *Lääkärilehti* **75**, 2778–2784 (2020).
162. Libby, P. *et al.* Atherosclerosis. *Nat. Rev. Dis. Prim.* **5**, 56 (2019).
163. Wilson, P. W. F. *et al.* Lipid measurements in the management of cardiovascular diseases: Practical recommendations a scientific statement from the national lipid association writing group. *J. Clin. Lipidol.* **15**, 629–648 (2021).
164. Friedewald, W. T., Levy, R. I. & Fredrickson, D. S. Estimation of the concentration of low-density lipoprotein cholesterol in plasma, without use of the preparative ultracentrifuge. *Clin. Chem.* **18**, 499–502 (1972).
165. Martin, S. S. *et al.* Comparison of a novel method vs the Friedewald equation for estimating low-density lipoprotein cholesterol levels from the standard lipid profile. *JAMA* **310**, 2061–2068 (2013).
166. Mineral Research Laboratory Mila. Cholesterol, LDL, oxidised. Available at: https://laboratorymila.com/cholesterol-ldl-oxidised/.
167. Langlois, M. R. *et al.* Quantifying Atherogenic Lipoproteins: Current and Future Challenges in the Era of Personalized Medicine and Very Low Concentrations of LDL Cholesterol. A Consensus Statement from EAS and EFLM. *Clin. Chem.* **64**, 1006–1033 (2018).
168. Suomalainen Lääkäriseura Duodecim. Dyslipidemiat (Dyslipidaemias). *Käypä hoito -suositus* (2021). Available at: https://www.kaypahoito.fi/hoi50025?tab=suositus.
169. van Deventer, H. E. *et al.* Non-HDL cholesterol shows improved accuracy for cardiovascular risk score classification compared to direct or calculated LDL cholesterol in a dyslipidemic population. *Clin. Chem.* **57**, 490–501 (2011).
170. Robinson, J. G., Wang, S., Smith, B. J. & Jacobson, T. A. Meta-analysis of the relationship between non-high-density lipoprotein cholesterol reduction and coronary heart disease risk. *J. Am. Coll. Cardiol.* **53**, 316–322 (2009).
171. Masana, L. *et al.* Substituting non-HDL cholesterol with LDL as a guide for lipid-lowering therapy increases the number of patients with indication for therapy. *Atherosclerosis* **226**, 471–475 (2013).
172. Cybulska, B., Kłosiewicz-Latoszek, L., Penson, P. E. & Banach, M. What do we know about the role of lipoprotein(a) in atherogenesis 57 years after its discovery? *Prog. Cardiovasc. Dis.* **63**, 219–227 (2020).
173. Puckey, L. & Knight, B. Dietary and genetic interactions in the regulation of plasma lipoprotein(a). *Curr. Opin. Lipidol.* **10**, 35–40 (1999).
174. Orsó, E. & Schmitz, G. Lipoprotein(a) and its role in inflammation, atherosclerosis and malignancies. *Clin. Res. Cardiol. Suppl.* **12**, 31–37 (2017).
175. Saleheen, D. *et al.* Apolipoprotein(a) isoform size, lipoprotein(a) concentration, and coronary artery disease: a mendelian randomisation analysis. *lancet. Diabetes Endocrinol.* **5**, 524–533 (2017).
176. Rehberger Likozar, A., Zavrtanik, M. & Šebeštjen, M. Lipoprotein(a) in atherosclerosis: from pathophysiology to clinical relevance and treatment options. *Ann. Med.* **52**, 162–177 (2020).

177. Enas, E. A., Varkey, B., Dharmarajan, T. S., Pare, G. & Bahl, V. K. Lipoprotein(a): An independent, genetic, and causal factor for cardiovascular disease and acute myocardial infarction. *Indian Heart J.* **71**, 99–112 (2019).
178. Kiechl, S. & Willeit, J. The mysteries of lipoprotein(a) and cardiovascular disease revisited. *Journal of the American College of Cardiology* **55**, 2168–2170 (2010).
179. Deb, A. & Caplice, N. M. Lipoprotein(a): new insights into mechanisms of atherogenesis and thrombosis. *Clin. Cardiol.* **27**, 258–264 (2004).
180. Labudovic, D. *et al.* Lipoprotein(a) - Link between Atherogenesis and Thrombosis. *Prague Med. Rep.* **120**, 39–51 (2019).
181. Nave, A. H. *et al.* Lipoprotein (a) as a risk factor for ischemic stroke: a meta-analysis. *Atherosclerosis* **242**, 496–503 (2015).
182. Nordestgaard, B. G. *et al.* Lipoprotein(a) as a cardiovascular risk factor: current status. *Eur. Heart J.* **31**, 2844–2853 (2010).
183. Willeit, P. *et al.* Baseline and on-statin treatment lipoprotein(a) levels for prediction of cardiovascular events: individual patient-data meta-analysis of statin outcome trials. *Lancet (London, England)* **392**, 1311–1320 (2018).
184. Zhang, Y. *et al.* Prognostic utility of lipoprotein(a) combined with fibrinogen in patients with stable coronary artery disease: a prospective, large cohort study. *J. Transl. Med.* **18**, 373 (2020).
185. Kardys, I. *et al.* Lipoprotein(a), interleukin-10, C-reactive protein, and 8-year outcome after percutaneous coronary intervention. *Clin. Cardiol.* **35**, 482–489 (2012).
186. Pineda, J. *et al.* The prognostic value of biomarkers after a premature myocardial infarction. *Int. J. Cardiol.* **143**, 249–254 (2010).
187. Ozkan, U., Ozcelik, F., Yildiz, M. & Budak, M. Lipoprotein(a) Gene Polymorphism Increases a Risk Factor for Aortic Valve Calcification. *J. Cardiovasc. Dev. Dis.* **6**, (2019).
188. Langsted, A., Kamstrup, P. R. & Nordestgaard, B. G. Lipoprotein(a): fasting and nonfasting levels, inflammation, and cardiovascular risk. *Atherosclerosis* **234**, 95–101 (2014).
189. O'Donoghue, M. L. *et al.* Lipoprotein(a), PCSK9 Inhibition, and Cardiovascular Risk. *Circulation* **139**, 1483–1492 (2019).
190. Bittner, V. A. *et al.* Effect of Alirocumab on Lipoprotein(a) and Cardiovascular Risk After Acute Coronary Syndrome. *J. Am. Coll. Cardiol.* **75**, 133–144 (2020).
191. Sabatine, M. S. *et al.* Evolocumab and Clinical Outcomes in Patients with Cardiovascular Disease. *N. Engl. J. Med.* **376**, 1713–1722 (2017).
192. Schwartz, G. G. *et al.* Alirocumab and Cardiovascular Outcomes after Acute Coronary Syndrome. *N. Engl. J. Med.* **379**, 2097–2107 (2018).
193. Doonan, L. M., Fisher, E. A. & Brodsky, J. L. Can modulators of apolipoproteinB biogenesis serve as an alternate target for cholesterol-lowering drugs? *Biochim. Biophys. acta. Mol. cell Biol. lipids* **1863**, 762–771 (2018).
194. Morita, S. Metabolism and Modification of Apolipoprotein B-Containing Lipoproteins Involved in Dyslipidemia and Atherosclerosis. *Biol. Pharm. Bull.* **39**, 1–24 (2016).
195. Davidson, N. O. & Shelness, G. S. APOLIPOPROTEIN B: mRNA editing, lipoprotein assembly, and presecretory degradation. *Annu. Rev. Nutr.* **20**, 169–193 (2000).
196. Oörni, K., Pentikäinen, M. O., Ala-Korpela, M. & Kovanen, P. T. Aggregation, fusion, and vesicle formation of modified low density lipoprotein particles: molecular mechanisms and effects on matrix interactions. *J. Lipid Res.* **41**, 1703–1714 (2000).
197. Skålén, K. *et al.* Subendothelial retention of atherogenic lipoproteins in early atherosclerosis. *Nature* **417**, 750–754 (2002).
198. Cantey, E. P. & Wilkins, J. T. Discordance between lipoprotein particle number and cholesterol content: an update. *Curr. Opin. Endocrinol. Diabetes. Obes.* **25**, 130–136 (2018).
199. Ohwada, T. *et al.* Apolipoprotein B correlates with intra-plaque necrotic core volume in stable coronary artery disease. *PLoS One* **14**, e0212539 (2019).

200. Barter, P. J. *et al.* Apo B versus cholesterol in estimating cardiovascular risk and in guiding therapy: report of the thirty-person/ten-country panel. *J. Intern. Med.* **259**, 247–258 (2006).
201. Cao, J. *et al.* A comparison of three apolipoprotein B methods and their associations with incident coronary heart disease risk over a 12-year follow-up period: The Multi-Ethnic Study of Atherosclerosis. *J. Clin. Lipidol.* **12**, 300–304 (2018).
202. Walldius, G. *et al.* High apolipoprotein B, low apolipoprotein A-I, and improvement in the prediction of fatal myocardial infarction (AMORIS study): a prospective study. *Lancet (London, England)* **358**, 2026–2033 (2001).
203. Walldius, G. & Jungner, I. Is there a better marker of cardiovascular risk than LDL cholesterol? Apolipoproteins B and A-I--new risk factors and targets for therapy. *Nutr. Metab. Cardiovasc. Dis.* **17**, 565–571 (2007).
204. Tian, M. *et al.* Comparison of Apolipoprotein B/A1 ratio, Framingham risk score and TC/HDL-c for predicting clinical outcomes in patients undergoing percutaneous coronary intervention. *Lipids Health Dis.* **18**, 202 (2019).
205. Sierra-Johnson, J. *et al.* Concentration of apolipoprotein B is comparable with the apolipoprotein B/apolipoprotein A-I ratio and better than routine clinical lipid measurements in predicting coronary heart disease mortality: findings from a multi-ethnic US population. *Eur. Heart J.* **30**, 710–717 (2009).
206. Karjalainen, M. K. *et al.* Apolipoprotein A-I concentrations and risk of coronary artery disease: A Mendelian randomization study. *Atherosclerosis* **299**, 56–63 (2020).
207. Karasek, D., Vaverkova, H., Cibickova, L., Gajdova, J. & Kubickova, V. Apolipoprotein B vs non-high-density lipoprotein cholesterol: Association with endothelial hemostatic markers and carotid intima-media thickness. *J. Clin. Lipidol.* **11**, 442–449 (2017).
208. Dennis, E. A., Cao, J., Hsu, Y.-H., Magrioti, V. & Kokotos, G. Phospholipase A2 enzymes: physical structure, biological function, disease implication, chemical inhibition, and therapeutic intervention. *Chem. Rev.* **111**, 6130–6185 (2011).
209. Stafforini, D. M. Biology of platelet-activating factor acetylhydrolase (PAF-AH, lipoprotein associated phospholipase A2). *Cardiovasc. drugs Ther.* **23**, 73–83 (2009).
210. Howard, K. M., Miller, J. E., Miwa, M. & Olson, M. S. Cell-specific regulation of expression of plasma-type platelet-activating factor acetylhydrolase in the liver. *J. Biol. Chem.* **272**, 27543–27548 (1997).
211. Tsoukatos, D. C. *et al.* Platelet-activating factor acetylhydrolase and transacetylase activities in human aorta and mammary artery. *J. Lipid Res.* **49**, 2240–2249 (2008).
212. Jackisch, L. *et al.* Differential expression of Lp-PLA2 in obesity and type 2 diabetes and the influence of lipids. *Diabetologia* **61**, 1155–1166 (2018).
213. Tellis, C. C. & Tselepis, A. D. Pathophysiological role and clinical significance of lipoprotein-associated phospholipase A_2 (Lp-PLA_2) bound to LDL and HDL. *Curr. Pharm. Des.* **20**, 6256–6269 (2014).
214. Zalewski, A. & Macphee, C. Role of lipoprotein-associated phospholipase A2 in atherosclerosis: biology, epidemiology, and possible therapeutic target. *Arterioscler. Thromb. Vasc. Biol.* **25**, 923–931 (2005).
215. Münzel, T. & Gori, T. Lipoprotein-associated phospholipase A(2), a marker of vascular inflammation and systemic vulnerability. *European heart journal* **30**, 2829–2831 (2009).
216. O'Donoghue, M. L. *et al.* Effect of darapladib on major coronary events after an acute coronary syndrome: the SOLID-TIMI 52 randomized clinical trial. *JAMA* **312**, 1006–1015 (2014).
217. White, H. D. *et al.* Darapladib for preventing ischemic events in stable coronary heart disease. *N. Engl. J. Med.* **370**, 1702–1711 (2014).
218. Maher-Edwards, G., De'Ath, J., Barnett, C., Lavrov, A. & Lockhart, A. A 24-week study to evaluate the effect of rilapladib on cognition and cerebrospinal fluid biomarkers of Alzheimer's disease. *Alzheimer's Dement. (New York, N. Y.)* **1**, 131–140 (2015).

219. Staurenghi, G. *et al.* Darapladib, a lipoprotein-associated phospholipase A2 inhibitor, in diabetic macular edema: a 3-month placebo-controlled study. *Ophthalmology* **122**, 990–996 (2015).
220. Thompson, A. *et al.* Lipoprotein-associated phospholipase A(2) and risk of coronary disease, stroke, and mortality: collaborative analysis of 32 prospective studies. *Lancet (London, England)* **375**, 1536–1544 (2010).
221. Ge, P.-C. *et al.* Synergistic Effect of Lipoprotein-Associated Phospholipase A2 with Classical Risk Factors on Coronary Heart Disease: A Multi-Ethnic Study in China. *Cell. Physiol. Biochem. Int. J. Exp. Cell. Physiol. Biochem. Pharmacol.* **40**, 953–968 (2016).
222. Tibaut, M. *et al.* Markers of Atherosclerosis: Part 1 - Serological Markers. *Heart. Lung Circ.* **28**, 667–677 (2019).
223. Summers, S. A. Could Ceramides Become the New Cholesterol? *Cell Metab.* **27**, 276–280 (2018).
224. Larsen, P. J. & Tennagels, N. On ceramides, other sphingolipids and impaired glucose homeostasis. *Mol. Metab.* **3**, 252–260 (2014).
225. Merrill, A. H. J. *et al.* Sphingolipid biosynthesis de novo by rat hepatocytes in culture. Ceramide and sphingomyelin are associated with, but not required for, very low density lipoprotein secretion. *J. Biol. Chem.* **270**, 13834–13841 (1995).
226. Laaksonen, R. *et al.* Plasma ceramides predict cardiovascular death in patients with stable coronary artery disease and acute coronary syndromes beyond LDL-cholesterol. *Eur. Heart J.* **37**, 1967–1976 (2016).
227. Kauhanen, D. *et al.* Development and validation of a high-throughput LC-MS/MS assay for routine measurement of molecular ceramides. *Anal. Bioanal. Chem.* **408**, 3475–3483 (2016).
228. Wiesner, P., Leidl, K., Boettcher, A., Schmitz, G. & Liebisch, G. Lipid profiling of FPLC-separated lipoprotein fractions by electrospray ionization tandem mass spectrometry. *J. Lipid Res.* **50**, 574–585 (2009).
229. Ståhlman, M. *et al.* Dyslipidemia, but not hyperglycemia and insulin resistance, is associated with marked alterations in the HDL lipidome in type 2 diabetic subjects in the DIWA cohort: impact on small HDL particles. *Biochim. Biophys. Acta* **1831**, 1609–1617 (2013).
230. Schissel, S. L. *et al.* Rabbit aorta and human atherosclerotic lesions hydrolyze the sphingomyelin of retained low-density lipoprotein. Proposed role for arterial-wall sphingomyelinase in subendothelial retention and aggregation of atherogenic lipoproteins. *J. Clin. Invest.* **98**, 1455–1464 (1996).
231. Tarasov, K. *et al.* Molecular lipids identify cardiovascular risk and are efficiently lowered by simvastatin and PCSK9 deficiency. *J. Clin. Endocrinol. Metab.* **99**, E45-52 (2014).
232. Cheng, J. M. *et al.* Plasma concentrations of molecular lipid species in relation to coronary plaque characteristics and cardiovascular outcome: Results of the ATHEROREMO-IVUS study. *Atherosclerosis* **243**, 560–566 (2015).
233. Havulinna, A. S. *et al.* Circulating Ceramides Predict Cardiovascular Outcomes in the Population-Based FINRISK 2002 Cohort. *Arterioscler. Thromb. Vasc. Biol.* **36**, 2424–2430 (2016).
234. Ridker, P. M. A Test in Context: High-Sensitivity C-Reactive Protein. *J. Am. Coll. Cardiol.* **67**, 712–723 (2016).
235. Boncler, M., Wu, Y. & Watala, C. The Multiple Faces of C-Reactive Protein-Physiological and Pathophysiological Implications in Cardiovascular Disease. *Molecules* **24**, (2019).
236. Kaptoge, S. *et al.* C-reactive protein concentration and risk of coronary heart disease, stroke, and mortality: an individual participant meta-analysis. *Lancet (London, England)* **375**, 132–140 (2010).
237. Penson, P. E. *et al.* Associations between very low concentrations of low density lipoprotein cholesterol, high sensitivity C-reactive protein, and health outcomes in the Reasons for Geographical and Racial Differences in Stroke (REGARDS) study. *Eur. Heart J.* **39**, 3641–3653 (2018).

238. Albert, M. A., Danielson, E., Rifai, N. & Ridker, P. M. Effect of statin therapy on C-reactive protein levels: the pravastatin inflammation/CRP evaluation (PRINCE): a randomized trial and cohort study. *JAMA* **286**, 64–70 (2001).
239. Ridker, P. M. *et al.* Measurement of C-reactive protein for the targeting of statin therapy in the primary prevention of acute coronary events. *N. Engl. J. Med.* **344**, 1959–1965 (2001).
240. Ridker, P. M. *et al.* Rosuvastatin to prevent vascular events in men and women with elevated C-reactive protein. *N. Engl. J. Med.* **359**, 2195–2207 (2008).
241. Lawler, P. R. *et al.* Targeting cardiovascular inflammation: next steps in clinical translation. *Eur. Heart J.* **42**, 113–131 (2021).
242. Arroyo-Espliguero, R. *et al.* C-reactive protein elevation and disease activity in patients with coronary artery disease. *Eur. Heart J.* **25**, 401–408 (2004).
243. Sattar, N. *et al.* C-reactive protein and prediction of coronary heart disease and global vascular events in the Prospective Study of Pravastatin in the Elderly at Risk (PROSPER). *Circulation* **115**, 981–989 (2007).
244. Arroyo-Espliguero, R., Avanzas, P., Quiles, J. & Kaski, J. C. Predictive value of coronary artery stenoses and C-reactive protein levels in patients with stable coronary artery disease. *Atherosclerosis* **204**, 239–243 (2009).
245. Held, C. *et al.* Inflammatory Biomarkers Interleukin-6 and C-Reactive Protein and Outcomes in Stable Coronary Heart Disease: Experiences From the STABILITY (Stabilization of Atherosclerotic Plaque by Initiation of Darapladib Therapy) Trial. *J. Am. Heart Assoc.* **6**, (2017).
246. Pradhan, A. D., Aday, A. W., Rose, L. M. & Ridker, P. M. Residual Inflammatory Risk on Treatment With PCSK9 Inhibition and Statin Therapy. *Circulation* **138**, 141–149 (2018).
247. Bohula, E. A. *et al.* Inflammatory and Cholesterol Risk in the FOURIER Trial. *Circulation* **138**, 131–140 (2018).
248. Nissen, S. E. *et al.* Statin therapy, LDL cholesterol, C-reactive protein, and coronary artery disease. *N. Engl. J. Med.* **352**, 29–38 (2005).
249. Arroyo-Espliguero, R., Viana-Llamas, M. C., Silva-Obregón, A. & Avanzas, P. The Role of C-reactive Protein in Patient Risk Stratification and Treatment. *Eur. Cardiol.* **16**, e28 (2021).
250. Piepoli, M. F. *et al.* 2016 European Guidelines on cardiovascular disease prevention in clinical practice: The Sixth Joint Task Force of the European Society of Cardiology and Other Societies on Cardiovascular Disease Prevention in Clinical Practice (constituted by representat. *Eur. Heart J.* **37**, 2315–2381 (2016).
251. Tuñón, J. *et al.* Identifying the anti-inflammatory response to lipid lowering therapy: a position paper from the working group on atherosclerosis and vascular biology of the European Society of Cardiology. *Cardiovasc. Res.* **115**, 10–19 (2019).
252. Ohta, H. *et al.* Disruption of tumor necrosis factor-alpha gene diminishes the development of atherosclerosis in ApoE-deficient mice. *Atherosclerosis* **180**, 11–17 (2005).
253. Zhang, H. *et al.* Role of TNF-alpha in vascular dysfunction. *Clin. Sci. (Lond).* **116**, 219–230 (2009).
254. Jovinge, S. *et al.* Evidence for a role of tumor necrosis factor alpha in disturbances of triglyceride and glucose metabolism predisposing to coronary heart disease. *Metabolism.* **47**, 113–118 (1998).
255. Irace, C. *et al.* Effect of anti TNFalpha therapy on arterial diameter and wall shear stress and HDL cholesterol. *Atherosclerosis* **177**, 113–118 (2004).
256. Dixon, W. G. *et al.* Reduction in the incidence of myocardial infarction in patients with rheumatoid arthritis who respond to anti-tumor necrosis factor alpha therapy: results from the British Society for Rheumatology Biologics Register. *Arthritis Rheum.* **56**, 2905–2912 (2007).
257. Soeki, T. & Sata, M. Inflammatory Biomarkers and Atherosclerosis. *Int. Heart J.* **57**, 134–139 (2016).
258. Dinarello, C. A. Proinflammatory cytokines. *Chest* **118**, 503–508 (2000).
259. Waehre, T. *et al.* Increased expression of interleukin-1 in coronary artery disease with downregulatory effects of HMG-CoA reductase inhibitors. *Circulation* **109**, 1966–1972 (2004).

260. Kirii, H. *et al.* Lack of interleukin-1beta decreases the severity of atherosclerosis in ApoE-deficient mice. *Arterioscler. Thromb. Vasc. Biol.* **23**, 656–660 (2003).
261. Katz, M. F., Farber, H. W., Dodds-Stitt, Z., Cruikshank, W. W. & Beer, D. J. Serotonin-stimulated aortic endothelial cells secrete a novel T lymphocyte chemotactic and growth factor. *J. Leukoc. Biol.* **55**, 567–573 (1994).
262. Mizia-Stec, K. *et al.* Serum tumour necrosis factor-alpha, interleukin-2 and interleukin-10 activation in stable angina and acute coronary syndromes. *Coron. Artery Dis.* **14**, 431–438 (2003).
263. Hartman, J. & Frishman, W. H. Inflammation and atherosclerosis: a review of the role of interleukin-6 in the development of atherosclerosis and the potential for targeted drug therapy. *Cardiol. Rev.* **22**, 147–151 (2014).
264. Hurst, S. M. *et al.* Il-6 and its soluble receptor orchestrate a temporal switch in the pattern of leukocyte recruitment seen during acute inflammation. *Immunity* **14**, 705–714 (2001).
265. Brasier, A. R. The nuclear factor-kappaB-interleukin-6 signalling pathway mediating vascular inflammation. *Cardiovasc. Res.* **86**, 211–218 (2010).
266. Schieffer, B. *et al.* Impact of interleukin-6 on plaque development and morphology in experimental atherosclerosis. *Circulation* **110**, 3493–3500 (2004).
267. Koenig, W. & Khuseyinova, N. Biomarkers of atherosclerotic plaque instability and rupture. *Arterioscler. Thromb. Vasc. Biol.* **27**, 15–26 (2007).
268. Li, H., Liu, W. & Xie, J. Circulating interleukin-6 levels and cardiovascular and all-cause mortality in the elderly population: A meta-analysis. *Arch. Gerontol. Geriatr.* **73**, 257–262 (2017).
269. Cushing, S. D. *et al.* Minimally modified low density lipoprotein induces monocyte chemotactic protein 1 in human endothelial cells and smooth muscle cells. *Proc. Natl. Acad. Sci. U. S. A.* **87**, 5134–5138 (1990).
270. Gu, L. *et al.* Absence of monocyte chemoattractant protein-1 reduces atherosclerosis in low density lipoprotein receptor-deficient mice. *Mol. Cell* **2**, 275–281 (1998).
271. Ni, W. *et al.* New anti-monocyte chemoattractant protein-1 gene therapy attenuates atherosclerosis in apolipoprotein E-knockout mice. *Circulation* **103**, 2096–2101 (2001).
272. Frangogiannis, N. G. The mechanistic basis of infarct healing. *Antioxid. Redox Signal.* **8**, 1907–1939 (2006).
273. Deo, R. *et al.* Association among plasma levels of monocyte chemoattractant protein-1, traditional cardiovascular risk factors, and subclinical atherosclerosis. *J. Am. Coll. Cardiol.* **44**, 1812–1818 (2004).
274. de Lemos, J. A. *et al.* Association between plasma levels of monocyte chemoattractant protein-1 and long-term clinical outcomes in patients with acute coronary syndromes. *Circulation* **107**, 690–695 (2003).
275. Sugiyama, S. *et al.* Macrophage myeloperoxidase regulation by granulocyte macrophage colony-stimulating factor in human atherosclerosis and implications in acute coronary syndromes. *Am. J. Pathol.* **158**, 879–891 (2001).
276. Kampoli, A.-M. *et al.* Clinical utility of biomarkers in premature atherosclerosis. *Curr. Med. Chem.* **19**, 2521–2533 (2012).
277. Tibaut, M. & Petrovič, D. Oxidative Stress Genes, Antioxidants and Coronary Artery Disease in Type 2 Diabetes Mellitus. *Cardiovasc. Hematol. Agents Med. Chem.* **14**, 23–38 (2016).
278. Zhang, R. *et al.* Association between myeloperoxidase levels and risk of coronary artery disease. *JAMA* **286**, 2136–2142 (2001).
279. Teng, N. *et al.* The roles of myeloperoxidase in coronary artery disease and its potential implication in plaque rupture. *Redox Rep.* **22**, 51–73 (2017).
280. Pawlus, J., Hołub, M., Kozuch, M., Dabrowska, M. & Dobrzycki, S. Serum myeloperoxidase levels and platelet activation parameters as diagnostic and prognostic markers in the course of coronary disease. *Int. J. Lab. Hematol.* **32**, 320–328 (2010).

281. Samsamshariat, S. Z., Basati, G., Movahedian, A., Pourfarzam, M. & Sarrafzadegan, N. Elevated plasma myeloperoxidase levels in relation to circulating inflammatory markers in coronary artery disease. *Biomark. Med.* **5**, 377–385 (2011).
282. Tretjakovs, P. *et al.* Circulating adhesion molecules, matrix metalloproteinase-9, plasminogen activator inhibitor-1, and myeloperoxidase in coronary artery disease patients with stable and unstable angina. *Clin. Chim. Acta.* **413**, 25–29 (2012).
283. Heslop, C. L., Frohlich, J. J. & Hill, J. S. Myeloperoxidase and C-reactive protein have combined utility for long-term prediction of cardiovascular mortality after coronary angiography. *J. Am. Coll. Cardiol.* **55**, 1102–1109 (2010).
284. Baseri, M. *et al.* Myeloperoxidase levels predicts angiographic severity of coronary artery disease in patients with chronic stable angina. *Adv. Biomed. Res.* **3**, 139 (2014).
285. Meuwese, M. C. *et al.* Serum myeloperoxidase levels are associated with the future risk of coronary artery disease in apparently healthy individuals: the EPIC-Norfolk Prospective Population Study. *J. Am. Coll. Cardiol.* **50**, 159–165 (2007).
286. Rebeiz, A. G. *et al.* Plasma myeloperoxidase concentration predicts the presence and severity of coronary disease in patients with chest pain and negative troponin-T. *Coron. Artery Dis.* **22**, 553–558 (2011).
287. Narula, J. *et al.* Histopathologic characteristics of atherosclerotic coronary disease and implications of the findings for the invasive and noninvasive detection of vulnerable plaques. *J. Am. Coll. Cardiol.* **61**, 1041–1051 (2013).
288. van Velzen, J. E. *et al.* Comprehensive assessment of spotty calcifications on computed tomography angiography: comparison to plaque characteristics on intravascular ultrasound with radiofrequency backscatter analysis. *J. Nucl. Cardiol. Off. Publ. Am. Soc. Nucl. Cardiol.* **18**, 893–903 (2011).
289. Myasoedova, V. A., Chistiakov, D. A., Grechko, A. V & Orekhov, A. N. Matrix metalloproteinases in pro-atherosclerotic arterial remodeling. *J. Mol. Cell. Cardiol.* **123**, 159–167 (2018).
290. Gough, P. J., Gomez, I. G., Wille, P. T. & Raines, E. W. Macrophage expression of active MMP-9 induces acute plaque disruption in apoE-deficient mice. *J. Clin. Invest.* **116**, 59–69 (2006).
291. Marino-Puertas, L., Goulas, T. & Gomis-Rüth, F. X. Matrix metalloproteinases outside vertebrates. *Biochim. Biophys. acta. Mol. cell Res.* **1864**, 2026–2035 (2017).
292. Cauwe, B., Van den Steen, P. E. & Opdenakker, G. The biochemical, biological, and pathological kaleidoscope of cell surface substrates processed by matrix metalloproteinases. *Crit. Rev. Biochem. Mol. Biol.* **42**, 113–185 (2007).
293. Kowara, M., Cudnoch-Jedrzejewska, A., Opolski, G. & Wlodarski, P. MicroRNA regulation of extracellular matrix components in the process of atherosclerotic plaque destabilization. *Clin. Exp. Pharmacol. Physiol.* **44**, 711–718 (2017).
294. Dabek, J., Glogowska-Ligus, J. & Szadorska, B. Transcription activity of MMP-2 and MMP-9 metalloproteinase genes and their tissue inhibitor (TIMP-2) in acute coronary syndrome patients. *J. Postgrad. Med.* **59**, 115–120 (2013).
295. Turu, M. M. *et al.* Intraplaque MMP-8 levels are increased in asymptomatic patients with carotid plaque progression on ultrasound. *Atherosclerosis* **187**, 161–169 (2006).
296. Dhillon, O. S. *et al.* Matrix metalloproteinase-2 predicts mortality in patients with acute coronary syndrome. *Clin. Sci. (Lond).* **118**, 249–257 (2009).
297. Inokubo, Y. *et al.* Plasma levels of matrix metalloproteinase-9 and tissue inhibitor of metalloproteinase-1 are increased in the coronary circulation in patients with acute coronary syndrome. *Am. Heart J.* **141**, 211–217 (2001).
298. Blankenberg, S. *et al.* Plasma concentrations and genetic variation of matrix metalloproteinase 9 and prognosis of patients with cardiovascular disease. *Circulation* **107**, 1579–1585 (2003).

299. Garvin, P., Jonasson, L., Nilsson, L., Falk, M. & Kristenson, M. Plasma Matrix Metalloproteinase-9 Levels Predict First-Time Coronary Heart Disease: An 8-Year Follow-Up of a Community-Based Middle Aged Population. *PLoS One* **10**, e0138290 (2015).
300. Tuomainen, A. M. *et al.* Serum matrix metalloproteinase-8 concentrations are associated with cardiovascular outcome in men. *Arterioscler. Thromb. Vasc. Biol.* **27**, 2722–2728 (2007).
301. Goncalves, I. *et al.* Elevated Plasma Levels of MMP-12 Are Associated With Atherosclerotic Burden and Symptomatic Cardiovascular Disease in Subjects With Type 2 Diabetes. *Arterioscler. Thromb. Vasc. Biol.* **35**, 1723–1731 (2015).
302. de Lemos, J. A. Increasingly sensitive assays for cardiac troponins: a review. *JAMA* **309**, 2262–2269 (2013).
303. Parmacek, M. S. & Solaro, R. J. Biology of the troponin complex in cardiac myocytes. *Prog. Cardiovasc. Dis.* **47**, 159–176 (2004).
304. Westermann, D., Neumann, J. T., Sörensen, N. A. & Blankenberg, S. High-sensitivity assays for troponin in patients with cardiac disease. *Nat. Rev. Cardiol.* **14**, 472–483 (2017).
305. Takeda, S., Yamashita, A., Maeda, K. & Maéda, Y. Structure of the core domain of human cardiac troponin in the Ca(2+)-saturated form. *Nature* **424**, 35–41 (2003).
306. Rasmussen, M. & Jin, J.-P. Troponin Variants as Markers of Skeletal Muscle Health and Diseases. *Front. Physiol.* **12**, 747214 (2021).
307. Apple, F. S. & Collinson, P. O. Analytical characteristics of high-sensitivity cardiac troponin assays. *Clin. Chem.* **58**, 54–61 (2012).
308. Reichlin, T. *et al.* Incremental value of copeptin for rapid rule out of acute myocardial infarction. *J. Am. Coll. Cardiol.* **54**, 60–68 (2009).
309. Mingels, A. *et al.* Reference population and marathon runner sera assessed by highly sensitive cardiac troponin T and commercial cardiac troponin T and I assays. *Clin. Chem.* **55**, 101–108 (2009).
310. FDA. 510(k) substantial equivalence determination desicion summary. *US Food & Drug Administration* (2017). Available at: https://www.accessdata.fda.gov/cdrh_docs/reviews/K162895.pdf.
311. Omland, T. *et al.* A sensitive cardiac troponin T assay in stable coronary artery disease. *N. Engl. J. Med.* **361**, 2538–2547 (2009).
312. Omland, T. *et al.* Prognostic value of cardiac troponin I measured with a highly sensitive assay in patients with stable coronary artery disease. *J. Am. Coll. Cardiol.* **61**, 1240–1249 (2013).
313. Everett, B. M. *et al.* Troponin and Cardiac Events in Stable Ischemic Heart Disease and Diabetes. *N. Engl. J. Med.* **373**, 610–620 (2015).
314. White, H. D. *et al.* Association of contemporary sensitive troponin I levels at baseline and change at 1 year with long-term coronary events following myocardial infarction or unstable angina: results from the LIPID Study (Long-Term Intervention With Pravastatin in Ischaemic. *J. Am. Coll. Cardiol.* **63**, 345–354 (2014).
315. Bansal, N. *et al.* High-sensitivity troponin T and N-terminal pro-B-type natriuretic peptide (NT-proBNP) and risk of incident heart failure in patients with CKD: the Chronic Renal Insufficiency Cohort (CRIC) Study. *J. Am. Soc. Nephrol.* **26**, 946–956 (2015).
316. McGill, D., Talaulikar, G., Potter, J. M., Koerbin, G. & Hickman, P. E. Over time, high-sensitivity TnT replaces NT-proBNP as the most powerful predictor of death in patients with dialysis-dependent chronic renal failure. *Clin. Chim. Acta.* **411**, 936–939 (2010).
317. Tentzeris, I. *et al.* Complementary role of copeptin and high-sensitivity troponin in predicting outcome in patients with stable chronic heart failure. *Eur. J. Heart Fail.* **13**, 726–733 (2011).
318. Barlera, S. *et al.* Predictors of mortality in 6975 patients with chronic heart failure in the Gruppo Italiano per lo Studio della Streptochinasi nell'Infarto Miocardico-Heart Failure trial: proposal for a nomogram. *Circ. Heart Fail.* **6**, 31–39 (2013).

319. Masson, S. *et al.* Serial measurement of cardiac troponin T using a highly sensitive assay in patients with chronic heart failure: data from 2 large randomized clinical trials. *Circulation* **125**, 280–288 (2012).
320. Blankenberg, S. *et al.* Contribution of 30 biomarkers to 10-year cardiovascular risk estimation in 2 population cohorts: the MONICA, risk, genetics, archiving, and monograph (MORGAM) biomarker project. *Circulation* **121**, 2388–2397 (2010).
321. Blankenberg, S. *et al.* Troponin I and cardiovascular risk prediction in the general population: the BiomarCaRE consortium. *Eur. Heart J.* **37**, 2428–2437 (2016).
322. Carthew, R. W. & Sontheimer, E. J. Origins and Mechanisms of miRNAs and siRNAs. *Cell* **136**, 642–655 (2009).
323. Arroyo, J. D. *et al.* Argonaute2 complexes carry a population of circulating microRNAs independent of vesicles in human plasma. *Proc. Natl. Acad. Sci. U. S. A.* **108**, 5003–5008 (2011).
324. Cortez, M. A. *et al.* MicroRNAs in body fluids--the mix of hormones and biomarkers. *Nat. Rev. Clin. Oncol.* **8**, 467–477 (2011).
325. Weber, J. A. *et al.* The microRNA spectrum in 12 body fluids. *Clin. Chem.* **56**, 1733–1741 (2010).
326. Dlouhá, D. & Hubáček, J. A. Regulatory RNAs and cardiovascular disease - with a special focus on circulating microRNAs. *Physiol. Res.* **66**, S21–S38 (2017).
327. Raitoharju, E., Oksala, N. & Lehtimäki, T. MicroRNAs in the atherosclerotic plaque. *Clin. Chem.* **59**, 1708–1721 (2013).
328. Creemers, E. E., Tijsen, A. J. & Pinto, Y. M. Circulating microRNAs: novel biomarkers and extracellular communicators in cardiovascular disease? *Circ. Res.* **110**, 483–495 (2012).
329. Wang, K. *et al.* Comparing the MicroRNA spectrum between serum and plasma. *PLoS One* **7**, e41561 (2012).
330. Rawlings-Goss, R. A., Campbell, M. C. & Tishkoff, S. A. Global population-specific variation in miRNA associated with cancer risk and clinical biomarkers. *BMC Med. Genomics* **7**, 53 (2014).
331. Fichtlscherer, S. *et al.* Circulating microRNAs in patients with coronary artery disease. *Circ. Res.* **107**, 677–684 (2010).
332. Elmén, J. *et al.* Antagonism of microRNA-122 in mice by systemically administered LNA-antimiR leads to up-regulation of a large set of predicted target mRNAs in the liver. *Nucleic Acids Res.* **36**, 1153–1162 (2008).
333. Dong, J. *et al.* Potential Role of Lipometabolism-Related MicroRNAs in Peripheral Blood Mononuclear Cells as Biomarkers for Coronary Artery Disease. *J. Atheroscler. Thromb.* **24**, 430–441 (2017).
334. Moore, K. J., Rayner, K. J., Suárez, Y. & Fernández-Hernando, C. The role of microRNAs in cholesterol efflux and hepatic lipid metabolism. *Annu. Rev. Nutr.* **31**, 49–63 (2011).
335. Marquart, T. J., Allen, R. M., Ory, D. S. & Baldán, A. miR-33 links SREBP-2 induction to repression of sterol transporters. *Proc. Natl. Acad. Sci. U. S. A.* **107**, 12228–12232 (2010).
336. Iliopoulos, D., Drosatos, K., Hiyama, Y., Goldberg, I. J. & Zannis, V. I. MicroRNA-370 controls the expression of microRNA-122 and Cpt1alpha and affects lipid metabolism. *J. Lipid Res.* **51**, 1513–1523 (2010).
337. Faccini, J. *et al.* Circulating miR-155, miR-145 and let-7c as diagnostic biomarkers of the coronary artery disease. *Sci. Rep.* **7**, 42916 (2017).
338. Li, X. *et al.* miR-155 acts as an anti-inflammatory factor in atherosclerosis-associated foam cell formation by repressing calcium-regulated heat stable protein 1. *Sci. Rep.* **6**, 21789 (2016).
339. Das, A., Samidurai, A. & Salloum, F. N. Deciphering Non-coding RNAs in Cardiovascular Health and Disease. *Front. Cardiovasc. Med.* **5**, 73 (2018).
340. Cheng, H. S. *et al.* MicroRNA-146 represses endothelial activation by inhibiting pro-inflammatory pathways. *EMBO Mol. Med.* **5**, 1017–1034 (2013).
341. Sondermeijer, B. M. *et al.* Platelets in patients with premature coronary artery disease exhibit upregulation of miRNA340* and miRNA624*. *PLoS One* **6**, e25946 (2011).

342. Schulte, C. *et al.* Comparative Analysis of Circulating Noncoding RNAs Versus Protein Biomarkers in the Detection of Myocardial Injury. *Circ. Res.* **125**, 328–340 (2019).
343. Karakas, M. *et al.* Circulating microRNAs strongly predict cardiovascular death in patients with coronary artery disease-results from the large AtheroGene study. *Eur. Heart J.* **38**, 516–523 (2017).
344. Esteller, M. Non-coding RNAs in human disease. *Nat. Rev. Genet.* **12**, 861–874 (2011).
345. Fang, Y. & Fullwood, M. J. Roles, Functions, and Mechanisms of Long Non-coding RNAs in Cancer. *Genomics. Proteomics Bioinformatics* **14**, 42–54 (2016).
346. Kashi, K., Henderson, L., Bonetti, A. & Carninci, P. Discovery and functional analysis of lncRNAs: Methodologies to investigate an uncharacterized transcriptome. *Biochim. Biophys. Acta* **1859**, 3–15 (2016).
347. Xiong, G., Jiang, X. & Song, T. The overexpression of lncRNA H19 as a diagnostic marker for coronary artery disease. *Rev. Assoc. Med. Bras.* **65**, 110–117 (2019).
348. Chen, J. & Dang, J. LncRNA CASC11 was downregulated in coronary artery disease and inhibits transforming growth factor-β1. *J. Int. Med. Res.* **48**, 300060519889187 (2020).
349. Xu, Y. & Shao, B. Circulating lncRNA IFNG-AS1 expression correlates with increased disease risk, higher disease severity and elevated inflammation in patients with coronary artery disease. *J. Clin. Lab. Anal.* **32**, e22452 (2018).
350. Cho, H. *et al.* Long noncoding RNA ANRIL regulates endothelial cell activities associated with coronary artery disease by up-regulating CLIP1, EZR, and LYVE1 genes. *J. Biol. Chem.* **294**, 3881–3898 (2019).
351. Hu, Y.-W. *et al.* Long noncoding RNA NEXN-AS1 mitigates atherosclerosis by regulating the actin-binding protein NEXN. *J. Clin. Invest.* **129**, 1115–1128 (2019).
352. Shang, J., Li, Q.-Z., Zhang, J.-Y. & Yuan, H.-J. FAL1 regulates endothelial cell proliferation in diabetic arteriosclerosis through PTEN/AKT pathway. *Eur. Rev. Med. Pharmacol. Sci.* **22**, 6492–6499 (2018).
353. Zhang, L., Zhou, C., Qin, Q., Liu, Z. & Li, P. LncRNA LEF1-AS1 regulates the migration and proliferation of vascular smooth muscle cells by targeting miR-544a/PTEN axis. *J. Cell. Biochem.* **120**, 14670–14678 (2019).
354. Hennessy, E. J. *et al.* The long noncoding RNA CHROME regulates cholesterol homeostasis in primate. *Nat. Metab.* **1**, 98–110 (2019).
355. Li, X. *et al.* Overexpression of GAS5 inhibits abnormal activation of Wnt/β-catenin signaling pathway in myocardial tissues of rats with coronary artery disease. *J. Cell. Physiol.* **234**, 11348–11359 (2019).
356. Guo, F. *et al.* The interplay of LncRNA ANRIL and miR-181b on the inflammation-relevant coronary artery disease through mediating NF-κB signalling pathway. *J. Cell. Mol. Med.* **22**, 5062–5075 (2018).
357. Hu, Y. & Hu, J. Diagnostic value of circulating lncRNA ANRIL and its correlation with coronary artery disease parameters. *Brazilian J. Med. Biol. Res. = Rev. Bras. Pesqui. medicas e Biol.* **52**, e8309 (2019).
358. Cai, Y. *et al.* Circulating 'LncPPARδ' From Monocytes as a Novel Biomarker for Coronary Artery Diseases. *Medicine (Baltimore).* **95**, e2360 (2016).
359. Ebadi, N. *et al.* Dysregulation of autophagy-related lncRNAs in peripheral blood of coronary artery disease patients. *Eur. J. Pharmacol.* **867**, 172852 (2020).
360. Lin, T. M., Galbert, S. P., Kiefer, D., Spellacy, W. N. & Gall, S. Characterization of four human pregnancy-associated plasma proteins. *Am. J. Obstet. Gynecol.* **118**, 223–236 (1974).
361. Lin, T. M. & Halbert, S. P. Placental localization of human pregnancy--associated plasma proteins. *Science* **193**, 1249–1252 (1976).
362. Overgaard, M. T. *et al.* Messenger ribonucleic acid levels of pregnancy-associated plasma protein-A and the proform of eosinophil major basic protein: expression in human reproductive and nonreproductive tissues. *Biol. Reprod.* **61**, 1083–1089 (1999).

363. Gude, M. F. *et al.* PAPP-A, IGFBP-4 and IGF-II are secreted by human adipose tissue cultures in a depot-specific manner. *Eur. J. Endocrinol.* **175**, 509–519 (2016).
364. Qin, X., Byun, D., Strong, D. D., Baylink, D. J. & Mohan, S. Studies on the role of human insulin-like growth factor-II (IGF-II)-dependent IGF binding protein (hIGFBP)-4 protease in human osteoblasts using protease-resistant IGFBP-4 analogs. *J. bone Miner. Res. Off. J. Am. Soc. Bone Miner. Res.* **14**, 2079–2088 (1999).
365. Bayes-Genis, A. *et al.* Insulin-like growth factor binding protein-4 protease produced by smooth muscle cells increases in the coronary artery after angioplasty. *Arterioscler. Thromb. Vasc. Biol.* **21**, 335–341 (2001).
366. Conover, C. A. *et al.* Cytokine stimulation of pregnancy-associated plasma protein A expression in human coronary artery smooth muscle cells: inhibition by resveratrol. *Am. J. Physiol. Cell Physiol.* **290**, C183-8 (2006).
367. Chen, B.-K. *et al.* Molecular regulation of the IGF-binding protein-4 protease system in human fibroblasts: identification of a novel inducible inhibitor. *Endocrinology* **143**, 1199–1205 (2002).
368. Thomsen, J. *et al.* PAPP-A proteolytic activity enhances IGF bioactivity in ascites from women with ovarian carcinoma. *Oncotarget* **6**, 32266–32278 (2015).
369. Espelund, U. S. *et al.* Insulin-Like Growth Factor Bioactivity, Stanniocalcin-2, Pregnancy-Associated Plasma Protein-A, and IGF-Binding Protein-4 in Pleural Fluid and Serum From Patients With Pulmonary Disease. *J. Clin. Endocrinol. Metab.* **102**, 3526–3534 (2017).
370. Folkersen, J., Grudzinskas, J. G., Hindersson, P., Teisner, B. & Westergaard, J. G. Pregnancy-associated plasma protein A: circulating levels during normal pregnancy. *Am. J. Obstet. Gynecol.* **139**, 910–914 (1981).
371. Wald, N. J., Watt, H. C. & Hackshaw, A. K. Integrated screening for Down's syndrome based on tests performed during the first and second trimesters. *N. Engl. J. Med.* **341**, 461–467 (1999).
372. Brizot, M. L. *et al.* Gene expression of human pregnancy-associated plasma protein-A in placenta from trisomic pregnancies. *Placenta* **17**, 33–36 (1996).
373. Smith, G. C. S. *et al.* Early pregnancy levels of pregnancy-associated plasma protein a and the risk of intrauterine growth restriction, premature birth, preeclampsia, and stillbirth. *J. Clin. Endocrinol. Metab.* **87**, 1762–1767 (2002).
374. Poon, L. C. Y., Maiz, N., Valencia, C., Plasencia, W. & Nicolaides, K. H. First-trimester maternal serum pregnancy-associated plasma protein-A and pre-eclampsia. *Ultrasound Obstet. Gynecol. Off. J. Int. Soc. Ultrasound Obstet. Gynecol.* **33**, 23–33 (2009).
375. Smith, G. C. S. *et al.* Early-pregnancy origins of low birth weight. *Nature* **417**, 916 (2002).
376. Kristensen, T., Oxvig, C., Sand, O., Møller, N. P. & Sottrup-Jensen, L. Amino acid sequence of human pregnancy-associated plasma protein-A derived from cloned cDNA. *Biochemistry* **33**, 1592–1598 (1994).
377. Boldt, H. B. *et al.* Mutational analysis of the proteolytic domain of pregnancy-associated plasma protein-A (PAPP-A): classification as a metzincin. *Biochem. J.* **358**, 359–367 (2001).
378. Laursen, L. S. *et al.* Cell surface targeting of pregnancy-associated plasma protein A proteolytic activity. Reversible adhesion is mediated by two neighboring short consensus repeats. *J. Biol. Chem.* **277**, 47225–47234 (2002).
379. Oxvig, C., Sand, O., Kristensen, T., Gleich, G. J. & Sottrup-Jensen, L. Circulating human pregnancy-associated plasma protein-A is disulfide-bridged to the proform of eosinophil major basic protein. *J. Biol. Chem.* **268**, 12243–12246 (1993).
380. Overgaard, M. T. *et al.* Expression of recombinant human pregnancy-associated plasma protein-A and identification of the proform of eosinophil major basic protein as its physiological inhibitor. *J. Biol. Chem.* **275**, 31128–31133 (2000).
381. Overgaard, M. T. *et al.* Inhibition of proteolysis by the proform of eosinophil major basic protein (proMBP) requires covalent binding to its target proteinase. *FEBS Lett.* **560**, 147–152 (2004).

382. Conover, C. A. *et al.* Transgenic overexpression of pregnancy-associated plasma protein-A in murine arterial smooth muscle accelerates atherosclerotic lesion development. *Am. J. Physiol. Heart Circ. Physiol.* **299**, H284-91 (2010).
383. Mazerbourg, S. *et al.* Pregnancy-associated plasma protein-A (PAPP-A) in ovine, bovine, porcine, and equine ovarian follicles: involvement in IGF binding protein-4 proteolytic degradation and mRNA expression during follicular development. *Endocrinology* **142**, 5243–5253 (2001).
384. Monget, P. *et al.* Pregnancy-associated plasma protein-A is involved in insulin-like growth factor binding protein-2 (IGFBP-2) proteolytic degradation in bovine and porcine preovulatory follicles: identification of cleavage site and characterization of IGFBP-2 degradation. *Biol. Reprod.* **68**, 77–86 (2003).
385. Gyrup, C. & Oxvig, C. Quantitative analysis of insulin-like growth factor-modulated proteolysis of insulin-like growth factor binding protein-4 and -5 by pregnancy-associated plasma protein-A. *Biochemistry* **46**, 1972–1980 (2007).
386. Boldt, H. B. *et al.* The Lin12-notch repeats of pregnancy-associated plasma protein-A bind calcium and determine its proteolytic specificity. *J. Biol. Chem.* **279**, 38525–38531 (2004).
387. Laursen, L. S. *et al.* Substrate specificity of the metalloproteinase pregnancy-associated plasma protein-A (PAPP-A) assessed by mutagenesis and analysis of synthetic peptides: substrate residues distant from the scissile bond are critical for proteolysis. *Biochem. J.* **367**, 31–40 (2002).
388. Jepsen, M. R. *et al.* Stanniocalcin-2 inhibits mammalian growth by proteolytic inhibition of the insulin-like growth factor axis. *J. Biol. Chem.* **290**, 3430–3439 (2015).
389. Kløverpris, S. *et al.* Stanniocalcin-1 Potently Inhibits the Proteolytic Activity of the Metalloproteinase Pregnancy-associated Plasma Protein-A. *J. Biol. Chem.* **290**, 21915–21924 (2015).
390. Bayes-Genis, A. *et al.* Pregnancy-Associated Plasma Protein a As a Marker of Acute Coronary Syndromes. *N. Engl. J. Med.* **345**, 1022–1029 (2001).
391. Harrington, S. C., Simari, R. D. & Conover, C. A. Genetic deletion of pregnancy-associated plasma protein-A is associated with resistance to atherosclerotic lesion development in apolipoprotein E-deficient mice challenged with a high-fat diet. *Circ. Res.* **100**, 1696–1702 (2007).
392. Bale, L. K., Chakraborty, S. & Conover, C. A. Inducible reduction in pregnancy-associated plasma protein-A gene expression inhibits established atherosclerotic plaque progression in mice. *Endocrinology* **155**, 1184–1187 (2014).
393. Conover, C. A., Bale, L. K. & Oxvig, C. Targeted Inhibition of Pregnancy-Associated Plasma Protein-A Activity Reduces Atherosclerotic Plaque Burden in Mice. *J. Cardiovasc. Transl. Res.* **9**, 77–79 (2016).
394. Boldt, H. B. *et al.* Effects of mutated pregnancy-associated plasma protein-a on atherosclerotic lesion development in mice. *Endocrinology* **154**, 246–252 (2013).
395. Tang, S.-L. *et al.* PAPP-A negatively regulates ABCA1, ABCG1 and SR-B1 expression by inhibiting LXRα through the IGF-I-mediated signaling pathway. *Atherosclerosis* **222**, 344–354 (2012).
396. Blankenberg, S., Barbaux, S. & Tiret, L. Adhesion molecules and atherosclerosis. *Atherosclerosis* **170**, 191–203 (2003).
397. Peng, L., Yang, K., Jiang, W. & Yi, B. Methods to observe and weaken the influence of pregnancy-associated plasma protein-A on endothelial cell function. *Ann. Clin. Lab. Sci.* **44**, 399–404 (2014).
398. Tousoulis, D., Kampoli, A.-M., Tentolouris, C., Papageorgiou, N. & Stefanadis, C. The role of nitric oxide on endothelial function. *Curr. Vasc. Pharmacol.* **10**, 4–18 (2012).
399. Wobst, J., Schunkert, H. & Kessler, T. Genetic alterations in the NO-cGMP pathway and cardiovascular risk. *Nitric oxide Biol. Chem.* **76**, 105–112 (2018).
400. Lacolley, P., Regnault, V., Nicoletti, A., Li, Z. & Michel, J.-B. The vascular smooth muscle cell in arterial pathology: a cell that can take on multiple roles. *Cardiovasc. Res.* **95**, 194–204 (2012).

401. Resch, Z. T., Simari, R. D. & Conover, C. A. Targeted disruption of the pregnancy-associated plasma protein-A gene is associated with diminished smooth muscle cell response to insulin-like growth factor-I and resistance to neointimal hyperplasia after vascular injury. *Endocrinology* **147**, 5634–5640 (2006).
402. Wu, X.-F. *et al.* Level of Pregnancy-associated Plasma Protein-A Correlates With Coronary Thin-cap Fibroatheroma Burden in Patients With Coronary Artery Disease: Novel Findings From 3-Vessel Virtual Histology Intravascular Ultrasound Assessment. *Medicine (Baltimore).* **95**, e2563 (2016).
403. Cirillo, P. *et al.* Pregnancy-associated plasma protein-A promotes TF procoagulant activity in human endothelial cells by Akt-NF-κB axis. *J. Thromb. Thrombolysis* **42**, 225–232 (2016).
404. Grover, S. P. & Mackman, N. Tissue Factor: An Essential Mediator of Hemostasis and Trigger of Thrombosis. *Arterioscler. Thromb. Vasc. Biol.* **38**, 709–725 (2018).
405. Steffensen, L. B. *et al.* Stanniocalcin-2 overexpression reduces atherosclerosis in hypercholesterolemic mice. *Atherosclerosis* **248**, 36–43 (2016).
406. Yamamoto, K. *et al.* Contrasting effects of stanniocalcin-related polypeptides on macrophage foam cell formation and vascular smooth muscle cell migration. *Peptides* **82**, 120–127 (2016).
407. Suomalainen Lääkäriseura Duodecim. Sepelvaltimotautikohtaus (Acute coronary syndrome). *Käypä hoito -suositus* (2022). Available at: https://www.kaypahoito.fi/hoi50130#A2.
408. Terkelsen, C. J. *et al.* Temporal course of pregnancy-associated plasma protein-A in angioplasty-treated ST-elevation myocardial infarction patients and potential significance of concomitant heparin administration. *Am. J. Cardiol.* **103**, 29–35 (2009).
409. Hajek, P. *et al.* Influence of concomitant heparin administration on pregnancy-associated plasma protein-A levels in acute coronary syndrome with ST segment elevation. *Arch. Med. Sci.* **7**, 977–983 (2011).
410. Jespersen, C. H. B., Vestergaard, K. R., Schou, M., Teisner, B. & Iversen, K. The effect of heparin on pregnancy associated plasma protein-A concentration in healthy, non-pregnant individuals. *Clin. Biochem.* **48**, 757–761 (2015).
411. Tertti, R. *et al.* Intravenous administration of low molecular weight and unfractionated heparin elicits a rapid increase in serum pregnancy-associated plasma protein A. *Clin. Chem.* **55**, 1214–1217 (2009).
412. Wittfooth, S. *et al.* Studies on the effects of heparin products on pregnancy-associated plasma protein A. *Clin. Chim. Acta.* **412**, 376–381 (2011).
413. Hjortebjerg, R. *et al.* PAPP-A and IGFBP-4 fragment levels in patients with ST-elevation myocardial infarction treated with heparin and PCI. *Clin. Biochem.* **48**, 322–328 (2015).
414. Postnikov, A. B. *et al.* N-terminal and C-terminal fragments of IGFBP-4 as novel biomarkers for short-term risk assessment of major adverse cardiac events in patients presenting with ischemia. *Clin. Biochem.* **45**, 519–524 (2012).
415. Hjortebjerg, R. *et al.* Insulin-Like Growth Factor Binding Protein 4 Fragments Provide Incremental Prognostic Information on Cardiovascular Events in Patients With ST-Segment Elevation Myocardial Infarction. *J. Am. Heart Assoc.* **6**, (2017).
416. Wittfooth, S. Free PAPP-A: A novel marker in acute coronary syndrome patients [PhD thesis]. (University of Turku, Turku, Finland, 2009).
417. Qin, Q. P. *et al.* Molecular distinction of circulating pregnancy-associated plasma protein A in myocardial infarction and pregnancy. *Clin. Chem.* **51**, 75–83 (2005).
418. Wittfooth, S. *et al.* Immunofluorometric point-of-care assays for the detection of acute coronary syndrome-related noncomplexed pregnancy-associated plasma protein A. *Clin. Chem.* **52**, 1794–1801 (2006).
419. Tuunainen, E. *et al.* Direct immunoassay for free pregnancy-associated plasma protein A (PAPP-A). *J Appl Lab Med* **3**, 438–449 (2018).

420. Guven, A. *et al.* A coronary proatherosclerotic marker: Pregnancy-associated plasma protein A and its association with coronary calcium score and carotid intima-media thickness. *Adv. Clin. Exp. Med.* **26**, 467–473 (2017).
421. Heeschen, C. *et al.* Pregnancy-associated plasma protein-A levels in patients with acute coronary syndromes: comparison with markers of systemic inflammation, platelet activation, and myocardial necrosis. *J. Am. Coll. Cardiol.* **45**, 229–237 (2005).
422. Elesber, A. A. *et al.* Pregnancy associated plasma protein-A and risk stratification of patients presenting with chest pain in the emergency department. *Int. J. Cardiol.* **117**, 365–369 (2007).
423. McCann, C. J. *et al.* Novel biomarkers in early diagnosis of acute myocardial infarction compared with cardiac troponin T. *Eur. Heart J.* **29**, 2843–2850 (2008).
424. Iversen, K. K. *et al.* Pregnancy associated plasma protein A, a potential marker for vulnerable plaque in patients with non-ST-segment elevation acute coronary syndrome. *Clin. Biochem.* **42**, 828–834 (2009).
425. Body, R. *et al.* Low soluble P-selectin may facilitate early exclusion of acute myocardial infarction. *Clin. Chim. Acta.* **412**, 614–618 (2011).
426. Hajek, P. *et al.* High positive predictive value of PAPP-A for acute coronary syndrome diagnosis in heparin-naive patients. *J. Thromb. Thrombolysis* **34**, 99–105 (2012).
427. Schaub, N. *et al.* Markers of plaque instability in the early diagnosis and risk stratification of acute myocardial infarction. *Clin. Chem.* **58**, 246–256 (2012).
428. Wlazeł, R. N., Rysz, J. & Paradowski, M. Examination of serum pregnancy-associated plasma protein A clinical value in acute coronary syndrome prediction and monitoring. *Arch. Med. Sci.* **9**, 14–20 (2013).
429. Mehrpooya, M., Malekkandi, M., Arabloo, M., Zebardast, J. & Sattartabar, B. The Role of Insulin-Like Growth Factor-1 and Pregnancy-Associated Plasma Protein-A in Diagnosis of Acute Coronary Syndrome and Its Related Morbidities. *Adv. J. Emerg. Med.* **4**, e18 (2020).
430. Kavsak, P. A. *et al.* PAPP-A as a marker of increased long-term risk in patients with chest pain. *Clin. Biochem.* **42**, 1012–1018 (2009).
431. Iversen, K. K. *et al.* Usefulness of pregnancy-associated plasma protein A in patients with acute coronary syndrome. *Am. J. Cardiol.* **104**, 1465–1471 (2009).
432. Iversen, K. K. *et al.* Pregnancy-associated plasma protein-A, a marker for outcome in patients suspected for acute coronary syndrome. *Clin. Biochem.* **43**, 851–857 (2010).
433. Lund, J. *et al.* Free vs total pregnancy-associated plasma protein A (PAPP-A) as a predictor of 1-year outcome in patients presenting with non-ST-elevation acute coronary syndrome. *Clin. Chem.* **56**, 1158–1165 (2010).
434. Bonaca, M. P. *et al.* Prospective evaluation of pregnancy-associated plasma protein-a and outcomes in patients with acute coronary syndromes. *J. Am. Coll. Cardiol.* **60**, 332–338 (2012).
435. von Haehling, S. *et al.* Value of serum pregnancy-associated plasma protein A for predicting cardiovascular events among patients presenting with cardiac chest pain. *CMAJ* **185**, E295-303 (2013).
436. Cosin-Sales, J. *et al.* Relationship among pregnancy associated plasma protein-A levels, clinical characteristics, and coronary artery disease extent in patients with chronic stable angina pectoris. *Eur. Heart J.* **26**, 2093–2098 (2005).
437. Mueller, T., Dieplinger, B., Poelz, W. & Haltmayer, M. Increased pregnancy-associated plasma protein-A as a marker for peripheral atherosclerosis: results from the Linz Peripheral Arterial Disease Study. *Clin. Chem.* **52**, 1096–1103 (2006).
438. Heider, P. *et al.* Is serum pregnancy-associated plasma protein A really a potential marker of atherosclerotic carotid plaque stability? *Eur. J. Vasc. Endovasc. Surg. Off. J. Eur. Soc. Vasc. Surg.* **39**, 668–675 (2010).
439. Elesber, A. A. *et al.* Prognostic value of circulating pregnancy-associated plasma protein levels in patients with chronic stable angina. *Eur. Heart J.* **27**, 1678–1684 (2006).

440. Consuegra-Sanchez, L. *et al.* Prognostic value of circulating pregnancy-associated plasma protein-A (PAPP-A) and proform of eosinophil major basic protein (pro-MBP) levels in patients with chronic stable angina pectoris. *Clin. Chim. Acta.* **391**, 18–23 (2008).
441. Iversen, K. K. *et al.* Pregnancy associated plasma protein-A as a marker for myocardial infarction and death in patients with stable coronary artery disease: a prognostic study within the CLARICOR Trial. *Atherosclerosis* **214**, 203–208 (2011).
442. Schulz, O. *et al.* Pregnancy-associated plasma protein A values in patients with stable cardiovascular disease: use of a new monoclonal antibody-based assay. *Clin. Chim. Acta.* **412**, 880–886 (2011).
443. Zengin, E. *et al.* The utility of pregnancy-associated plasma protein A for determination of prognosis in a cohort of patients with coronary artery disease. *Biomark. Med.* **9**, 731–741 (2015).
444. Nilsson, E. *et al.* Pregnancy Associated Plasma Protein-A as a Cardiovascular Risk Marker in Patients with Stable Coronary Heart Disease During 10 Years Follow-Up-A CLARICOR Trial Sub-Study. *J. Clin. Med.* **9**, (2020).
445. de Lemos, J. A., McGuire, D. K. & Drazner, M. H. B-type natriuretic peptide in cardiovascular disease. *Lancet (London, England)* **362**, 316–322 (2003).
446. Ponikowski, P. *et al.* 2016 ESC Guidelines for the diagnosis and treatment of acute and chronic heart failure: The Task Force for the diagnosis and treatment of acute and chronic heart failure of the European Society of Cardiology (ESC)Developed with the special contribution o. *Eur. Heart J.* **37**, 2129–2200 (2016).
447. Dembic, M., Hedley, P. L., Torp-Pedersen, C., Kober, L. & Christiansen, M. Pregnancy-associated plasma protein-A (PAPP-A) and the proform of the eosinophil major basic protein (ProMBP) are associated with increased risk of death in heart failure patients. *Scand. J. Clin. Lab. Invest.* **77**, 352–357 (2017).
448. Konev, A. A. *et al.* CT-IGFBP-4 as a novel prognostic biomarker in acute heart failure. *ESC Hear. Fail.* **7**, 434–444 (2020).
449. Tromp, J. *et al.* Biomarker Correlates of Coronary Microvascular Dysfunction in Heart Failure With Preserved Ejection Fraction. *Circulation* **140**, 1359–1361 (2019).
450. Chandramouli, C. *et al.* Sex differences in proteomic correlates of coronary microvascular dysfunction among patients with heart failure and preserved ejection fraction. *Eur. J. Heart Fail.* (2022). doi:10.1002/ejhf.2435
451. Fantasia, I. *et al.* Fetal major cardiac defects and placental dysfunction at 11-13 weeks' gestation. *Ultrasound Obstet. Gynecol. Off. J. Int. Soc. Ultrasound Obstet. Gynecol.* **51**, 194–198 (2018).
452. Ott, W. J. The accuracy of antenatal fetal echocardiography screening in high- and low-risk patients. *Am. J. Obstet. Gynecol.* **172**, 1741–1749 (1995).
453. Ghi, T., Huggon, I. C., Zosmer, N. & Nicolaides, K. H. Incidence of major structural cardiac defects associated with increased nuchal translucency but normal karyotype. *Ultrasound Obstet. Gynecol. Off. J. Int. Soc. Ultrasound Obstet. Gynecol.* **18**, 610–614 (2001).
454. Alanen, J. *et al.* First trimester combined screening biochemistry in detection of congenital heart defects. *J. Matern. neonatal Med. Off. J. Eur. Assoc. Perinat. Med. Fed. Asia Ocean. Perinat. Soc. Int. Soc. Perinat. Obstet.* **32**, 3272–3277 (2019).
455. Hematian, M. N. *et al.* A prospective cohort study on association of first-trimester serum biomarkers and risk of isolated foetal congenital heart defects. *Biomarkers Biochem. Indic. Expo. response, susceptibility to Chem.* **26**, 747–751 (2021).
456. Bansal, M. Cardiovascular disease and COVID-19. *Diabetes Metab. Syndr.* **14**, 247–250 (2020).
457. Sattar, Y. *et al.* COVID-19 cardiovascular epidemiology, cellular pathogenesis, clinical manifestations and management. *Int. J. Cardiol. Hear. Vasc.* **29**, 100589 (2020).
458. Babapoor-Farrokhran, S. *et al.* Myocardial injury and COVID-19: Possible mechanisms. *Life Sci.* **253**, 117723 (2020).

459. Sanchez, B. G., Gasalla, J. M., Sánchez-Chapado, M., Bort, A. & Diaz-Laviada, I. Increase in Ischemia-Modified Albumin and Pregnancy-Associated Plasma Protein-A in COVID-19 Patients. *J. Clin. Med.* **10**, (2021).
460. Trilla, C. *et al.* First-trimester SARS-CoV-2 infection: clinical presentation, inflammatory markers and obstetric outcomes. *Fetal Diagn. Ther.* (2022). doi:10.1159/000523974
461. Di Mascio, D. *et al.* Outcome of coronavirus spectrum infections (SARS, MERS, COVID-19) during pregnancy: a systematic review and meta-analysis. *Am. J. Obstet. Gynecol. MFM* **2**, 100107 (2020).
462. Kumar, A. *et al.* Pregnancy-associated plasma protein-A regulates myoblast proliferation and differentiation through an insulin-like growth factor-dependent mechanism. *J. Biol. Chem.* **280**, 37782–37789 (2005).
463. von Lode, P., Rosenberg, J., Pettersson, K. & Takalo, H. A europium chelate for quantitative point-of-care immunoassays using direct surface measurement. *Anal. Chem.* **75**, 3193–3201 (2003).
464. Eriksson, S. *et al.* Negative interference in cardiac troponin I immunoassays from a frequently occurring serum and plasma component. *Clin. Chem.* **49**, 1095–1104 (2003).
465. CLSI. *Evaluation of derection capability for clinical laboratory measurement procedures; approved guideline - second edition. CLSI document EP17-A2*. (2012).
466. CLSI. *Evalutaion of precision performance of quantitative measuremnt methods; approved guideline - second edition. CLSI document EP5-A2*. (2004).
467. Savukoski, T. *et al.* Novel sensitive cardiac troponin I immunoassay free from troponin I-specific autoantibody interference. *Clin. Chem. Lab. Med.* **52**, 1041–1048 (2014).
468. Warnick, G. R., Cheung, M. C. & Albers, J. J. Comparison of current methods for high-density lipoprotein cholesterol quantitation. *Clin. Chem.* **25**, 596–604 (1979).
469. Kajander, S. *et al.* Cardiac positron emission tomography/computed tomography imaging accurately detects anatomically and functionally significant coronary artery disease. *Circulation* **122**, 603–613 (2010).
470. Tuunainen, E. *et al.* Free PAPP-A as a biomarker: heparin-induced release is not related to coronary atherosclerotic burden. *Clin. Chem. Lab. Med.* **57**, e155–e158 (2019).
471. Maaniitty, T. *et al.* Prognostic Value of Coronary CT Angiography With Selective PET Perfusion Imaging in Coronary Artery Disease. *JACC. Cardiovasc. Imaging* **10**, 1361–1370 (2017).
472. Nesterov, S. V *et al.* Myocardial perfusion quantitation with 15O-labelled water PET: high reproducibility of the new cardiac analysis software (Carimas). *Eur. J. Nucl. Med. Mol. Imaging* **36**, 1594–1602 (2009).
473. Danad, I. *et al.* Quantitative assessment of myocardial perfusion in the detection of significant coronary artery disease: cutoff values and diagnostic accuracy of quantitative [(15)O]H2O PET imaging. *J. Am. Coll. Cardiol.* **64**, 1464–1475 (2014).
474. Center for Drug Evaluation and Research. Guidance for Industry: Bioanalytical method validation. *FDA* Available at: https://www.fda.gov/downloads/Drugs/Guidance/ucm070107.pdf. (Accessed October 2017).
475. Andreasson, U. *et al.* A Practical Guide to Immunoassay Method Validation. *Front. Neurol.* **6**, 179 (2015).
476. Overgaard, M. T. *et al.* Pregnancy-associated plasma protein-A2 (PAPP-A2), a novel insulin-like growth factor-binding protein-5 proteinase. *J. Biol. Chem.* **276**, 21849–21853 (2001).
477. Gutierrez-Leonard, H. *et al.* Pregnancy-associated plasma protein-A (PAPP-A) as a possible biomarker in patients with coronary artery disease. *Ir. J. Med. Sci.* (2016). doi:10.1007/s11845-016-1515-6
478. Nichenametla, G. & Thomas, V. S. Evaluation of Serum Pregnancy Associated Plasma Protein-A & Plasma D-Dimer in Acute Coronary Syndrome. *J. Clin. Diagn. Res.* **10**, BC01-3 (2016).
479. Al-Mohaissen, M. A. *et al.* A Plaque Disruption Index Identifies Patients with Non-STE-Type 1 Myocardial Infarction within 24 Hours of Troponin Positivity. *PLoS One* **11**, e0164315 (2016).

480. O'Donoghue, M. L. *et al.* Multimarker Risk Stratification in Patients With Acute Myocardial Infarction. *J. Am. Heart Assoc.* **5**, (2016).
481. Kavsak, P. A., Xu, L., Yusuf, S. & McQueen, M. J. High-sensitivity cardiac troponin I measurement for risk stratification in a stable high-risk population. *Clin. Chem.* **57**, 1146–1153 (2011).
482. Caselli, C. *et al.* Effect of Coronary Atherosclerosis and Myocardial Ischemia on Plasma Levels of High-Sensitivity Troponin T and NT-proBNP in Patients With Stable Angina. *Arterioscler. Thromb. Vasc. Biol.* **36**, 757–764 (2016).
483. Di Angelantonio, E. *et al.* Major lipids, apolipoproteins, and risk of vascular disease. *JAMA* **302**, 1993–2000 (2009).
484. Fernández-Friera, L. *et al.* Normal LDL-Cholesterol Levels Are Associated With Subclinical Atherosclerosis in the Absence of Risk Factors. *J. Am. Coll. Cardiol.* **70**, 2979–2991 (2017).
485. Paana, T. *et al.* Cardiac troponin elevations in marathon runners. Role of coronary atherosclerosis and skeletal muscle injury. The MaraCat Study. *Int. J. Cardiol.* (2019). doi:10.1016/j.ijcard.2019.08.019
486. Grundy, S. M. *et al.* 2018 AHA/ACC/AACVPR/AAPA/ABC/ACPM/ADA/AGS/APhA/ASPC/NLA/PCNA Guideline on the Management of Blood Cholesterol: A Report of the American College of Cardiology/American Heart Association Task Force on Clinical Practice Guidelines. *J. Am. Coll. Cardiol.* **73**, e285–e350 (2019).
487. Winther, S. *et al.* Incorporating Coronary Calcification Into Pre-Test Assessment of the Likelihood of Coronary Artery Disease. *J. Am. Coll. Cardiol.* **76**, 2421–2432 (2020).
488. Gaemperli, O., Saraste, A. & Knuuti, J. Cardiac hybrid imaging. *Eur. Hear. journal. Cardiovasc. Imaging* **13**, 51–60 (2012).
489. Hjortebjerg, R. IGFBP-4 and PAPP-A in normal physiology and disease. *Growth Horm. IGF Res.* **41**, 7–22 (2018).
490. Juarez-Orozco, L. E. *et al.* Impact of a decreasing pre-test probability on the performance of diagnostic tests for coronary artery disease. *Eur. Hear. journal. Cardiovasc. Imaging* **20**, 1198–1207 (2019).
491. Gyrup, C., Christiansen, M. & Oxvig, C. Quantification of proteolytically active pregnancy-associated plasma protein-A with an assay based on quenched fluorescence. *Clin. Chem.* **53**, 947–954 (2007).

TURUN
YLIOPISTO
UNIVERSITY
OF TURKU

Painosalama, Turku, Finland 2022

ISBN 978-951-29-9048-1 (PRINT)
ISBN 978-951-29-9049-8 (PDF)
ISSN 2736-9390 (Print)
ISSN 2736-9684 (Online)